On the Machinability of Ductile and Strain Hardening Materials - Models and Methods for Analyzing Machinability

Schultheiss, Fredrik

2013

On the Machinability of Ductile and Strain Hardening Materials

- Models and Methods for Analyzing Machinability

Fredrik Schultheiss

LUND
UNIVERSITY

Division of Production and Materials Engineering
ISBN 978-91-7473-728-8 (printed)
ISBN 978-91-7473-729-5 (pdf)
LUTMDN(TMMV-1065)/1-152(2013)

Printed in Sweden by Media-Tryck, Lund University
Lund 2013

Abstract

As quality and performance demands on today's products increases, more and more advanced materials are being used during modern production. The problem is however that this in turn place new demands on the machining processes utilized. Even though a significant amount of research has been published on the machining of these materials knowledge is still limited in several crucial areas. A problem with machining research is that it often relies heavily on quantitative data primarily obtained through experimental investigations. Due to the substantial amount of potentially different machining cases it could be difficult to generalize the obtained results to other scenarios. In this dissertation it has been attempted to model the investigated phenomena through using universal physical relationships. Even though this might result in a larger modeling error for the specific case investigated the author sees a great advantage of being able to have a physical explanation to the obtained results.

The aim of this dissertation has been to increase the knowledge on, and to a certain extent predict, the machinability of some common ductile and strain hardening materials. The research has focused on evaluating duplex stainless steel, Ti6Al4V and Alloy 718. However, the proposed models have been constructed in a way as to aid future implementation for other workpiece materials. A central pillar of the research has been the influence of the stagnation point and the related minimum chip thickness. This aspect influences all machining operations and could potentially have a significant impact on the machinability, not least for ductile and strain hardening materials. During this research it was found that even though cutting conditions have a major influence on the value of the minimum chip thickness, material factors such as ductility and strain hardening should not be neglected as these also influence the obtained value. In turn, it was found that the minimum chip thickness could to a certain extent be used to explain the obtained workpiece surface roughness. Also, the tool surface roughness was found to have a determinate influence on the mechanics of the machining process.

During the present research it was also found that it is difficult to predict the tool life using conventional models for the investigated materials, essentially due to their high

strength at elevated temperatures, adhesive behavior during machining, and low thermal conductivity. The influence of these properties commonly results in rapid and unpredictable wear of the cutting tool. Plastic deformation of the cutting tool is always a concern when machining these materials and a first step towards establishing a method for measuring the initiation of plastic deformation by using the measured cutting force has been proposed. Also, through using a proposed method for determining the potential machinability of a specific workpiece material these effects could be reduced through the use of reasonable process parameters before commencing production.

Methods for improving the machining process in terms of for example part cost or sustainability has been developed as part of this research. Even though each of these methods only improves a small part of the whole production process these improvements should not be neglected as all parts of the process should be optimized in order to achieve a truly sustainable and cost efficient machining process.

Keywords:

Machinability, Duplex stainless steel, Ti6Al4V, Alloy 718, Minimum chip thickness, Contact condition, Surface topography, Tool wear, Part cost, Sustainable machining, Polar diagram.

Sammanfattning

Allteftersom kraven på kvalité och prestanda hos dagens produkter ökar används alltmer avancerade material som en del av modern produktion. Problemet som uppstår är dock att dessa material ställer nya krav på tillverkningsprocessen och då inte minst vid skärande bearbetning. Trots att en betydande mängd forskning redan har publicerats vad gäller skärande bearbetning av dessa material saknas fortfarande genomgripande kunskap inom flera viktiga delområden. Ett problem med forskning inom skärande bearbetning är att den ofta förlitar sig i huvudsak på kvantitativ data, primärt erhållen genom experimentella försök. Detta gör att de erhållna resultaten kan vara svåra att generalisera till andra bearbetningsfall. I denna avhandling har en ansats gjorts att tolka de erhållna resultaten med hjälp av fundamentala fysikaliska principer. Även om detta potentiellt resulterar i ett större modellfel så ser författaren stora fördelar med att kunna ge en fysikalisk tolkning av de erhållna resultaten.

Målet med denna avhandling har varit att öka kunskapen om, samt i viss utsträckning även förutsäga skärbarheten hos några vanligt förekommande duktila och deformationshårdnande material. Forskningen har primärt fokuserat på studier av skärbarheten hos duplexa rostfria stål, Ti6Al4V samt Alloy 718. Inflytandet från stagnationspunkten vid skärande bearbetning samt det närbesläktade fenomenet med en minsta teoretisk spåntjocklek har varit av central betydelse för denna forskning. Denna faktor påverkar alla bearbetningsprocesser och har en betydande inverkan på skärbarheten, inte minst för duktila och deformationshårdnande material. Som en del av denna forskning upptäcktes att den minsta teoretiska spåntjockleken har ett signifikant och i viss utsträckning förutsägbart inflytande på den bearbetade ytans topografi för samtliga undersökta material. Det visade sig även att storleken hos den minsta teoretiska spåntjockleken är relaterad till flera olika processparametrar så som använd skärdata samt även arbetsmaterialet duktilitet och deformationshårdnande. Det konstaterades även att skärverktygets ytfinhet har en mätbar inverkan på bearbetningsprocessen.

Som ett led av denna forskning iakttogs hur svårt det är att förutsäga skärverktygens livslängd vid bearbetning av dessa material primärt på grund av deras höga hållfasthet även vid förhöjd temperatur, adhesiva uppträdande under skärprocessen samt även

deras förhållandevis låga termiska konduktivitet. Således är deformation och annan nedbrytning av skärverktyget alltid ett potentiellt problem vid bearbetning av dessa material. Genom att använda den presenterade metoden för att bestämma den potentiella skärbarheten hos ett givet arbetsmaterial kan denna problematik potentiellt reduceras genom användning av rimliga processparametrar redan under initieringen av produktionen.

Även praktiska metoder för att förbättra bearbetningsprocessen i form av till exempel lägre detaljkostnad eller ökad hållbarhet från ett miljö- och samhällsperspektiv har presenterats som del av denna forskning. Trotts att de föreslagna metoderna enbart förbättrar en liten del av produktionsprocessen bör de inte försummas då alla delar av en tillverkningsprocess måste optimeras för att erhålla en reellt hållbar och kostnadseffektiv produktionsprocess.

Nyckelord:

Skärbarhet, Duplexa rostfria stål, Ti6Al4V, Alloy 718, Minsta teoretiska spåntjockleken, Kontaktförhållande, Yttopografi, Verktygsförslitning, Detaljkostnad, Hållbar bearbetning, Polära skärbarhetsdiagram.

Acknowledgment

The research presented in this dissertation would not have been possible without the help of a substantial amount of people and organizations. With the obvious risk of forgetting someone I would like to express my sincere gratitude to the following.

First of all I would like to express my gratitude to my supervisor Professor Jan-Eric Ståhl. If it would not have been for his guidance, encouragement and bright ideas this dissertation would never have been imaginable. I would also like to thank Professor Jinming Zhou and Dr. Volodymyr Bushlya for their support.

I would like to thank everyone involved in the ShortCut research project funded by SSF/ProViking for their invaluable assistance and funding during my research. Likewise, I would like to thank the Sustainable Production Initiative, SPI, cooperation between Lund University and Chalmers University of Technology for partially funding the latter part of my research.

Furthermore, I would like to express my sincere gratitude to Dr. Sören Hägglund at Seco Tools AB for his valuable input on my research, not least on my attempts to model the tool life. Similarly, I would like to thank Dr. Rachid M'Saoubi, Tommy Lehtola and everyone else at the R&D department at Seco Tools AB in Fagersta for their assistance. In addition I am also grateful for the assistance received from Bengt Högrelius whom even though he is now retired appears to be as engaged as ever in machining research.

I would also like to express my appreciation towards all my coauthors for the numerous papers we achieved together. In particular I would like to mention Tech. Lic. Mathias Agmell who help me with the FEM-simulations, Dr. Mikael Fallqvist who did not give up on teaching me the finer arts of tribology, Dr. Linhong Xu for her assistance in evaluating the potential machinability model and M.Sc. Manoucheher Vosough for his knowledge on the machining of Ti6Al4V. Likewise, I would like to express my gratefulness towards Mustafa Gatea for his assistance in performing the necessary measurements.

Further, I would like to express my sincere gratitude towards all my colleagues at the Division of Production and Materials Engineering at Lund University. Without your assistance and camaraderie I would never have been able to complete this research.

Finally, I would like to express my gratitude towards my family for their encouragement and belief in my pursuit of knowledge.

Lund, November 2013

Fredrik Schultheiss

Appended publications

This dissertation is primarily based on the following publications, which will be referred to in the text by their Roman numerals. The publications are appended at the end of this dissertation.

I *Machinability of Duplex Stainless Steels – A Study with Focus on the Tool Wear Behaviour*
F. Schultheiss, J.-E. Ståhl
Proceedings of the 4th International Swedish Production Symposium, (2011) 271-277

II *General Conception of Polar Diagrams for the Evaluation of the Potential Machinability of Workpiece Materials*
L. Xu, F. Schultheiss, M. Andersson, J.-E. Ståhl
International Journal of Machining and Machinability of Materials, 14 (2013) 24-44

III *Experimental Study on the Minimum Chip Thickness during the Machining of Duplex Stainless Steel*
F. Schultheiss, M. Agmell, B. Högrelius, V. Bushlya, J.-E. Ståhl
Proceedings of AMST '11 Advanced manufacturing systems and technology, (2011) 175-189

IV *Influence of the Tool Surface Micro Topography on the Tribological Characteristics in Metal Cutting: Part I Experimental Observations of Contact Conditions*
M. Fallqvist, F. Schultheiss, R. M'Saoubi, M. Olsson, J.-E. Ståhl
Wear, 298-299 (2013) 87-98

V *Influence of the Tool Surface Micro Topography on the Tribological Characteristics in Metal Cutting – Part II Theoretical Calculations of Contact Conditions*
F. Schultheiss, M. Fallqvist, R. M'Saoubi, M. Olsson, J.-E. Ståhl
Wear, 298-299 (2013) 23-31

VI *A Method for Identification of Geometrical Tool Changes during Machining of Titanium Alloy Ti6Al4V*
M. Vosough, F. Schultheiss, M. Agmell, J.-E. Ståhl
International Journal of Advanced Manufacturing Technology, 67 (2013) 339-348

VII *Cost Based Process Optimization by Incrementally Changing the Cutting Data during Sustainable Machining*
F. Schultheiss, B. Lundqvist, J.-E. Ståhl
Advanced Materials Research, 576 (2012) 742-746

VIII *Sustainable Machining through Increasing the Cutting Tool Utilization*
F. Schultheiss, J. Zhou, E. Gröntoft, J.-E. Ståhl
Journal of Cleaner Production, 59 (2013) 298-307

Other publications by the author not appended to this dissertation.

IX *Cost Optimization by Incremental Production Improvements of Metal Cutting Operations*
F. Schultheiss, M. Jönsson, B. Lundqvist, J.-E. Ståhl
Proceedings of the 4th International Swedish Production Symposium, (2011) 540-547

X *Analytical and Experimental Determination of the R_a Surface Roughness during Turning*
J.-E. Ståhl, F. Schultheiss, S. Hägglund
Proceedings of the 1st CIRP Conference on Surface Integrity, Procedia Engineering, 19 (2011) 349-356

XI *Analytical Calculation of the Equivalent Chip Thickness for Cutting Tools and its Influence on the Calculated Tool Life*
J.-E. Ståhl, F. Schultheiss
Advanced Materials Research, 576 (2012) 80-86

XII *A Sustainable Approach for Milling of Duplex Stainless Steel by Increasing the Cutting Tool Utilization*
F. Schultheiss, J. Zhou, E. Gröntoft, J.-E. Ståhl
Proceedings of the 5th International Swedish Production Symposium, (2012) 171-177

XIII *Analytical Calculation of the R_a Surface Roughness during Turning*
J.-E. Ståhl, F. Schultheiss, S. Hägglund
Proceedings of the 5th International Swedish Production Symposium, (2012) 185-189

XIV *A Step towards Sustainable Machining Through Increasing the Cutting Tool Utilization*
F. Schultheiss, J. Zhou, E. Gröntoft, J.-E. Ståhl
Proceedings of the International Conference on Sustainable Intelligent Manufacturing SIM 2013, (2013) 191-196

XV *Influence of the workpiece material properties on the cutting forces*
F. Schultheiss, V. Bushlya, J.-E. Ståhl
To be submitted to the 6th International Swedish Production Symposium, 2014

XVI *Influence of the minimum chip thickness on the obtained surface roughness during turning operations*
F. Schultheiss, S. Hägglund, V. Bushlya, J.-E. Ståhl
To be submitted to the 2nd CIRP Conference on Surface Integrity, 2014

Authors contribution

The author has made the following contributions to the appended publications.

I Schultheiss performed a major part of the planning, experiments and data analysis. He also wrote a major part of the paper.

II Schultheiss wrote a major part of the paper as based on previous work by Andersson and Ståhl [1]. He also contributed with reflections related to the use of the proposed model for ductile and strain hardening materials. Xu compiled fundamental material properties related to the investigated workpiece materials.

III Schultheiss had a major role in planning and performing the experiments as well as conducting the analytical calculations. He also wrote a major part of the paper except for the section discussing numerical simulation which was written by Agmell. Högrelius assisted by performing the quick-stop experiments.

IV Fallqvist performed the experiments and wrote a major part of the paper assisted by M'Saoubi. Schultheiss contributed by writing the section regarding the contact condition on the rake face as well as analyzing a minor part of the obtained data.

V Schultheiss performed a major part of analyzing the obtained data as well as writing the paper. Fallqvist performed the required experiments assisted by M'Saoubi. The load analysis implemented in the paper was based on theory by Ståhl.

VI Schultheiss performed a major part of the data analysis as well as wrote a major part of the paper as based on a draft written by Vosough. Vosough also performed a major part of the experiments based on planning by Ståhl. The section on numerical simulations was written by Agmell.

VII Schultheiss performed a major part of the planning, analysis of obtained data, and writing of the paper based on experimental data obtained by Lundqvist.

VIII Schultheiss performed part of the planning and experimental work as well as a major part of the data analysis and writing of the paper assisted by Zhou and Gröntoft. Gröntoft performed some additional experimental work specifically focusing on the milling process.

Contents

Symbols and abbreviations

Selected symbols and abbreviations used throughout the dissertation.

A	Chip area
A_{cl}	Axial force acting on the clearance face
a_p	Depth of cut
A_{pl}	Ploughing area
A_r	Axial force acting on the rake face
b_1	Theoretical chip width
b_2	Obtained chip width
BUE	Built-up edge
Cr	Cutting resistance
CVD	Chemical vapor deposition
D_n	Strain hardening factor
f	Feed
F_c	Main cutting force
F_f	Feed force
F_p	Passive force
h_1	Theoretical chip thickness
h_{1min}	Minimum chip thickness
h_2	Obtained chip thickness
h_{2min}	Measured minimum chip thickness
h_e	Equivalent chip thickness
HV	Vickers hardness
k	Thermal conductivity
k_c	Specific cutting force
l_c	Active cutting edge length
P	Power consumption
P_m	Motor power consumption
r	Nose radius
R_a	Arithmetic mean surface roughness
R_{cl}	Radial force acting on the clearance face
R_{max}	Maximum peak-to-valley surface roughness
R_{mean}	Theoretical surface centerline
R_r	Radial force acting on the rake face
r_β	Tool edge radius
SIFT	Stepwise increased feed test
T_{cl}	Tangential force acting on the clearance face
T_r	Tangential force acting on the rake face
VB	Width of the flank wear land
VB_N	Maximum width of the flank wear land
VB_S	Width of the synthetic wear land
v_c	Cutting speed
V_{rel}	Relative chip flow volume

Greek symbols.

μ_{cl}	Contact condition on the clearance face	v_{ch}	Chip flow angle
μ_r	Contact condition on the rake face	ρ_r	Friction angle
γ	Rake angle	σ_{UTS}	Ultimate tensile strength
δ	Angular coordinate	σ_Y	Yield strength
δ_0	Angular coordinate at $h_1(\delta) = 0$	ϕ	Shear angle
δ_{h1min}	Angular coordinate at $h_1(\delta) = h_{1min}$	φ_A	Axial load function
ε_b	Elongation at rupture	φ_{DF}	Tool deterioration factor
η	Machine tool efficiency	φ_R	Radial load function
κ	Major cutting edge angle	φ_T	Tangential load function
λ_h	Chip compression ratio	$\chi_{vc,comp}$	Cutting speed compensation factor

"The whole of science is nothing more than a refinement of everyday thinking."

Albert Einstein, Physics and Reality
Journal of the Franklin Institute, 221 (1936) 349-382.

1 Introduction

Machining processes are an essential part of modern production. It has been estimated that more than 80% of all manufactured products have been machined at some point before they are completed [2]. According to Gardner Business Media Inc. the worldwide annual production of machine tools (metal cutting and metal forming) was approximately US$93 billion during 2012 [3]. The same company estimates that US$3.6 billion was spent on metal cutting tools including grinding wheels and other abrasives during the same time period [4]. Even though it is difficult to find a precise definition of a metal cutting or machining process, in essence a machining process could be stated as intended to remove unwanted material from the workpiece in the form of a chip. This material removal is achieved through straining a local region of the workpiece until it is sheared off through using the relative motion of the tool in relation to the workpiece [5]. Thus, selected parts of the workpiece material can be removed. Primarily, machining processes can be considered as including turning, milling, drilling, boring, shaping, broaching and reaming processes.

1.1 Background and Aim

Research in the field of machining has been conducted for more than a century and even though significant advances have been made through the years similar questions are still being asked by modern scientists. As for research on all manufacturing process the aim of machining research is to strive towards products with a higher quality at a lower manufacturing cost. In addition, new difficult to machine materials are constantly being added to the market resulting in a need for continued research in the machining area. Different kinds of ductile and strain hardening materials are part of these new, difficult to machine materials and thus a viable subject for further research. One group of such comparatively new ductile and strain hardening materials is duplex stainless. Duplex stainless steel was invented about 70 years ago with the aim of increasing the oxidation resistance of stainless steel while at the same time maintaining an acceptable material cost [6, 7]. This was achieved by creating a dual phase material with approximately equal amounts of ferrite and austenite. A drawback

of duplex stainless steels is however that they in general are considered as having a low machinability as compared to conventional steels. Also, comparatively little is currently known on the exact behavior of duplex stainless steel during conventional machining operations. Other difficult to machine materials such as Ti6Al4V and Alloy 718 have possibly been investigated a bit further even though comparatively little has been published on the machinability of these ductile and strain hardening materials as compared to more common workpiece materials such as carbon steels. As a result the aim of this study has been to investigate the machinability of an assortment of ductile and strain hardening materials and in particular try to decipher the underlying reasons for their specific behavior. It was also of high interest to try and predict the behavior of different kinds of workpiece materials at varying process conditions and thus in the future being able to optimize the machining of this type of materials.

As published by Ståhl [8], several different research areas are commonly investigated during production research, Figure 1.1. Often several of these areas are addressed within a single study.

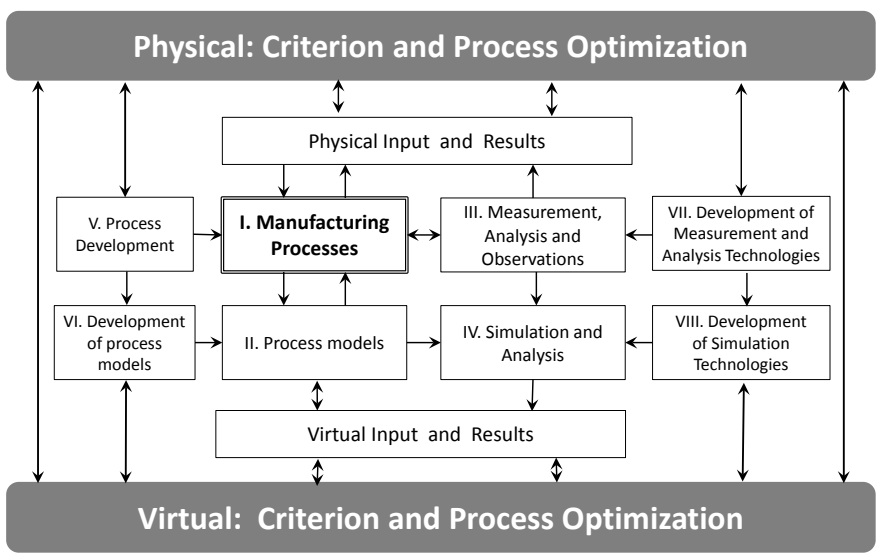

Figure 1.1 Fundamental research areas during production research [8].

For the research incorporated in this dissertation several of these research areas have been investigated to a varying extent. Predominantly the research presented in this dissertation has focused on the manufacturing process itself. The machining process has been analyzed through several different sets of quantitative measurements and observations. In addition, models of the process has been developed and compared to

the obtained data. This has been done in order to gain a better understanding of the machining process and thus in the future being able to predict the behavior while varying different process parameters. This knowledge could then be used to optimize the machining process for instance towards a lower manufacturing cost or a more sustainable and robust machining process.

1.2 Hypothesis

As based on previous publications on the behavior of metal cutting processes the following hypothesis were established for this study:

1. Machinability can be predicted through understanding the fundamental physical processes active during any machining process.
2. The potential machinability of a workpiece material can be predicted through knowledge of the material properties.
3. The stagnation zone and related minimum chip thickness has a measurable, significant influence on the machinability during any machining process.

1.3 Research Questions

In the light of the hypotheses the following research questions were determined.

RQ1. Can the obtained machinability be attributed to one or more physical phenomena during the machining process and thus be predicted?
RQ2. Could any part of the machinability for a specific workpiece material be analyzed without prior knowledge on the machining process?
RQ3. How should the machinability of a new machining operation be analyzed in order to aid the choice of appropriate process parameters?

1.4 Delimitations

In general it could be stated that the machinability is primarily dependent upon the workpiece material, machine tool, and process parameters including the tool material, tool geometry and cutting data. Since a considerable amount of different combinations of these variables exist it is impossible to validate the theories presented

in this dissertation for all potential combinations. Thus, only selected machining cases are discussed and validated in this dissertation. However, all experiments presented were carefully documented in order to increase the reproducibility of the performed experiments as well as to allow for future experiments to further investigate the validity of the presented methods and models. Thus, the following delimitations were employed during this research.

- The research has primarily been focused on machining of duplex stainless steel, Ti6Al4V and Alloy 718. However, in some cases alternative workpiece materials have been used either as a comparison or to further investigate the validity of the presented methods and models.
- The research has primarily been limited to longitudinal turning operations along with milling in one case. Since a continuous machining process with a single, stationary cutting tool was thought of as suitable for analyzing a considerable part of the fundamental physical process occurring during any machining process.
- The research has been limited to cemented carbide cutting tools since these are generally recommended by the tool manufacturers while machining the investigated workpiece materials as well as other ductile and strain hardening materials. That said, no claims are made that the selected tool grades and geometries are the optimum choice for each machining case investigated.

1.5 Outline of the Dissertation

This dissertation has the following structure:

Chapter 1: Introduction
Chapter 1 introduces the research topic and presents the research questions.

Chapter 2: Research Methodology
Chapter 2 describes the author's research philosophy and introduces the research methodology implemented for obtaining the results presented in this dissertation.

Chapter 3: Frame of Reference
Chapter 3 is a brief introduction into the field of machining research and more particularly machinability investigations.

Chapter 4: Machinability Investigations
Chapter 4 summarizes and discusses the results obtained by the author as a part of his research and is intended to address the research questions.

Chapter 5: Conclusions
Chapter 5 contains the main conclusions obtained as a part of this research with a particular emphasis on how this research answers the research questions.

Chapter 6: Future Research
Chapter 6 ends the dissertation with proposals for future research to further investigate the research topic.

1.6 Result Implementation

As a result of the general strive towards producing better products, more and more companies are using difficult to machine materials in their products. For example the use of ductile and strain hardening materials such as duplex stainless steel, Ti6Al4V and Alloy 718 is becoming increasingly common during production. The results presented in this dissertation are primarily intended to increase the production efficiency while producing different parts out of these materials. This can be done by better understanding the obtained results after any machining operation and thus entwines with the scientific goal of better understanding the machining process and consequently being able to predict the obtained results. Ståhl [8] has previously published a principle illustration on how product development and production continuously interact, successively improving the production efficiency while reducing the part cost, Figure 1.2.

The research presented in this dissertation could be attributed to several different parts of this improvement process. For instance, a model for assisting in predicting the potential machinability of a workpiece material has been presented. The evaluation of the influence of the workpiece material on the product quality as well as part cost and production sustainability should be performed before the initiation of production, possible even in cooperation with the early product development stages. Also, the so called incremental production improvement process has been introduced as part of this research, which could be considered as being a part of the continual improvements conducted during the production development phase. A principle illustration of the approximate location of the papers appended to this dissertation in relation to proposed development procedure can be found in Figure 1.3.

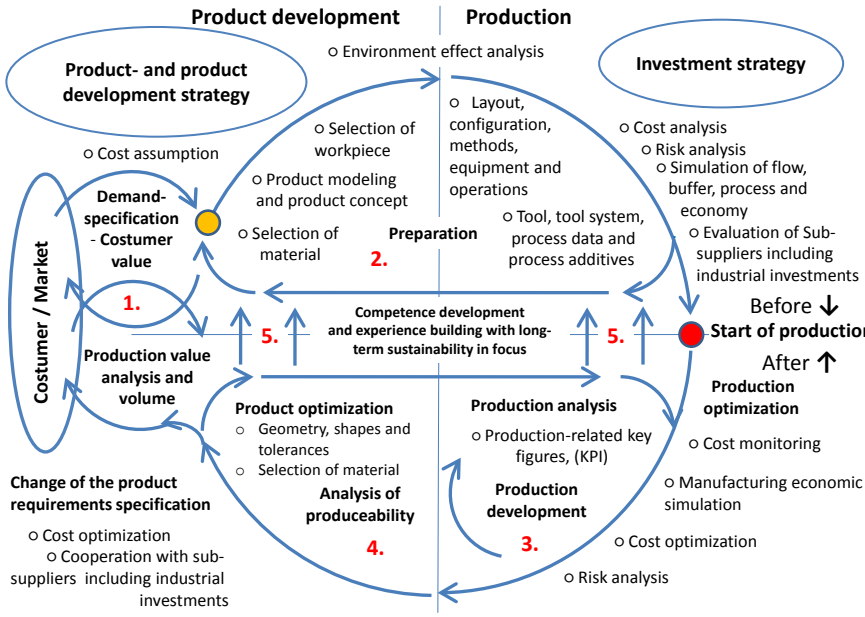

Figure 1.2 Graphic illustration of the continual interaction between product development and production [8, 9].

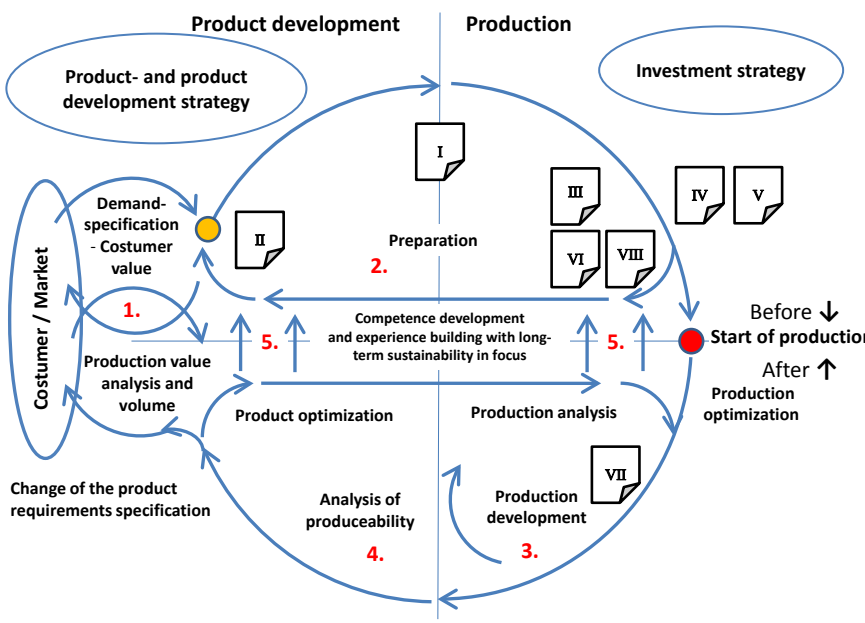

Figure 1.3 Approximate location of the appended publications in the production development process, adapted and modified from [8].

2 Research Methodology

Research on machining processes has been conducted for more than a century. For instance Taylor published his by now well-known equation during 1906 [10]. This publication is also of interest from a research methodology perspective as in the same publication Taylor also introduces what he considered as being the proper way of researching machining operations. According to Taylor, research on any machining operation implied careful experimental investigations through which reliable quantitative data could be obtained. Traditionally machining research relies heavily on quantitative data mainly obtained through experimental investigations. Even though experimental investigations may be a suitable choice for this research area it is still important to recognize the possibilities and limitations this implies as compared to other research methods. Thus, this section is intended to describe the author's research philosophy and the research methodology used during the research presented in this dissertation with special attention to the research methods implemented.

The research presented in this dissertation is an applied, practical research as opposed to basic research during which knowledge is sought for its own sake [11]. In general it could be stated that the goal of the research has been to contribute to the current fundamental knowledge on machining processes and thus aiding in creating a better process model based on the underlying physical properties of the machining process (so called mechanistic models).

2.1 Research Philosophy and Approach

Traditionally there exist two major research traditions, positivist and interpretivist. The positivist research tradition is based on the notion that knowledge may only obtained through observations and experience (empiricism). Thus, positivist research is mainly associated with quantitative research methods. As a comparison, interpretivist research is commonly associated with qualitative research methods [12]. In the current work predominantly a positivist research approach has been adopted.

Bell [13] states that experimental research can only be used in order to investigate cause and effect. This given that the investigated properties are measurable as well as possible to control by the researcher. This implies that certain qualitative studies may also be needed in order to fully analyze and understand a machining process as well as understanding the implication for other parts of the production process or even the community as a whole. A majority of all the results presented in this dissertation are quantitative and in general obtained through one or more experimental investigations. However, since not all parts of a machining process may be analyzed through quantitative data some additional qualitative data have also been collected and analyzed. For instance the difficulty of removing a chip with an adequate size from the machining process is hard to measure in quantitative terms and thus has to be evaluated qualitatively. The implications of combining quantitative and qualitative methods during a single study have been debated by several different authors during the last decade. As stated by Sale et al. [14], since the two methods are incommensurate any combination of the two could not be used for triangulation purposes. However, they could instead be used as complement to each other.

2.2 Research Methods

Although the methodology varied somewhat between the different studies conducted as a part of this research, in general it could be stated that the following approach was taken. First of all a research problem was identified. This was commonly done through literature reviews as well as informal discussions with persons with different kinds of knowledge about the process. When a research problem had been identified the first part of the solution was to conduct a more thorough literature review. This was done both to gain a better understanding of the current knowledge within the specific field as well as to investigate if any hypothesis related to the investigated problem previously had been presented by other authors. This knowledge could then be used as a foundation for further research.

During the research presented in this dissertation, experimental investigations where commonly performed in a laboratory environment or in some cases at related companies. The reason for choosing this research method was primarily the general aim of finding the relation between different quantitative parameters influencing the machining process. In addition, it is possible to control at least some of the parameters influencing the machining process. Thus, it was found that experimental research design was suitable for the research presented in this dissertation.

Principally two different experimental research approaches could be considered, phenomenological and predictive, depending on the order of the performed research activities [15]. The first of these, the phenomenological research approach, implies the creation of a theoretical model of the investigated phenomenon as based on analytical knowledge. Depending on circumstances these models could range from relatively simple models of only one equation to more complex models relaying on a large range of different equations and assumptions of the inner mechanics of a machining process. After the creation of a hypothetical model it is then attempted to validate the model for the specific problem investigated. This is primarily done through analyzing quantitative data obtained through experimental investigations. A schematic illustration of the phenomenological research approach can be found in Figure 2.1. The validation process is further described in section 2.3.

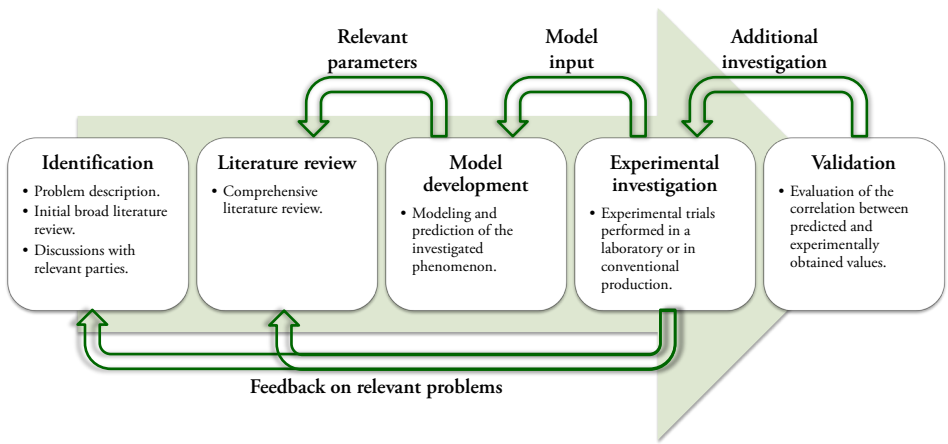

Figure 2.1 Schematic illustration of the implemented research methodology.

Even though there exists a significant knowledge on how different parameters influence each other during a machining process much is still unknown. This in combination with the large amount of different parameters possibly influencing each other implies that it is often unsuitable to divide the machining process into smaller parts during an experimental investigation. This might imply a certain degree of error of the obtained results due to disturbances from irrelevant parameters but at the same time the potential influence of any unknown parameter on the investigated phenomenon is not neglected. In cases where the influence of different process is unknown at the initiation of research, the predictive research approach is a suitable alternative. The predictive research approach starts with the acquisition of experimental data after the two initial steps of "identification" and "literature review" as illustrated in Figure 2.1. The next step of the predictive research approach is then

to create a model which to the fullest extent possible correlates with the obtained, experimental data. The accuracy of the model is commonly described through how well the model is able to predict the experimentally obtained results.

Even though slight variations occurred during the large amount of experiments conducted as a part of this research, in general it could be stated that a factorial experimental design was used as defined by Montgomery [16]. The reason for choosing this experimental design was the desire not only to observe the influence of a single factor but to also study any potential interaction between factors influencing the observed response variables. Repeated measurements of the observed variables were usually performed as well as replication of the performed experiments in selected cases. Also, in one of the studies laboratory experimental investigations were complemented through conducting field experiments at a selected company. The field experiments were primarily performed in order to increase the external validity of the obtained results.

As several different empirical studies have been performed as a part of this research it was decided to introduce the details of each of these at appropriate sections of the dissertation as well as in the appended papers. However, a short description of the methodology used as a part of each appended paper can be found in the following subsections.

2.2.1 Paper I

This paper presents research on the machinability of three different duplex stainless steels. During the study presented in this paper it was chosen to focus on evaluating the machinability of SAF 2507, SAF 2205 and LDX 2101 as these constitute a significant amount of the duplex stainless steel commercially produced today. As part of this study several different experiments were carried out in a laboratory environment for each of the three materials. All experiments were performed in conventional machine tools through longitudinally turning round bars ranging from about 100 mm to 150 mm in diameter depending on material. The experiments were performed by using commercially available CNMG120412 coated cemented carbide cutting tools mounted in a DCLNL3232P12 tool holder set at a major cutting edge angle of 90°. Conventional flood cooling using a large amount of cutting fluid was applied during all experiments with the exception of the quick-stop experiments during which no cutting fluid was used for practical reasons. The experiments were performed as a series of different feeds ranging from 0.1 mm/rev to 0.5 mm/rev while several different cutting speeds were used. The cutting speeds were in the range of

100 m/min up to the cutting speed where the tool failed, in some cases as high as 300 m/min. All other cutting data remained constant for the experiments performed while evaluating the obtained cutting forces and tool deterioration. Some experiments were also performed in order to model the tool life for each of these workpiece materials during which all three factors constituting the cutting data (depth of cut, feed and cutting speed) were varied. Additional tests were performed through using so called quick-stop equipment. With the help of this equipment it was possible to stop the turning process fast enough to obtain a workpiece with the chip still attached without significantly altering the conditions close to the cutting edge. Thus a "frozen" machining process could be obtained, suitable for further investigation. Some authentic industrial machining cases were also studied in order to evaluate the current situation while machining these materials as well as evaluating the tool wear obtained during commercial production.

2.2.2 Paper II

This paper presents the general use of polar diagrams for describing the potential machinability during machining operations. This research is analytical in nature and based on previous publications by other authors. As such no new experiments were performed.

2.2.3 Paper III

The research presented in this paper examines the influence of different process parameters on the size of the minimum chip thickness during longitudinal turning. The minimum chip thickness of three different kinds of duplex stainless steel (SAF 2507, SAF 2205 and LDX 2101), Ti6Al4V and Alloy 718 was experimentally evaluated. All of the machined workpieces were supplied as round bars having a diameter ranging from about 100 mm to 150 mm depending on material. Each different material was machined by using commercially available coated cemented carbide CNMG1204XX cutting tools mounted in a DCLNR2525M12 tool holder. The major cutting edge angle remained constant at κ = 95° during all these experiments. In addition to workpiece material, feed, nose radius and tool edge radius was also varied in order to evaluate the influence of each of these properties, individually or in combination, on the size of h_{2min}. The h_{2min} value was obtained through evaluating the difference between the obtained widths of the chips as compared to the theoretically expected values according to a model presented in the paper. Some of the chips obtained during these experiments were mounted in epoxy

and polished, allowing for examination of the chip cross-section by using a light optical microscope. A second method used for measuring the chips was by using a digital micrometer. For each of the measuring points presented in this paper 100 random measurements were performed while using a micrometer in order to attain a sufficient statistical foundation. Some additional orthogonal turning experiments were also performed in order to evaluate the size and influence of any potential chip widening during the circumstances investigated.

2.2.4 Paper IV

The research published in this paper was aimed at evaluating the influence of the tool surface micro topography on the tribological characteristics during metal cutting operations. During the experiments conducted as part of this research commercially available cemented carbide inserts (TPUN160308) were used as substrates. These substrates were first coated with a 5 µm thick Ti(C,N) layer deposited at 860°C through using chemical vapor deposition (CVD). These inserts were then also coated with a 3 µm thick α-Al_20_3 layer deposited at 1020°C through also using CVD. The inserts were then polished in order to obtain three different surface micro topographies in addition to the as-deposited. Some experimental inserts also had a synthetic flank wear of 200 µm. In addition to conventional pin-on-disc experiments, orthogonal turning experiments were performed at different feeds ranging from 0.025 mm/rev to 0.3 mm/rev. The depth of cut and cutting speed remained constant at a_p = 3 mm and v_c = 240 m/min for all machining cases investigated. During all of these machining experiments the cutting forces and the subsurface micro hardness were measured. The micro hardness was measured by using a Vickers indenter at 5 g for which the loading and unloading were performed for 30 s, respectively, with a holding time of 15 s. The obtained coating surface micro topography, tendency toward built-up layer formation as well as prevailing wear mechanics was identified, measured and evaluated through using optical profilometry, FEG-SEM and EDX analysis.

2.2.5 Paper V

This paper is a continuation of the research presented in the previous paper, Paper IV, based on the same experimental results although evaluated from a different perspective. As such, no additional experiments were performed as a part of this research.

2.2.6 Paper VI

The research presented in this paper evaluates a new method for evaluating geometrical tool changes during machining of Ti6Al4V. A central part of this research was the application of so called Stepwise Increased Feed Test (SIFT) experiments during which the obtained cutting force was measured and evaluated. During these SIFT experiments the feed is incrementally increased during a longitudinal turning operation while all other process parameters remain constant. The data obtained from these SIFT experiments were then used in order to calculate the load functions during the machining process. These could then be used to calculate a tool deterioration factor as presented in the paper. The method presented in the paper was validated by using it to evaluate two different coated cemented carbide tool grades, both of which having the same geometry CNMG120408, while machining Ti6Al4V. During the research presented in this paper the feed f was varied in the range of 0.05 to 0.35 mm/rev with a major cutting edge angle κ = 90° during all experiments. All SIFT experiments was initiated by a warm-up phase at f = 0.10 mm/rev at the same cutting speed and depth of cut as later used for the specific experiment. The reason for using this warm-up phase was the intention of having conditions similar to those during continuous machining, e.g. temperatures and stresses, at the initiation of the measuring series. In addition to the feed, the cutting speed was also varied in the range of 60 to 130 m/min depending on tool grade. A set of FEM simulations were also performed in order to evaluate the behavior of the cutting forces at low values of the theoretical chip thickness.

2.2.7 Paper VII

This paper presents a novel approach for incrementally improving the production process. As part of the validation of the proposed method experimental trials were performed at a participating company. The preformed experiments were based on a product produced by the participating company. Through systematically varying the cutting data as based on the original values used by the company, Table 2.1, and carefully evaluating and recording the obtained tool wear and scrap rate. This information was then used in order to compare the outcome of the machining process while using each cutting data combination through for example calculating the part cost for each case investigated.

Table 2.1 Variation of the cutting data implemented during this study as a function of the original cutting data use by the company.

Machining case nr.	**0**	**1**	**2**	**3**	**4**	**5**	**6**	**7**	**8**
Variation of feed f[%]	0	-10	+10	0	0	-10	+10	-10	+10
Variation of cutting speed v_c [%]	0	0	0	-10	+10	-10	-10	+10	+10

2.2.8 Paper VIII

This paper introduces a novel approach for increasing the cutting tool utilization, in some cases resulting in a tool life twice that of a conventional machining process. Even though the fundamental principle is equivalent for both milling and turning operations, the practical differences between the two processes resulted in the need for slightly different approaches for achieving the sought after increase in tool life. As a result two different sets of experiments were necessary for evaluating the implementation on each of the two machining processes, turning and milling, respectively.

The milling experiment was performed by face milling SAF 2304 duplex stainless steel while initially using a right-rotating R220.53-0100-09-7 milling head with SEEX09T3AFTN commercially available coated cemented carbide inserts. When the tool wear approached the flank wear criterion VB = 300 µm on the major cutting edge, the inserts were shifted into the left-rotating L220.53-0100-09-7A milling head and the process was repeated. In both cases the cutting parameters remained constant at cutting speed v_c = 80 m/min, depth of cut a_p = 2 mm and feed per tooth f_z = 0.15 mm/tooth. These parameters were chosen to coincide with the appropriate range of cutting data for semi-finishing operations of SAF 2304 in industrial applications.

The turning experiments were performed by longitudinal turning a bar of AISI 4340 alloy steel. Initially the experiments were conducted by turning the workpiece with a feed direction towards the chuck of the lathe. Then, after the cutting tool had sustained sufficient wear, the feed direction was reversed. The inserts used during these experiments were commercially available CNMG120412 coated cemented carbide inserts placed in a DCLNL3225P12 or DCLNR3225P12 tool holder, depending on the feed direction. In total, 5 different turning experiments were performed at varying values of the cutting data, Table 2.2.

Table 2.2 Cutting data used for the 5 turning experiments.

Experiment	v_c [m/min]	f [mm/rev]	a_p [mm]
1	200	0.25	2.5
2	260	0.25	2.5
3	170	0.30	2.5
4	270	0.30	2.5
5	220	0.40	2.5

2.3 Validity and Reliability

The two parameters validity and reliability are commonly used for describing the quality of scientific research. As such understanding and evaluation of these parameters was thought of as essential during the current research in order to obtain results contributing to the scientific knowledge within its field. The following subsections discuss how these parameters have been evaluated and improved during the current research.

2.3.1 Validity

According to Oberkampf et al. [17] validation may be defined as "the assessment of the accuracy of a computational simulation by comparison with experimental data". As most of the results obtained as a part of this research is quantitative this definition of validation closely resembles the assessments performed as a part of this research. However, a problem arose in some cases as certain amounts of qualitative data were also collected. As a method for overcoming this obstacle it was attempted to use the validity definition as proposed by Yin [18]. Although this definition originally was intended for case study research no major disadvantage was perceived while using this definition as an addition to that defined by Oberkampf et al. during this research. It should however be remembered that the main part of this dissertation relies on quantitative research and thus this addition could be perceived as only having a minor influence.

Yin [18] lists three different kinds of validity: construct validity, internal validity and external validity. In short the construct validity is defined as concerning the choice of correct operative measurements of the investigated phenomenon as well as avoiding subjective judgments during the data collection phase. The internal validity concerns the creation of causal relationships in which the researcher demonstrates how a certain

condition leads to other conditions. Finally, external validity can be considered as equivalent to generalizability and describes how well the obtained results could be generalized to other scenarios. Throughout the whole of this study it has been attempted to strengthen the construct validity through studying previous publications by other researchers. The investigation of internal validity is an integral part of this research and was commonly achieved through comparing the predicted values obtained from the proposed methods and models with those obtained from experimental investigations. Concerning the external validity the significant amount of different combinations of parameters made it impossible to investigate all possible combinations. Thus, only a few carefully chosen scenarios were experimentally investigated to at least gain an initial prediction of the validity of the proposed methods and models. As published by Oberkampf et al. [17] any experimental data can only be used for assessing the correctness or accuracy of the specific case investigated. Thus, any generalization from experimentally obtained data should be done carefully with understanding of the potential errors introduced.

Yin [18] claims that there are two types of generalizations, statistical and analytical. Out of these two statistical generalizations is perhaps the most obvious type which describes how the generalization could be improved through extending the population investigated. In comparison analytical generalization refers to generalization as a result of theoretical knowledge and evaluation and is thus not related to the population investigated. In this dissertation both of these kinds of generalizations are used. In general it was attempted to investigate a substantial population even though practical restrictions were put on the potential size of the population during several cases. In addition it was attempted to achieve generalizations through using analytical evaluations primarily through the introduction of proposed models and methods design to be applicable during different machining situations as discussed for each model.

2.3.2 Reliability

Reliability is closely connected to repeatability during scientific research. As such, it describes to which degree the same result is obtainable through repeating the performed experiments. During the experimental research presented in this dissertation it is in most cases difficult to evaluate the reliability of the obtained results due to the large amount of unknown variables. However, in several cases the same experiments were repeated in order to investigate the variation of obtained results. In cases where the resultant behavior was anomalous an extra repetition of the experiment was performed as a general rule. Further, each set of experiments have

been carefully described in order to aid potential future researchers in repeating the experiments. In addition, all obtained results were carefully catalogued and stored for future reference.

3 Frame of Reference

Machinability is a widely used term in machining society. However, it is difficult to give a clear definition of machinability, especially in terms of quantities which are numerically measurable. As a result machinability research is still commonly confined to only discussing specific combinations of workpiece materials and process parameters impeding the comparison of different machining situations. Through better understanding both the influence of the workpiece material properties as well as the machining process itself this barrier could be lowered even though not completely overcome. Through conducting machinability research in a structured and consistent manner the obtained results from each machining case may be compared and thus be much more useful for a general practitioner. As an introduction to the field, the following section is intended to describe the fundamentals of any machining process with particular focus on the factors influencing the machinability during a general machining process.

3.1 Metal Cutting

Metal cutting as a manufacturing method has a long history starting at roughly 2000 BC at which hand held tools were used generally relying on the muscle strength of the user. Later on, at around AD 1500 muscle power was in many cases replaced by an external power source for example in the shape of a water wheel. At around the 1750s the use of machines and engines as a central source of power was introduced allowing for production to be carried out without the need of access to wind or water power. For instance a steam engine could be used to drive a whole array of different machine tools through the use of intricate drive belt systems. From approximately 1900 and onwards each machine tool has received its own individual power source in the form of an electric motor allowing the machine to be placed anywhere needed at the moment. Then, during the 1950s program controlled machine tools were developed replacing mechanical control with computer-controlled systems. This was then follow during the 1970s by the integration of the product development phase into the production process through the introduction of so called computer aided

manufacturing CAM [19]. Today, machining operations can still be considered as being a fundamental part of modern production. Recently it has been estimated that over US$100 billion are spent annually on metal cutting finishing operations worldwide [20].

A machining process can be defined as processes were a cutting tool plastically deforms the workpiece material in order to remove a certain amount of material from the workpiece referred to as a chip. Today, a wide range of metal cutting processes are used during conventional production, the most commonly encountered including turning, milling, drilling, boring, shaping, broaching and reaming processes. Although each of these processes may appear different from each other they still exhibit certain inherent similarities making it possible to transfer fundamental knowledge of one process to another, although sometimes with minor alterations. This should however be done with great care and knowledge of each individual process as to not distort the obtained results.

All machining operations rely on an individually active cutting edge for locally shearing the workpiece in such a way as to remove a chip. Depending on machining operation the process configuration varies somewhat but in general the term cutting data is defined as consisting of depth of cut a_p, feed f and cutting speed v_c. In addition to these several different distances and angles are needed to fully define any machining process. These differ somewhat depending on machining operation but for turning operations, which has been frequently used for the experiments presented in this dissertation, the following dimensions and angles are commonly encountered, Figure 3.1.

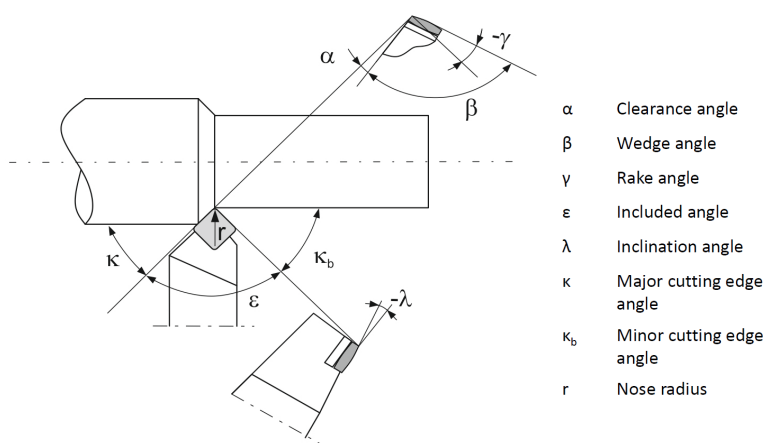

Figure 3.1 Commonly used dimensions and angles for describing the tool geometry in relation to the workpiece during conventional turning operations, adapted from Vieregge [21] as later published by Ståhl [5].

3.2 Machinability

"The machinability of an alloy is similar to the palatability of wine –
easily appreciated but not readily measured in quantitative terms"

This quote from Trent and Wright [22] partly exemplifies the problem of defining machinability. Even though machinability is a complex concept with a far from unequivocal meaning it is used in innumerable books, papers and discussions both in academia and industry. Several different authors have used slightly varying definitions of machinability. As an initial step, Ståhl [5] has published a holistic and somewhat diffuse definition of machinability. According to Ståhl machinability may be defined as:

"The behavior of the workpiece material during the cutting process and
the effect this has on the process results obtained."

Thus, the term machinability may be interpreted as involving the quality of the machined part and the obtained tool deterioration. In addition the concept includes how readily a particular combination of workpiece and machining process may be used for producing a specific part of adequate quality. Shaw [23] lists three main aspects that he claims should be included in the machinability concept: 1) Tool life, 2) Surface finish and 3) Power required to cut. A similar list of attributes have also been published by Kalpakjian and Schmid [24] who extends the list with an additional attribute 4) Chip control. The need to include chip control into machinability evaluations is further emphasized by Jawahir [25]. Trent and Wright [22] presents a slightly different set of properties when they define machinability as a function of: 1) Tool life, 2) Limiting rate of metal removal, 3) Cutting forces, 4) Surface finish and 5) Chip shape. Ståhl [5] has published a list of factors influencing the machinability which could be seen as a combination of the research presented by the previous authors with slight improvements mainly through the introduction of environmental factors. As a result these factors were considered as a suitable definition of the factors influencing machinability during the present research and will be considered while discussing machinability for the remainder of this dissertation.

1. Surface integrity
2. Chip geometry and properties
3. Energy consumption and cutting forces
4. Tool deterioration
5. Environmental factors

Traditionally machinability assessments have been based on one or more quantitative criteria such as tool life, material removal rate etc. Figure 3.2 [25]. Due to the inherent differences between different machining processes and situations it is difficult to attain a quantitative value of the machinability when comparing different machining situations [26]. Trent and Wright [22] emphasizes that even though knowledge of such machinability criteria may be practically useful they cannot be regarded as an evaluation of the machinability valid for the whole range of operations encountered industrially. As a result of the complexity of evaluating the machinability as a quantitative value no single definition has thus far been universally accepted even though several have been proposed [27-30].

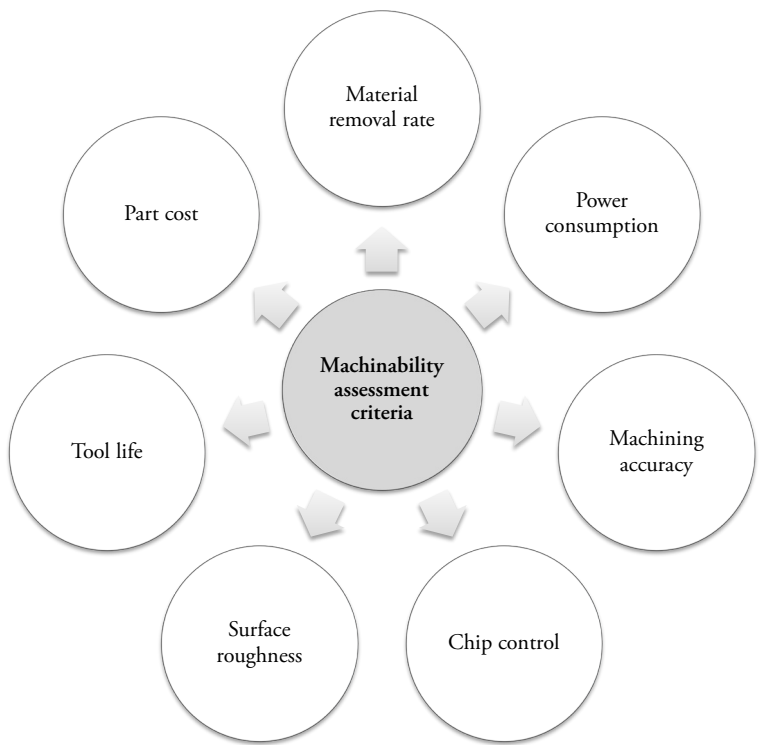

Figure 3.2 Traditionally used machinability assessment criteria, adapted from Jawahir [25].

A significant amount of research has previously been published in an attempt to better understand and predict the machinability during different machining operations. For instance Boubekri et al. [31] used a mathematical model for predicting the forces acting on the cutting tool during machining. They then used this information while evaluating the machinability of an assortment of different workpiece materials. Venkata Rao and Ghandi [28] distinguishes between two different types of models for evaluating the machinability of a workpiece material.

Their result prove that simultaneous consideration of different machinability criteria as well as material attributes could be used for evaluating the choice of appropriate cutting tools for a specific machining operation. Similarly, Chien and Chou [32] published a model for predicting the machinability of stainless steel as based on artificial neural networks which they considered as appropriate for determining optimum values of the cutting data. Stoić et al. [33] investigated the machinability of a mould steel. As part of their research they constructed a mathematical model for determining a machinability index. A later publication by Venkata Rao [34] presents a method for evaluating the machinability of different workpiece materials based on multiple attributes. Also, significant efforts has been put into investigating how to select appropriate cutting data in order to obtain an optimal machinability as described by several different authors e.g. [35-38]. Often these publications use fuzzy logic or neural networks primarily since it is difficult to analytically evaluate the machinability. Other publications have also investigated different process output parameters such as cutting forces, tool wear and surface roughness e.g. [39-41]. All of these models do however require a known combination of workpiece material and machining process.

3.2.1 Surface integrity

The surface characteristics of a manufactured part will have a direct influence on the performance of a specific product, influencing for instance frictional and wear behavior, effectiveness of lubrication, initiation of surface cracks, etc. [42]. As a result it is vital to evaluate the obtained surface integrity after any manufacturing process to ascertain that it confines to required quality standards. Evaluation of a machined surface can be divided into two parts, surface finish and surface integrity. The term surface finish is commonly used in order to described the geometric features of a surface while surface integrity has a wider definition also pertaining to all material properties influenced by the machined surface such as fatigue life, corrosion resistance, residual stresses, etc. [23, 24]. Out of all factors included in the surface integrity the surface finish is probably the most commonly measured and evaluated from an industrial perspective. Since the invention of the stylus equipment during the early 1930s it has been possible to obtain quantitative values of the surface roughness. As a result a whole arrange of different principles for evaluating the surface roughness has been developed [23]. Among a large assortment of different standards currently in use, the arithmetic mean surface roughness R_a is one of the most commonly used in industry. Other common definitions include the maximum peak-to-valley surface roughness R_{max} as well as the slightly modified mean peak-to-valley surface roughness

R_z. Depending on geographical region the root mean square surface roughness R_q may also be used. A summary of the main parameters influencing the surface roughness during a machining operation is schematically illustrated in Figure 3.3. Although the surface finish will be a result of the final finishing process as well as the near surface stress state (within 10 µm), the obtained surface integrity will depend on the whole series of manufacturing methods used while manufacturing a specific product [43]. Jawahir et al. [43] states that as a rule of thumb conventional machining processes will commonly produce compressive residual stresses in the machined surface. However, they also stress that this might not always be true for all machining processes partly due to the influence of preexisting stress conditions in the workpiece surface as well as the magnitude of the mechanical and thermal loads occurring during the machining process.

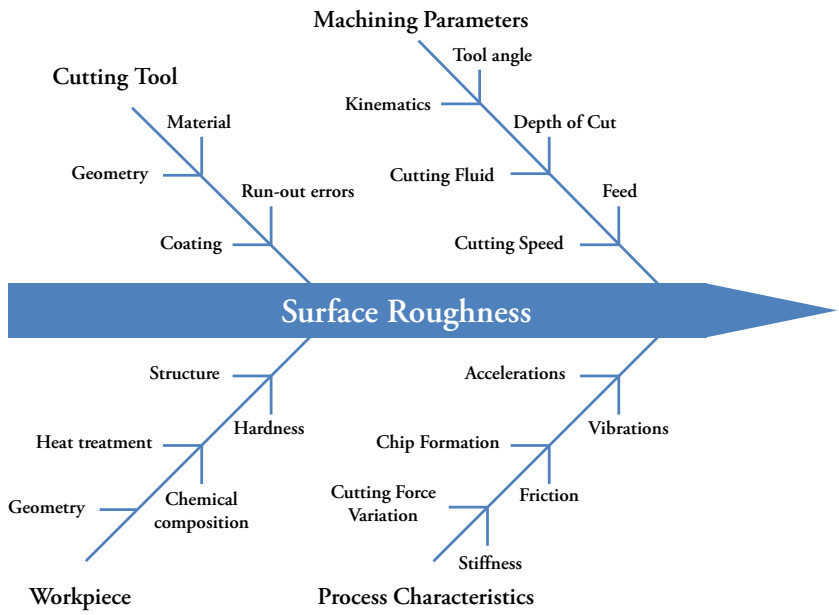

Figure 3.3 Schematic illustration of the different parametrs influencing the surface roughness during machining, adapted from Benardos [44].

3.2.2 Chip geometry and properties

Chip control during machining operations is of important practical concerns due to factors such as: 1) Personal safety, 2) Possible damage to the equipment or workpiece, 3) Handling and disposal of chips after machining and 4) Cutting forces, temperatures and tool life [23]. In general satisfactory chip breaking is sought where

the obtained chips are sufficiently short for easy removal from the cutting zone. This is however a highly ambiguous definition resulting in the need for a qualitative evaluation of the obtained chips. Thus, "good chip breaking" may vary significantly between different machining cases. Figure 3.4 illustrates an example of a classical division of chips into acceptable and non-acceptable chip forms as published by Ståhl [5].

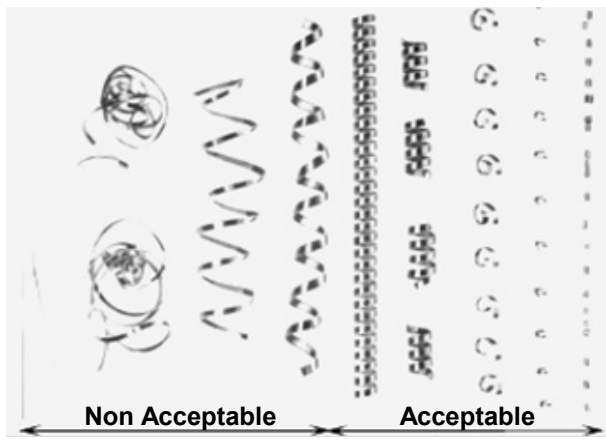

Figure 3.4 Example of a clasical division of chips into acceptable and non-acceptable chip forms [5].

In addition to chip breaking, it is also important that the chip flow direction and curvature is such that no chip hammering of either the cutting tool or machined surface occurs. Several authors have attempted to describe chips obtained from a machining process geometrically. For instance Spaans [45] has divided differing types of chips into the following categories as a function of their geometrical shape, Figure 3.5. Kluft et al. [46] claims that the chip form will primarily be influenced by three factors: upcurling, sidecurling and chip flow angle. Together with knowledge of the width, thickness and length of the chip this information could be used to define the chip form in its entirety according to Kluft et al. [46]. Jawahir and van Luttervelt [47] stress that improved methods for chip control is becoming increasingly relevant due to the major trend towards fully automated machining processes. Although a significant amount of research has been performed within this area several difficult questions still remains to be answer as listed by the authors.

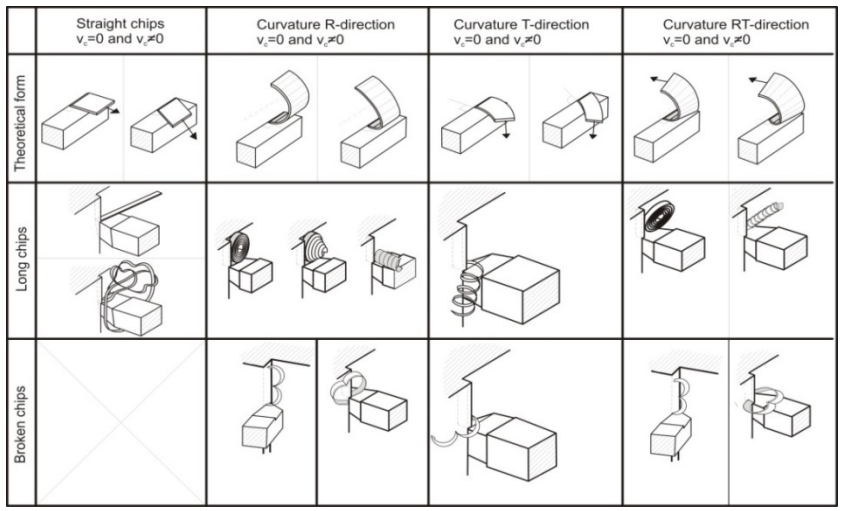

Figure 3.5 Systematic division of chips into different categories as a function of their form based on Spaans [45] as later modified and published by Ståhl [5].

3.2.3 Energy consumption and cutting forces

Conventionally the cutting force occurring during any machining operations is decomposed into three parts, the main cutting force F_c, the feed force F_f and the passive force F_p. Figure 3.6 illustrate how each of these forces are defined for a general turning application. Similar definitions apply to all other machining operations even though minor alterations may occur.

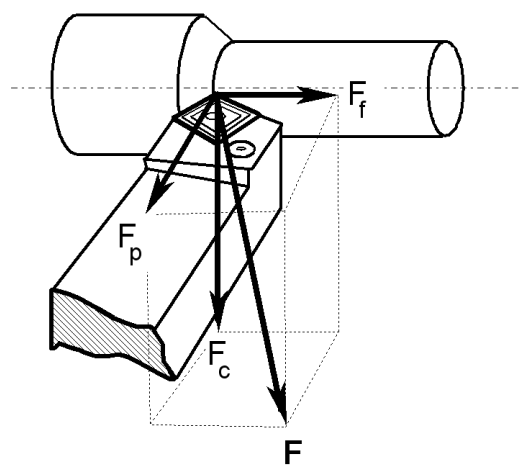

Figure 3.6 Principle cutting force components occurring during a conventional turning operation contributing to the resultant cutting force F, adapted from [48].

The three primary cutting forces may in turn be divided into several smaller parts depending on which surface and direction they are acting on. As illustrated in Figure 3.7 the cutting forces may be analyzed with respect to the surface they are acting on (clearance face indicated with "*cl*" and rake face indicated with "*r*"). They may also be divided into tangential *T*, radial *R* and axial *A* directions. Thus, six individual cutting forces can be defined, each contributing to the three previously described primary cutting force components according to Equation 3.1.

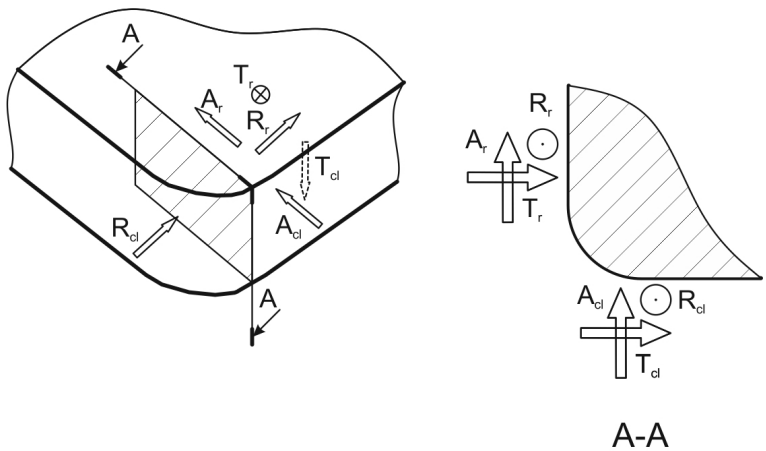

Figure 3.7 Principle division of the cutting forces with respect to the surfaces and directions they are acting on, adapted from [5].

$$\begin{aligned} F_c &= T_r + T_{cl} \\ F_f &= A_r + A_{cl} \\ F_p &= R_r + R_{cl} \end{aligned} \qquad 3.1$$

Knowledge of the main cutting force may be used to calculate the cutting resistance *Cr*. The cutting resistance is defined as the force per chip area sustained by the workpiece material during a specific machining process [5]. The power consumption during machining operations can be calculated as the product between the total cutting force acting in the tangential direction, i.e. the direction of the cutting speed vector, and the relative speed between the tool and workpiece. A universal mathematical relationship cannot be defined as different cutting operations have varying geometric characteristics which contribute to the cutting force component and various distributions of the relative velocity between the tool and workpiece materials.

Generically the cutting force acting in each of the speed directions contributes to the power consumption *P* during a cutting process, Equation 3.2. The three speed

directions v_f, v_p, and v_c are defined in the same direction as F_f, F_p and F_c respectively. For most machining cases the expression can be simplified to only calculating P_c. This since the value of both v_f and v_p are generally significantly smaller the v_c for conventional machining operations.

$$P = v_f \cdot F_f + v_p \cdot F_p + v_c \cdot F_c \approx P_c = v_c \cdot F_c \qquad 3.2$$

For a known value of the cutting resistance Cr or the specific cutting force k_c, the main cutting force may be calculated and thus also enabling calculation of the required cutting power, Equation 3.3.

$$P_c = v_c \cdot F_c = v_c \cdot h_1 \cdot b_1 \cdot Cr \qquad 3.3$$

The required motor power of the machine tool during any machining operation is always greater than the energy consumed by the cutting process. For a known efficiency of the machine tool η, the total energy required may be calculated as follows, Equation 3.4.

$$P_m = \frac{P_c}{\eta} \qquad 3.4$$

Knowledge of the cutting forces and the related power consumption during a machining process is crucial as this information is vital while dimensioning the machine tool and cutting tool as well as while determining which process parameters should be used during a specific machining operation. In addition, too large values of the cutting forces may result in a rapid deterioration of the cutting tool and should thus be avoided.

3.2.4 Tool deterioration

Understanding of the tool deterioration is an important field within the science of machining research. From an industrial perspective it is especially vital to be able to predict when to change a cutting tool during any given machining operation in order not to risk the quality of the machined part. Depending on the combination of machining process, tool material and geometry, and workpiece material many different kinds of tool wear may be observed. A problem with modeling tool life, especially for difficult to machine materials such as those investigated in this dissertation, is that several different types of tool deterioration often occurs in unison as exemplified in Figure 3.8.

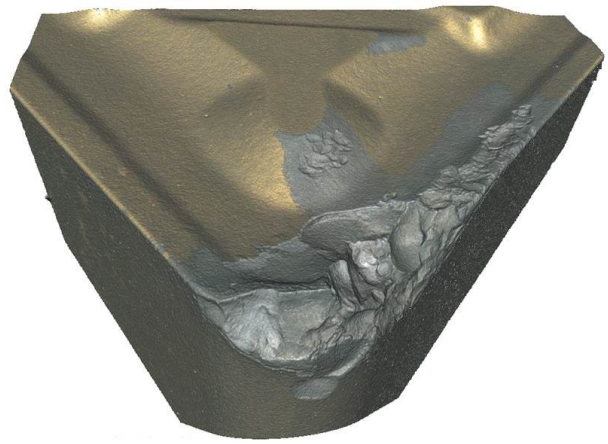

Figure 3.8 Example of tool deterioation obtained while machining duplex stainless steel SAF 2205.

Typically, the obtained tool deterioration can be classified into one or more of the following principle categories or mechanisms [23, 26]:

1. Adhesive wear
   A small amount of workpiece material may adhere to the cutting tool depending on process conditions in some cases forming so called built-up layers (BUL) or built-up edges (BUE). While the amount of adhered material gradually increases during the machining process the forces acting on the material will also increase until they reach a critical value at which the adhered material is sheared off from the cutting tool. While doing so the adhered material may also remove a small part of the cutting tool material resulting in wear of the tool.

2. Abrasive wear
   Abrasive wear of the cutting tool is a common occurrence and is primarily, although not entirely, caused by hard particles in the workpiece material. Commonly the size of the abrasive wear is evaluated through measuring either the average width of the flank wear land VB or the maximum width VB_N (often referred to as notch wear) as for instance described by ISO 3685:1993 [49].

3. Chemical wear
   Especially at high process temperatures chemical interaction between the cutting tool and the workpiece material or the surrounding air may become of increasing concern. Particularly over time chemical wear of the cutting tool may have a significant impact on the obtained tool life.

4. Fatigue
   Wear related to fatigue of the cutting tool is generally caused by a combination of high process temperatures and mechanical loads. Variations of the process temperature, the mechanical load or any combination of these may result in the initiation of cracks which over time could cause a fracture of the cutting tool.

A large array of different types of tool deterioration behaviors may be obtained based on these four primary categories as exemplified by Figure 3.9.

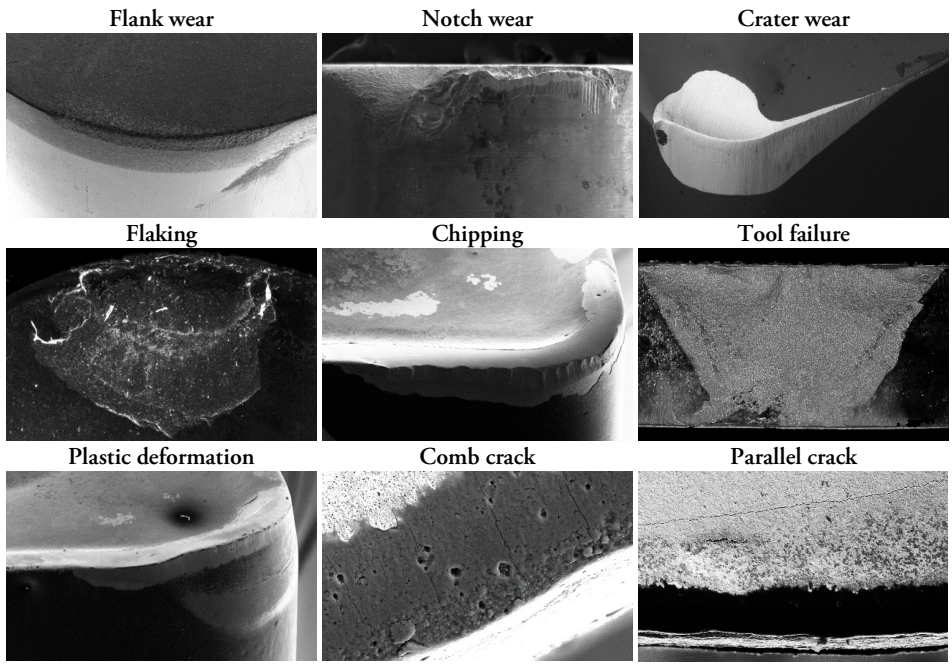

Figure 3.9 Commonly occurring types of tool wear.

A vast amount of research on tool life and ways of modeling and thus predicting this parameter have been published through the years by among others Taylor [10], Kronenberg [50] and Colding [51, 52]. During the research presented in this dissertation the tool life model as proposed by Colding was primarily used due to its widespread implementation in both industry and academia. This does however not necessarily imply that the Colding model produces the best possible results for all potential implementations.

3.2.5 Environmental factors

The United Nations has recognized sustainable development, including the important area of sustainable production, as an important challenge for our current and future society [53, 54]. As presented by Jovane et al. [55] the sustainable development domain could be divided into three separate regions which coincide to form the sustainable domain, Figure 3.10. Sustainable development is thus not only dependent upon environmental aspects but also economic and social considerations. Additionally, the same could also be said to apply to sustainable production.

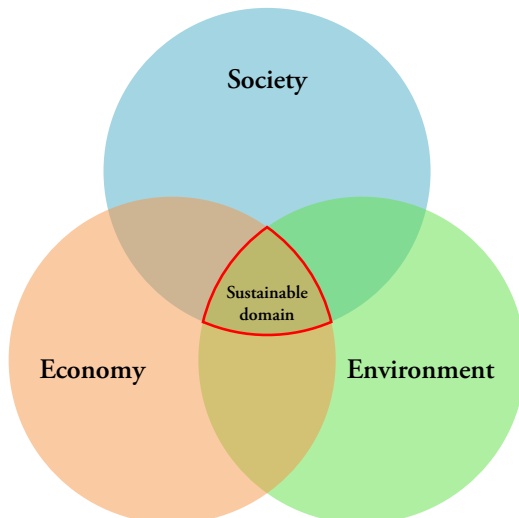

Figure 3.10 The sustainable domain, adapted from Jovane et al. [55].

Later, Ståhl [8] has published a extended version of this definition also including moral and ethics, Figure 3.11. A significant amount of research has been published on how to achieve sustainable machining. In essence the use of cutting fluid is considered as the primary obstacle while striving towards sustainable machining since discarded cutting fluid is hazardous to the environment and thus needs to be handled with great care. However, the whole machining process needs to be optimized in order to achieve a truly sustainable machining process.

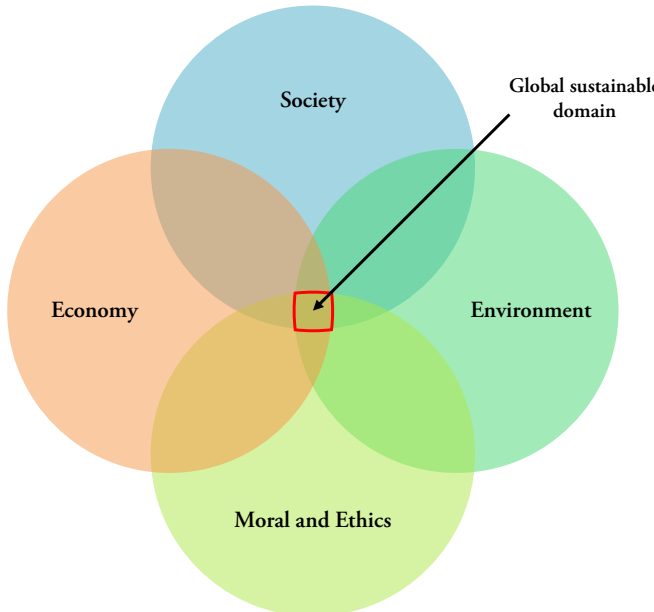

Figure 3.11 The sustainable domain as defined by Ståhl [8].

3.3 Ductile and Strain Hardening Materials

Ductility and strain hardening are two common material properties encountered when testing and describing any material. However, the research presented in this dissertation focuses on materials displaying sufficiently high values of both of these properties due to their substantial influence on the machining process. Although a large selection of different materials could be thought of as fitting into this description it was decided to primarily focus on duplex stainless steel, Ti6Al4V and Alloy 718 during this research. Although considerable differences exist between these materials they all display a comparatively high ductility and strain hardening as compared to more commonly machined materials such as carbon steels. For instance duplex stainless steel exhibits high values of both the ductility and strain hardening. In addition to these parameters Ti6Al4V exhibits an increased tendency towards chemical wear and thermal loads in the cutting zone. Finally, Alloy 718 partially exhibits all of the negative characteristics for the two previous types of materials as well as an increased material strength. This section will briefly introduce each of these materials with particular focus on factors potentially influential for the machining process.

3.3.1 Duplex stainless steel

Duplex stainless steel was invented roughly 100 years ago. The initial intention was to create a material which could withstand the chlorine containing cooling water used by the sulphite pulp industry. However, it was not until the introduction of the argon-oxygen-decarburization process during the late 1960s and early 1970s that duplex stainless steel grades could be commercially manufactured for more general engineering applications. Due to the new possibility of manufacturing duplex stainless steel with low carbon content in combination with high chromium and nitrogen contents a favorable balance between ferrite and austenite was obtainable. This was the starting point for using duplex stainless steel as an engineering material suitable for a wide range of applications [6].

As the name indicates, duplex stainless steel is a two phase material containing approximately equal amount of austenitic and ferritic phase. Often duplex stainless steels are divided into three different categories: "Lean duplex" having a comparatively low alloying content, "Conventional duplex" which includes the majority of all duplex stainless steels produced today, and "Super duplex" which has a comparatively high alloying content generally used for especially demanding applications. During this study three different grades of duplex stainless steel have been investigated (LDX 2101, SAF 2205 and SAF 2507) which together form a substantial part of all the duplex stainless steels commercially available on today's market. These materials were selected to cover all three types of duplex stainless steel according to previously (Lean duplex – LDX 2101, Conventional duplex – SAF 2205 and Super duplex – SAF 2507). The chemical composition according to nominal standards for each of these materials can be found in Table 3.1. Examples of the material structure for each of the three investigated materials can be found in Figure 3.12.

Table 3.1 Chemical composition according to nominal standards (wt. %)

Designation	C	Si	Mn	Cr	Ni	Mo	N
LDX 2101	0.03	0.4	5.0	21.5	1.5	0.3	0.22
SAF 2205	0.03	1.0	2.0	22.5	5.5	3.2	0.18
SAF 2507	0.06	0.8	1.2	25.0	7.0	4.0	0.30

Some selected material properties according to nominal standards for these three materials are presented in Table 3.2. As stated by Weibull [7], duplex stainless steel has a yield strength more than twice that of ordinary austenitic stainless steel without significant reductions in the obtained elongation at rupture or impact strength.

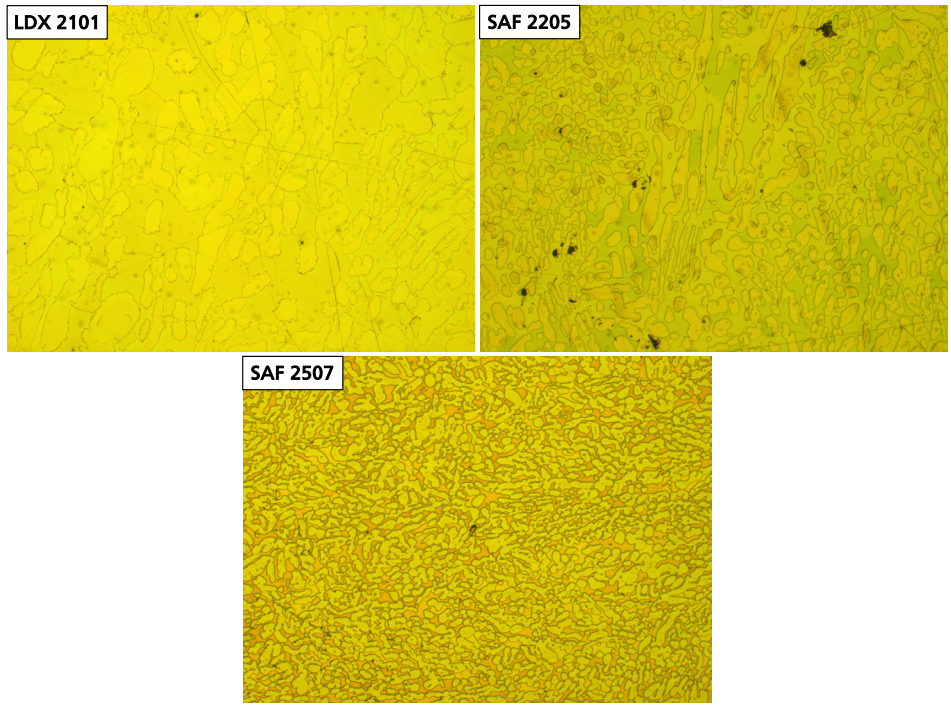

Figure 3.12 Examples of the microstructure for the three different types of duplex stainless steel investigated [56].

Table 3.2 Selected material properties according to nominal standards.

Designation	Hardness [HB]	Yield strength [N/mm^2]	Ultimate tensile strength [N/mm^2]	Elongation at rupture [%]	Thermal conductivity [W/mK]
LDX 2101	225	480	700	38	15
SAF 2205	250	510	750	25	15
SAF 2507	250	550	820	25	15

In order to evaluate the variation in hardness possibly contributing to the abrasiveness of each material 100 nano hardness indentations were performed as a grid on a randomly selected workpiece surface. The samples were first mounted and polished using commercially available equipment. Then the Berkovich hardness was measured at a load of 100 mN. Figure 3.13 illustrates the obtained hardness for each of the three materials where the right part illustrates the probability density for different hardness values and the left part illustrates the variation of the hardness over the investigated surfaces.

Duplex stainless steel is used for a number of different applications in the process industry, especially in cases where localized corrosion is a problem [57]. Typical

applications include equipment for sour gas wells, paper industry, pressure vessels, desalination plants, etc. [58]. According to previous publications, modern duplex stainless steel grades tend to have a low machinability in essence due to the same reasons as other types of stainless steel [59]. However, as expressed by Larsson and Lundqvist [60] this may not imply that duplex stainless steel has a worse machinability than other types of stainless steel if proper precautions are taken.

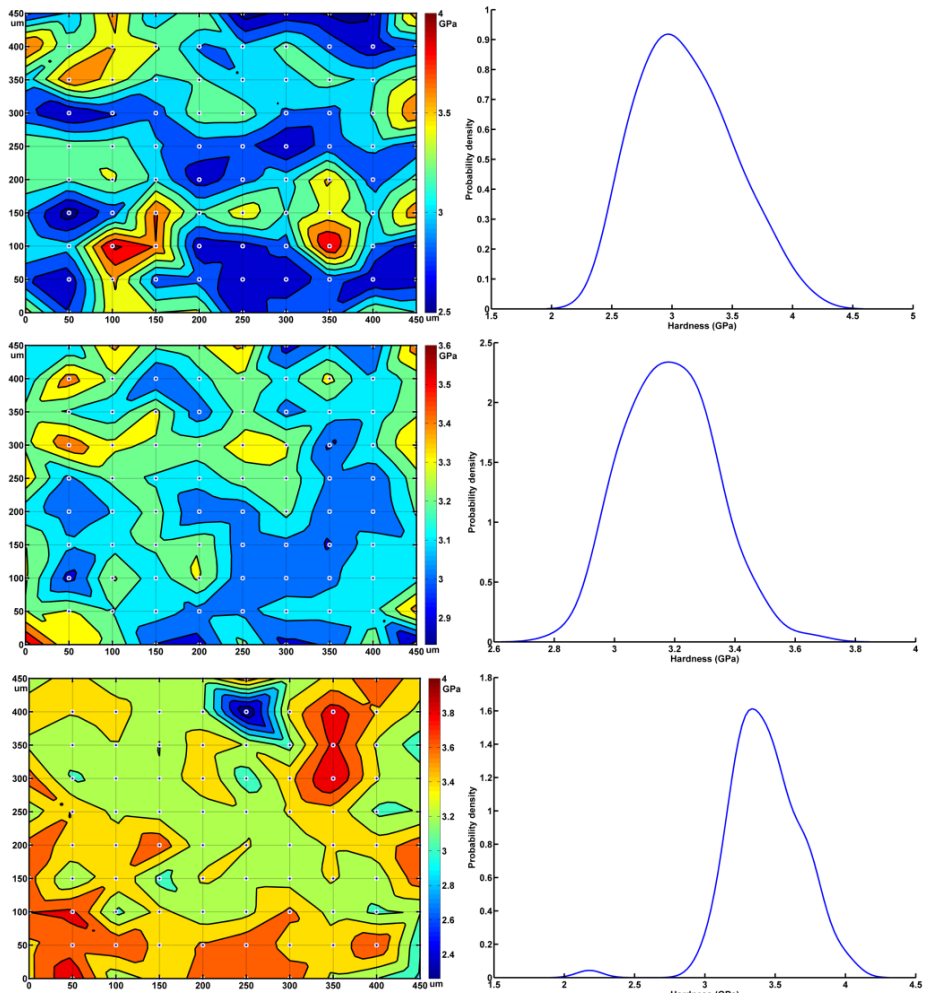

Figure 3.13 Berkovich hardness distribution for randomly selected samples of LDX 2101 (top), SAF 2205 (middle) and SAF 2507 (bottom).

3.3.2 Ti6Al4V

Even though Titanium was discovered in 1791 it was not until the second half of the twentieth century that it became widely available as engineering material [24, 61]. Titanium alloys have a high strength-to-weight ratio making them suitable for use in for example aircraft engines and airframe manufacture [62]. The high corrosion resistance also makes titanium suitable for use in for example chemical, petrochemical and offshore industry. In addition, an important application of titanium and its alloys is in the production of surgical implants [5]. Figure 3.14 illustrates an example of a typical Ti6Al4V microstructure.

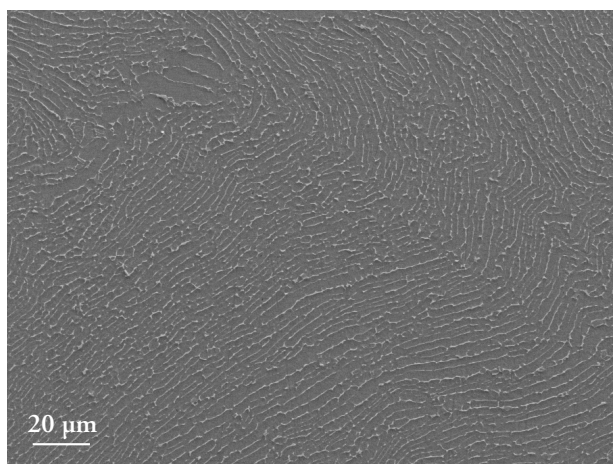

Figure 3.14 Example of the Ti6Al4V microstructure.

Titanium alloy Ti6Al4V is in common use for several different applications accounting for more than 50% of the titanium alloy production [63]. The chemical composition of Ti6Al4V according to nominal standards is presented in Table 3.3. Typical values of selected material properties are presented in Table 3.4.

Table 3.3 Chemical composition according to nominal standards (wt. %) [64].

Designation	N	C	H	Fe	O	Al	V	Ti
Ti6Al4V	max 0.05	max 0.08	max 0.012	max 0.25	max 0.13	5.5-6.5	3.5-4.5	Balance

Table 3.4 Typical values of selected material properties [64].

Designation	Hardness [HRC]	Yield strength [N/mm^2]	Ultimate tensile strength [N/mm^2]	Elongation at rupture [%]	Thermal conductivity [W/mK]
Ti6Al4V	31	870	940	15	9

Similar to the results obtained for duplex stainless steel, the Berkovich hardness was measured in a grid of 100 measuring points at a load of 100 mN, Figure 3.15.

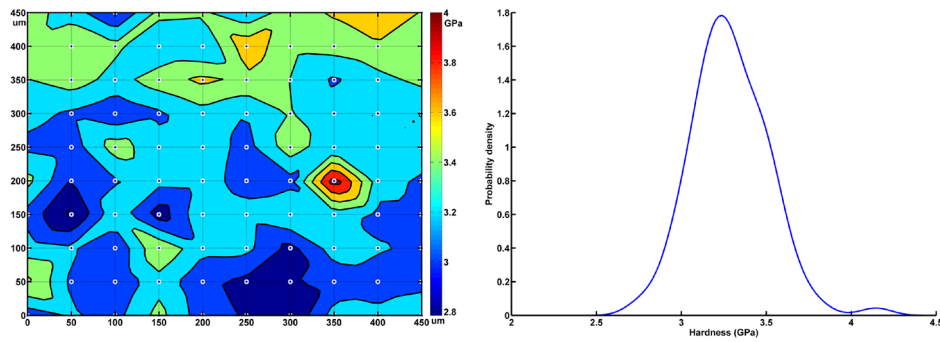

Figure 3.15 Berkovich hardness distribution for a randomly selected sample of Ti6Al4V.

The machinability of titanium and its alloys is generally considered as poor primarily due to several inherent properties of the material. Titanium is very chemically reactive and thus has a tendency to weld onto the cutting tool during machining operations. In addition, the low thermal conductivity of Titanium will result in an increased temperature during machining adversely affecting the tool life. Finally, Titanium has been reported as maintaining its high strength and low modulus of elasticity even at elevated temperatures further impairing the machinability [65].

3.3.3 Alloy 718

Alloy 718 is a heat resistant nickel-iron based superalloy developed in the late 1950's by the International Nickel Company primarily for use at intermediate temperatures. Initially Alloy 718 was used as turbine disk material in aircraft jet engines due to its relatively high resistance to creep and stress rupture as compared to other materials available during the same time period [66, 67]. An example of the typical microstructure of Alloy 718 can be found in Figure 3.16.

Today, Alloy 718 is potentially the most used superalloy on the market. One of the main reasons for the wide use of the material dates back to the cobalt crisis at the end of the 1970s. During this time the price of alloys containing cobalt increased making alloys not containing cobalt, such as Alloy 718, more attractive due to the lower price. Today Alloy 718 is used in for example jet engines, gas turbines and the nuclear industry primarily due to its high strength at elevated temperatures [68, 69]. The nominal composition of Alloy 718 can be found in Table 3.5. Typical values of some

selected material properties for wrought, solution annealed and aged Alloy 718 at room temperature can be found in Table 3.6.

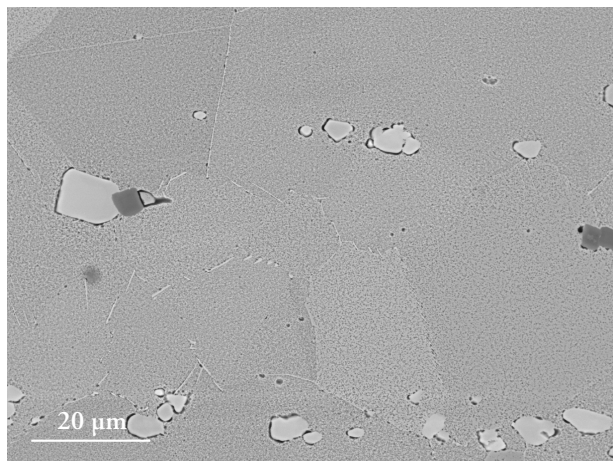

Figure 3.16 Example of the microstructure of Alloy 718.

Table 3.5 Chemical composition according to nominal standards (wt. %) [69].

Designation	Ni	Cr	Fe	C	Mo	Al	Ti	Nb	B	Mn	Si
Alloy 718	Balance	19	18.5	0.04	3.0	0.5	0.9	5.1	0.006	0.2	0.2

Table 3.6 Typical values of selected material properties for Alloy 718 [68].

Designation	Hardness [HB]	Yield strength [N/mm^2]	Ultimate tensile strength [N/mm^2]	Elongation at rupture [%]	Thermal conductivity [W/mK]
Alloy 718	422	1132	1491	20	11

In order to aid the comparison between the different materials investigated, the Berkovich hardness has been measured in a grid of 100 measurements at a load of 100 mN as previously reported for the four other workpiece materials investigated, Figure 3.17.

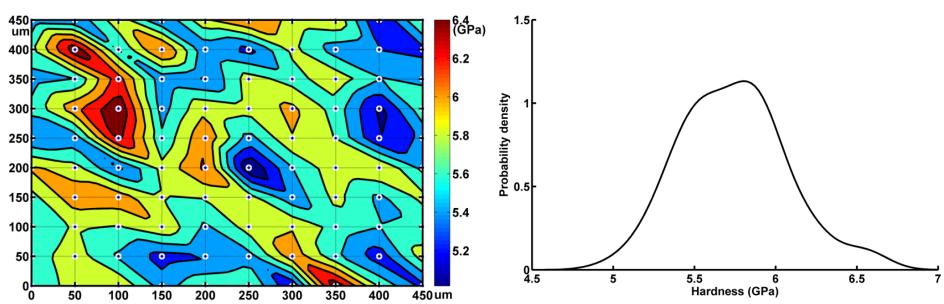

Figure 3.17 Berkovich hardness distribution for a randomly selected sample of Alloy 718.

Previous studies have reported that Alloy 718 is difficult to machine primarily due to two basic issues: short tool life and inadequate surface integrity of the machined surface. Several different traits of Alloy 718 have been reported as being responsible for this low machinability, primarily including [70]:

- A major part of the strength is maintained even at elevated temperatures.
- A high strain rate sensitivity and work hardening rate.
- Inclusions of highly abrasive carbide particles.
- Poor thermal conductivity.
- Adhesion of the workpiece material onto the cutting tool.

4 Machinability Investigations

If the machinability is investigated in a clear and consecutive manner the comparisons of the machinability for different machining cases become simpler. This will improve the usefulness of the obtained results both from an academic perspective as well as for the general practitioner. The following section attempts to describe and evaluate the results obtained by the author as a part of his research while investigating the machinability of ductile and strain hardening materials.

4.1 Influence of the Workpiece Material

A large amount of the literature published investigates a combination of workpiece material, cutting tool and machining operation. However, due to the large array of possible combinations of these factors there exists a need to evaluate the potential machinability of a specific workpiece material before involving the other factors influencing the machinability. Thus, an attempt was made to evaluate the potential machinability of a workpiece material while only knowing the material properties as commonly described on a materials certificate. The obtained results should then be applicable for any machining operation.

4.1.1 General conception of polar diagrams

Several previously published models for evaluating the machinability are limited to only being valid for a single combination of workpiece material and machining conditions. Thus, there is a need for a new model for evaluating the potential machinability of a workpiece material independently of the machining operation. A potential method for achieving this could be to evaluate the workpiece material properties and through comparing these to those of another material having a known machinability a comparative measure of the potential machinability may be acquired. The general conception of such a model was presented and discussed in Paper II.

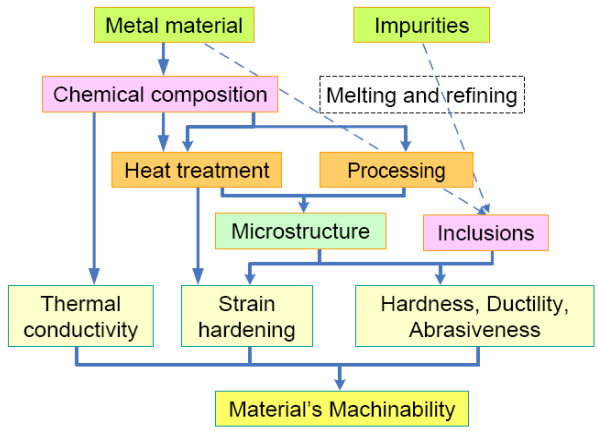

Figure 4.1 Factors influencing the workpiece material properties and thus in turn the machinability [5].

Several different material properties may be considered as influencing the machinability for a specific workpiece material. In essence, a complex relationship between mechanical properties, physical properties, microstructure, inclusion and the machinability of the workpiece could be thought to exist as principally illustrated in Figure 4.1. Five workpiece material properties have previously been recognized as influential on the potential machinability [1, 68, 69, 71-74]. These five material properties were specified as being the ductility, strain hardening, thermal conductivity, hardness and abrasiveness.

Ductility: A high ductility will in general result in a stronger adhesion between the workpiece material and cutting tool. Thus, reduced workpiece ductility will commonly decrease the adhesive wear of the cutting tool. Also, a low ductility is often beneficial for chip formation. In this context the elongation at rupture was used as a quantitative measurement of the workpiece material ductility.

Strain hardening: In general a high strain hardening will result in that a larger amount of energy is required for the formation of chips during metal cutting operations. Since an increased value of the strain hardening will result in an increase of the cutting resistance due to the increased workpiece material strength the attained cutting forces will increase. For quantitative evaluation of the strain hardening factor, D_n, the following relationship was introduced, Equation 4.1. In this equation σ_{UTS} is the ultimate tensile strength and σ_Y is the yield strength.

$$D_n = \frac{\sigma_{UTS}}{\sigma_Y} \qquad 4.1$$

Thermal conductivity: In general heat is generated due to plastic deformation of the workpiece material or friction during metal cutting operations. A high rate of heat removal is thus necessary in order to prevent a severe rise of temperature close to the cutting edge. This since high temperatures during machining operations may have detrimental effects on the product quality as well as resulting in excessive wear of the cutting tool. Thus, an increase of the workpiece material thermal conductivity will be beneficial for improving the material's machinability since it will assist in rapidly conducting heat away from the cutting zone. The thermal conductivity of the workpiece material was chosen as a direct quantitative measurement for this property.

Hardness: The hardness of a workpiece material strongly correlates to the deformation- and cutting resistance of the workpiece material. Thus, the hardness is an important factor when evaluating the machinability of a specific workpiece material primarily due to the influence on the obtained cutting forces. A low hardness is generally favorable except for the case of very ductile workpiece materials which tend to form built-up edges. Several different quantitative measurements may be used to evaluate the hardness of a workpiece material and any of these might be suitable for the intended application given that all investigated materials could be compared by using the same factor. Since the hardness of most workpiece materials could be measured by using the Brinell hardness, HB, this quantity was used during these comparisons.

Abrasiveness: Abrasive wear mechanism during machining operations is mainly related to the wear of the cutting tool. A high abrasiveness of the workpiece material tends to result in an increase of the tool wear and thus decreased machinability. In general terms abrasive wear of the cutting tool may be considered as the result of hard, abrasive particles of microscopic size embedded in the workpiece material, sliding against the cutting tool during the machining operation. High concentrations of such particles, for instance carbides or oxides, has been found to result in edge chipping and flank wear of the cutting tool [75]. It is difficult to obtain a quantitative measurement of the abrasiveness of a workpiece material especially since the commonly used pin-on-disc test requires a combination of two materials and thus is unsuitable for this application. This far no method for obtaining an appropriate measurement has been published and conclusively proven efficient even though some work on this topic has already been published. For instance Avdovic et al. [71] used the carbon content of Alloy 718 for estimating the abrasiveness. Even though this approach showed good results it is only valid for a single workpiece material and could thus not be generalized to all possible materials. A potential solution to this problem have been published by Ståhl [5]. Ståhl [5] uses a large number of micro hardness measurements in order to statistically evaluate the abrasiveness of a material

over a certain area. This approach shows great potentials for future use but since no conclusive evidence on the validity of this approach has thus far been published it is yet difficult to predict if these results could be incorporated into the polar diagrams.

All of the quantitative values used for these calculations were derived at room temperature. This simplification is mainly used due to the problem of determining the workpiece temperature during a machining operation as well as the material properties at these elevated temperatures. Even though this simplification might introduce an error into the comparison it is still beneficial from a practical standpoint due to the increased simplicity of obtaining appropriate input data. This far no conclusive indications have been observed suggesting that this simplification might have a major adverse influence on the obtained results. It is however of the outmost importance that all material properties for the investigated workpiece materials ought to be compared at equivalent conditions.

Knowledge of these material properties as well as those for a reference material can be used to create a polar diagram for describing the potential machinability of a workpiece material. These polar diagrams are intended to describe the potential machinability of the workpiece material in both an intuitive and direct manner. A fundamental assumption is that materials having similar polar diagrams could be machined through using similar cutting conditions. Thus, initial information on reasonable cutting conditions could be obtained without using any initial trials. In addition, with exception of the abrasiveness all of these material properties are commonly available on material data sheets supplied by the material manufacturer and thus this type of comparison could be performed without direct access to the workpiece material. A principle example of the intended procedure for implementation of the polar diagrams can be found in Figure 4.2.

A polar diagram as introduced by Andersson and Ståhl [1] is based on relative values of each of the five previously presented material properties as compared to a reference material. Depending on circumstances the choice of appropriate reference material may vary. However, for a general machining scenario AISI 4140 could be considered as a suitable reference material due to its average machinability as compared to the whole range of potential workpiece materials used during modern production. Thus, AISI 4140 has been used as reference material during this study. The choice of reference material is however not imperative since any reference material may be chosen as long as the obtained results are used in a consistent manner.

While employing the current method for evaluating the potential machinability each of the five material properties is assigned a relative value ranging from 0 to 10 where 0 indicates the highest machinability. For all material properties investigated those of

the reference material obtain the relative value 5. An example of a polar diagram can be found in Figure 4.3.

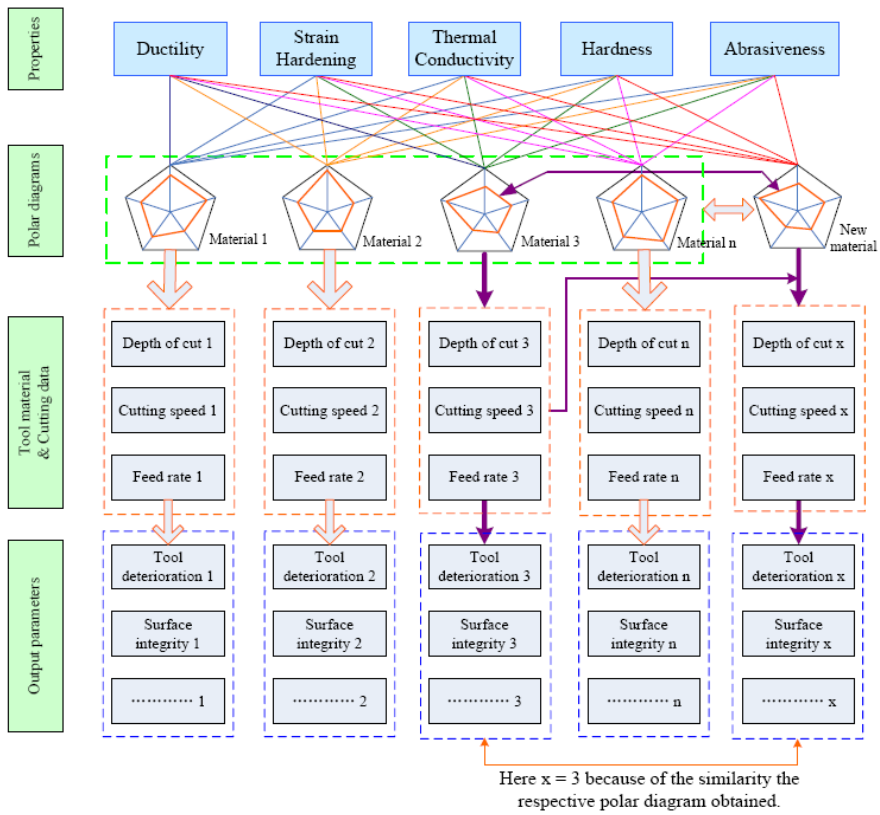

Figure 4.2 Principle system configuration while using polar diagrams illustrating different workpiece materials' potential machinability [76].

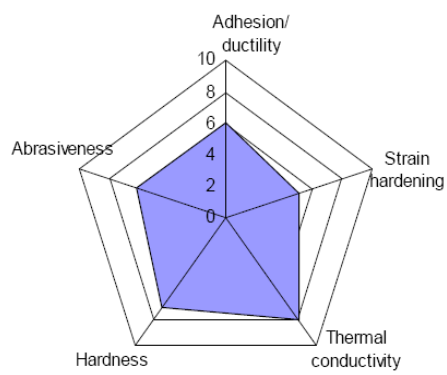

Figure 4.3 Principle illustration of a polar diagram for evaluating the potential machinability of a workpiece material [76].

The relative value for the ductility, strain hardening, hardness and abrasiveness used in the polar diagram can be calculated through using Equation 4.2. In this equation M_x is the relative value of the material property investigated, X is the measured value of the property, G_{min} and G_{max} are the minimum and maximum values corresponding to the maximum and minimum relative values and R is the value of the investigated material property for the reference material.

$$M_x = 5 + 5 \cdot \frac{X - R}{R - G_{\min}} \quad for \quad X < R$$
$$M_x = 5 + 5 \cdot \frac{X - R}{G_{\max} - R} \quad for \quad X > R \qquad 4.2$$

While calculating the relative value for the thermal conductivity a slightly different approach is needed since an increase of the thermal conductivity will result in an improved machinability as opposed to the relation for the other material properties. Thus, Equation 4.3 is introduced for these calculations. As can be noted from these two equations it is necessary to determine the extreme values G_{min} and G_{max} in advance. As long as these values are outside those of the obtained values for each material investigated no restrictions are placed on the chosen values given that they are used in a consistent manner. However, for practical reasons it could be beneficial if these values were chosen close to the extreme values of the investigated materials since this will increase the resolution of the obtained results and thus aid in future comparisons of the obtained data.

$$M_x = 5 + 5 \cdot \frac{R - X}{R - G_{\min}} \quad for \quad X < R$$
$$M_x = 5 + 5 \cdot \frac{R - X}{G_{\max} - R} \quad for \quad X > R \qquad 4.3$$

As a way of evaluating the proposed model a comparison with machinability data previously published by Chandrasekaran and Johansson [77] was performed. As no data on either thermal conductivity or abrasiveness of the materials were specified by the authors no comparison in this respect could be performed. In this comparison AISI 4140 was used as a reference material with material properties according to Table 4.1.

Table 4.1 Selected material properties for AISI 4140 [78].

Designation	Hardness [HB]	Yield strength [N/mm^2]	Ultimate tensile strength [N/mm^2]	Elongation at rupture [%]
AISI 4140	310	650	1000	12

Based on the material properties published by Chandrasekaran and Johansson [77] the following relative values could be obtained, Table 4.2. As no data was obtained on the thermal conductivity and abrasiveness of the investigated materials the relative values for both of these parameters were set to 5 in this comparison.

Table 4.2 Calculations of the relative material properties for SS 2375 and SS 2378 based on Chandrasekaran and Johansson [77].

Material property	G_{min}	G_{max}	SS 2375		SS 2378	
			Absolute value	Relative value	Absolute value	Relative value
Ductility [%]	1	60	40	9.0	35	7.0
Strain Hardening	0	40	0.9	3.7	1.3	4.5
Hardness [HB]	70	600	160	2.6	180	4.3

Through using the relative values of the material properties as found in Table 4.2, a polar diagram for each of the two materials could be obtained, Figure 4.4. Based on the results published by Chandrasekaran and Johansson [77], SS 2378 was expected to have a slightly worse machinability than SS 2378 which partially is corroborated by the result obtained during this comparison. This since SS 2378 exhibits a larger relative value of two of the investigated material properties as compared to SS 2375.

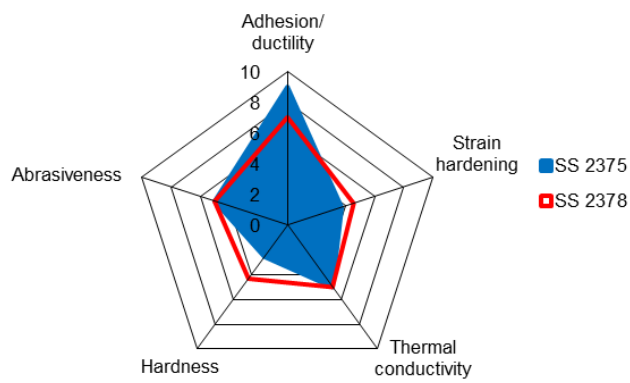

Figure 4.4 Comparision of the polar diagrams obtained for SS 2375 and SS 2378.

Through using this method the machinability of different kinds of materials may be compared. As an example polar diagrams of some selected stainless steels can be found in Figure 4.5. Note however that the value on the abrasiveness axle is only based on hypothetical values due to the previously described difficulties with quantifying abrasiveness in an appropriate and repeatable fashion.

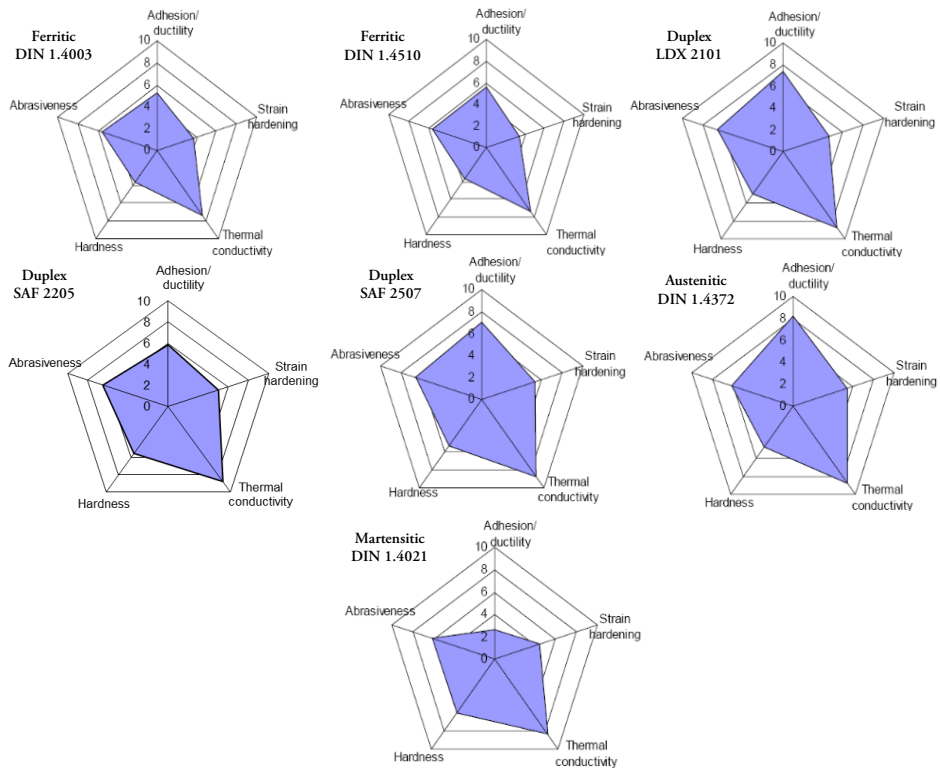

Figure 4.5 Polar diagrams for the evaluation of the potential machinability of some selected stainless steel materials, modified from [76].

4.1.2 Influence of the material on the cutting resistance

During a general machining operation the cutting resistance Cr is defined as the amount of energy needed per chip area to remove a chip for a certain combination of workpiece material and cutting tool. The cutting resistance may be calculated according to Equation 4.4 where F_c is the main cutting force, h_1 the theoretical chip thickness and b_1 is the theoretical chip width.

$$Cr = \frac{F_c}{h_1 \cdot b_1} \qquad 4.4$$

As stated in Paper VI the three cutting forces may be approximated as linearly dependent upon h_1 according to Equation 4.5 where F_c is the main cutting force, F_f the feed force and F_p the passive force, Figure 3.6. C_1, C_2, D_1, D_2, E_1 and E_2 are all model constants.

$$\begin{aligned} F_c &= C_2 + C_1 \cdot h_1 \\ F_f &= D_2 + D_1 \cdot h_1 \\ F_p &= E_2 + E_1 \cdot h_1 \end{aligned} \qquad 4.5$$

Through using Equation 4.5, Equation 4.4 may be rewritten according to Equation 4.6.

$$Cr = \frac{F_c}{h_1 \cdot b_1} = \frac{C_2 + C_1 \cdot h_1}{h_1 \cdot b_1} = \frac{C_1}{b_1} + \frac{C_2}{h_1 \cdot b_1} = \left\{ \begin{matrix} Cr_1 = \dfrac{C_1}{b_1} \\ Cr_2 = \dfrac{C_2}{b_1} \end{matrix} \right\} = Cr_1 + \frac{Cr_2}{h_1} \qquad 4.6$$

In this equation both Cr_1 and Cr_2 are constants out of which Cr_1 is primarily related to the energy consumption on the rake face of the cutting tool and Cr_2 is primarily related to the energy consumption on the clearance face of the cutting tool during a given machining operation. Due to this it is possible to assume that Cr_1 is primarily influenced by the workpiece material properties [5].

Another commonly used model for evaluating the obtained cutting forces has previously been presented by Kienzle [79]. Kienzle proposes the use of a so called specific cutting force. The specific cutting force, k_c, is defined according to Equation 4.7 where $k_{c1.1}$ is the unit specific cutting force and m_c is a model constant related to the cutting force. According to Ståhl [5] $k_{c1.1}$ is numerically approximately equal to Cr_1 with an acceptable accuracy.

$$k_c = k_{c1.1} \cdot h_1^{-m_c} \qquad 4.7$$

During any machining operation knowledge of the cutting resistance is beneficial due to the correlation between this factor and the cutting forces. However, a problem is that the cutting resistance needs to be determined experimentally. If the cutting resistance could be predicted before commencing production the waste of time and resources could be reduced. As part of the solution to this problem it was attempted to find a method for estimating the cutting resistance through only using the workpiece material properties commonly available on a material certificates. The obtained model is only intended as an aid when planning the machining of a new material and does not claim to produce accurate results during all machining scenarios.

Several different material properties could be considered as influencing the obtained cutting forces and thus the cutting resistance. Hastings et al. [80] have previously discussed the influence of the yield strength of the workpiece material on the obtained

cutting forces. One important statement in their article is that it is important to assess the material properties at conditions similar to those obtained during machining operations, e.g. elevated temperatures and high strain rates. Earlier work on this subject has also been published by Katsev [81] who mainly found that the ultimate tensile strength, hardness, elongation at rupture and impact toughness had a significant impact on the tool life which to a certain extent could be attributed to the obtained cutting forces.

As introduced in the previous section, section 4.1.1, 5 material properties have been identified as influential on the potential machinability of a workpiece material. Out of these it was theorized that primarily the hardness, yield strength, elongation at rupture and thermal conductivity of the workpiece material could be expected to influence the obtained cutting forces. In addition, these data could generally be derived from the data sheets supplied for any workpiece material. Consequently, it was attempted to only use these four material properties while modeling the Cr_1 value. The chosen material properties could be used to construct a large range of different models but after extensive testing it was found that the model according to Equation 4.8 produced the lowest coefficient of variation while comparing modeled to experimentally obtained values.

$$Cr_1 = \alpha \cdot HV^{\delta} + \beta \cdot \sigma_Y{}^{\nu} + \gamma \cdot \varepsilon_b{}^{\eta} + \xi \cdot k^{\omega} \qquad 4.8$$

In this equation the four material properties hardness HV, yield strength σ_Y, elongation at rupture ε_b and thermal conductivity k is combined with eight constants (α, β, δ, γ, η, ν, ξ and ω) in order to form a numerical model for calculating Cr_1. All constants in the equation need to be determined numerically, possibly implying the necessity for a significant amount of new experiments. However, through using previously published data sufficient information can be obtained for many machining cases. While evaluating the proposed model primarily two data sources were used as published by Ståhl [5] as well as König et al. [82]. Totally, the cutting resistances of 98 different materials were investigated.

During this research it was questioned whether all workpiece materials could be modeled as one entity or if the materials should be divided into smaller groups in order to obtain a more logical and structurally sound model. As an initial approach it was decided to model each material group according to ISO 513:2004 [83], each material group individually as well as all materials as a single entity. ISO 513:2004 defines 6 standardized material groups, Table 4.3.

Table 4.3 Standardized workpiece material groups according to ISO 513:2004.

ISO material group	Description
P	All kinds of steel and cast steels except stainless steels with austenitic structure
M	Stainless austenitic and austenitic/ferritic steel and cast steel.
K	Gray cast iron, cast iron with spheroid graphite and malleable cast iron.
N	Aluminum and other non-ferrous materials.
S	Heat-resistant special alloys based on iron, nickel, cobalt and/or titanium.
H	Hardened steel and cast iron materials.

Although the materials included in each material group may differ significantly this is still an initial approach towards dividing workpiece materials into groups as based on their properties during machining processes. It could be expected that the factors influencing the Cr_1 value for each material group are comparatively similar and thus a better model could be obtained if modeling each material group as a separate entity. For the materials used during this comparison, the Cr_1 values coefficient of variation was significantly smaller if modeling each material group as separate entity, Table 4.4, indicating potentials for a more accurate model.

Table 4.4 Obtained coefficients of variation for each ISO material group.

ISO material group	Number of materials	Mean Cr_1 value [N/mm^2]	Variation [%]
All materials	98	1510	34.6
P	56	1532	10.0
M	14	1627	14.2
K	3	916	7.9
N	11	553	19.8
S	10	2013	17.6
H	4	2621	13.8

In order to investigate the validity of this hypothesis each ISO material group was modeled individually in addition to all materials as one entity. In order to evaluate the accuracy of the modeled Cr_1 values the coefficient of variation V, as defined according to Equation 4.9, was used.

$$V = \frac{1}{n}\sum_{i=1}^{n}\left|\frac{Cr_{1,input} - Cr_{1,model}}{Cr_{1,input}}\right| \qquad 4.9$$

In Equation 4.9 n is the number of materials investigated. The index *input* indicates the previously known values and the index *model* refers to the value obtained from the model. The obtained coefficient of variation for each case investigated can be found in Table 4.5. Note that the proposed model containing 8 constants is inappropriate

for modeling the Cr_1 values of ISO material groups K and H due to the small amount of materials with a known Cr_1 value for these material groups. Thus, these material groups were excluded from this comparison.

As can be seen in Table 4.5 the model gives a coefficient of variation of more than 10% for several cases. Although this error is too big to ignore, given the large variation of the input data used, Table 4.4, the obtained modeling errors could still be seen as reasonably accurate. Further, it is of interest to note the comparatively good results while modeling all materials as one entity. Granted, the results are even better while only modeling the P materials but other than that the variation in accuracy appears negligible for all other material groups. This increased accuracy for ISO P materials could potentially be attributed to the smaller variation of Cr_1 values attained for this material group, Table 4.4. The differences between modeled and previously known values of Cr_1 are displayed in Figure 4.6 for both the case of modeling all materials as one entity as well as individually for each material group.

Table 4.5 Obtained coefficients of variation while modeling different ISO material groups.

ISO material group	V[%]	Number of materials
All materials	12.8	98
P	5.2	56
M	13.1	14
K	N.A.	3
N	12.6	11
S	16.2	10
H	N.A.	4

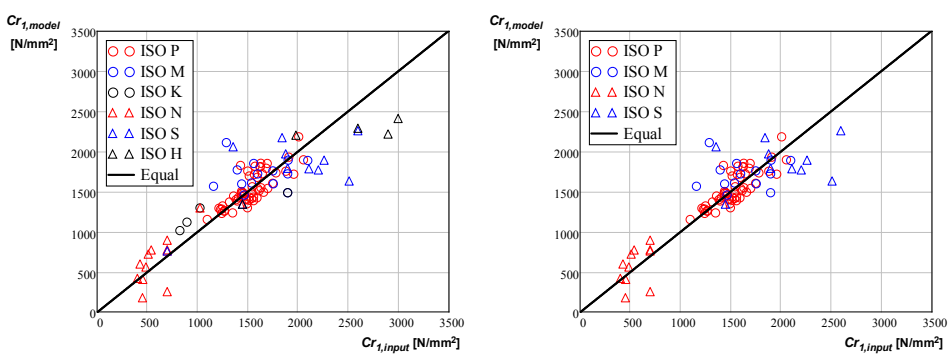

Figure 4.6 Comparison between modelled and measured Cr_1-values while modelling all materials as one entity (left) as well as each ISO material group individually (right). The solid line illustrates $Cr_{1,input} = Cr_{1,model}$.

Another way of comparing the obtained results is displayed in Figure 4.7. From these results it is possible to distinguish that the proposed model is especially well suited for

ISO P materials providing a relative small error. However, the model prediction is significantly worse for several other material groups including ISO M, ISO S and ISO H. Also, from this figure alone it is hard to distinguish any major differences between the two cases of modeling all workpiece materials as one entity as compared to each ISO material group individually.

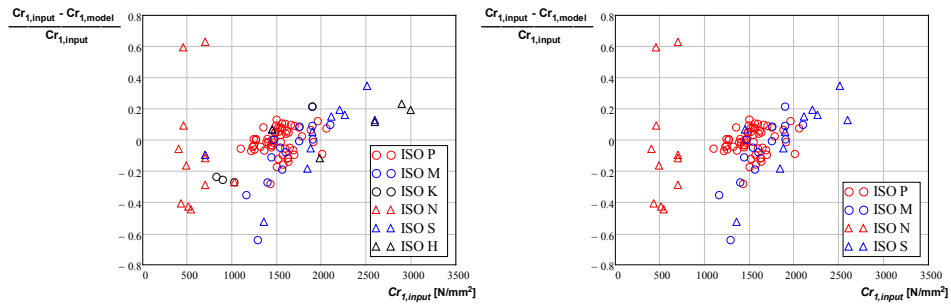

Figure 4.7 Relative comparisons between modelled and measured Cr_1-values while modelling all materials as one entity (left) as well as each ISO material group individually (right).

4.2 Analysis of the Obtained Product Quality

Surface integrity is an important aspect while evaluating the machinability during any machining operation. The surface integrity is primarily a combination of the quality of the machined surface, essentially described by the surface finish, as well as the material properties of the subsurface layer. Even though all parts of the surface integrity are essential for the quality of a machined part primarily the surface roughness has been studied this far. This due to the difficulty of measuring the properties of the subsurface layer commonly requiring destructive measurement methods. Also, the surface roughness is probably the part of the surface integrity which most commonly can be found on drawings in industry. Thus, the surface roughness is frequently the only parameter used during conventional production for evaluating if the machined surface fulfills the required quality criteria.

4.2.1 Analytical determination of R_a

The arithmetic mean surface roughness R_a is one of several different parameters commonly used for describing the deviation of a surface from an ideal level defined according to international standard (ISO 4287:1997 [84]). Several authors have published equations for calculating the R_a surface roughness during machining but

these are generally based on numerical adaptions to experimentally obtained data [85-89]. Also, in many practical cases the R_a surface roughness is estimated as a function of the R_{max} surface roughness [90]. It is however doubtful if any analytical ratio between the R_{max} and R_a surface roughness does exist. Efforts have thus been put into establishing an analytical model for calculating the R_a surface roughness as a function of the feed f and the tool nose radius r. Puhasmägi [91] has previously divided the combination of different feeds and tool nose radii into three different distinct machining cases, Figure 4.8. The proposed model is limited to surfaces created by only the nose radius of the cutting tool as previously described by several authors [91-93]. This machining case, case A, is principally illustrated in Figure 4.8.

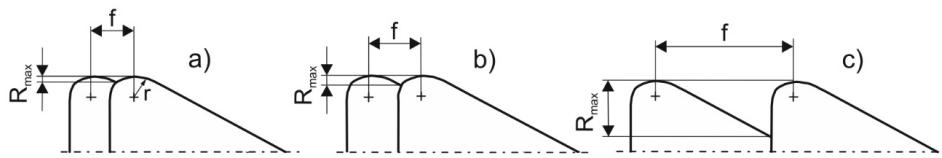

Figure 4.8 Principle illustration of three different combinations of feed and nose radius resulting in different machining cases, adapted from [91].

It can be analytically proven that machining case A impose a condition on the value of the feed f in relation to the tool nose radius r and minor cutting edge angle κ_b, Equation 4.10.

$$f \le 2 \cdot r \cdot \sin(\kappa_b) \tag{4.10}$$

The arithmetic mean surface roughness R_a is defined according to Equation 4.11 and describes the deviation of a surface from a theoretical centerline R_{mean} over a measuring length L_m according to Figure 4.9

$$R_a = \frac{1}{L_m} \cdot \int_0^{L_m} |y| \cdot dx \tag{4.11}$$

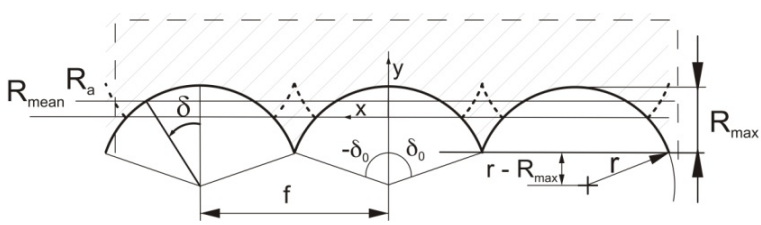

Figure 4.9 Principle illustration of a turned surface showing the feed f, tool nose radius r, maximum surface roughness R_{max}, arithmetic mean surface roughness R_a, mean surface roughness R_{mean}, angular coordinate δ and the angle $\pm\delta_0$, [94].

The angular position δ_0 as found in Figure 4.9 can be analytically calculated according to Equation 4.12.

$$\delta_0 = -\sin^{-1}\left(\frac{f}{2\cdot r}\right) \tag{4.12}$$

If the transition from major to minor cutting edge can be described as a circular arc the position along the edge line can be expressed through polar coordinates, Equation 4.13.

$$R(\delta) = r\cdot\left(1-\cos(\delta)\right) \tag{4.13}$$

As can be seen in Figure 4.9 the theoretical surface remaining on the workpiece after a longitudinal turning operation is created between the two angular positions $\pm\delta_0$. The average level of the surface in respect to the bottom line $R(\delta=0)$ can be calculated according to Equation 4.14.

$$R_{mean,\delta} = \frac{1}{2\cdot|\delta_0|}\cdot\int_{\delta_0}^{-\delta_0} r\cdot\left(1-\cos(\delta)\right)d\delta = \frac{2\cdot r\cdot\sin^{-1}\left(\frac{f}{2\cdot r}\right)-f}{2\cdot r\cdot\sin^{-1}\left(\frac{f}{2\cdot r}\right)} \tag{4.14}$$

In order to adapt this geometrical description to the definition of the R_a value the integration must be performed in the x direction, parallel to the machined surface. Thus, a change of coordinate system is required, Equation 4.15.

$$\begin{aligned} x &= r\cdot\sin\delta \Rightarrow \frac{dx}{d\delta} = r\cdot\cos\delta \\ y &= r\cdot\cos\delta \Rightarrow \frac{dy}{d\delta} = -r\cdot\sin\delta \end{aligned} \tag{4.15}$$

As a result Equation 4.14 may be rewritten according to Equation 4.16.

$$\begin{aligned} R_{mean} &= \frac{1}{2\cdot r\cdot\sin\left(|\delta_0|\right)}\cdot\int_{\delta_0}^{-\delta_0} r\cdot\left(1-\cos(\delta)\right)\cdot r\cdot\cos(\delta)\,d\delta \Rightarrow \\ R_{mean} &= r-\frac{r^2}{f}\cdot\sin^{-1}\left(\frac{f}{2\cdot r}\right)-\frac{r}{2}\cdot\sqrt{1-\frac{f^2}{4\cdot r^2}} \end{aligned} \tag{4.16}$$

Through using these equations the theoretical value of the arithmetic mean surface roughness may be calculated according to Equation 4.17. In order to avoid double compensation while changing the coordinate system $R_{mean,\delta}$ is used in this equation instead of R_{mean}.

$$R_{a,theoretical} = \frac{1}{2 \cdot r \cdot \sin\left(\left|\delta_0\right|\right)} \cdot \int_{\delta_0}^{-\delta_0} \left|R(\delta) - R_{mean,\delta}\right| \cdot r \cdot \cos(\delta) \cdot d\delta \qquad 4.17$$

The relationship found in Equation 4.17 describes the exact, analytical value of the arithmetic mean surface roughness. This equation however does not have any useful primitive function and thus needs to be solved numerically. It can however be noticed that the integral for calculating R_{mean} has a comparatively simple primitive function. Further, it has been found that the ratio between R_{mean} and R_a is approximately constants for all practically useful values of the feed and tool nose radius given that machining case A is maintained. Through using the ratio between R_{mean} and R_a an approximate equation for the R_a surface roughness can be determined, Equation 4.18.

$$R_{a,theoretical} \approx \frac{1}{1.29870} \cdot R_{mean} = 0.77 \cdot \left[r - \frac{r^2}{f} \cdot \sin^{-1}\left(\frac{f}{2 \cdot r}\right) - \frac{r}{2} \cdot \sqrt{1 - \frac{f^2}{4 \cdot r}} \right] \approx$$

$$\approx 0.77 \cdot \left(1 - \frac{\frac{f}{2 \cdot r}}{\sin^{-1}\left(\frac{f}{2 \cdot r}\right)} \right) \cdot r \qquad 4.18$$

4.2.2 Influence of the minimum chip thickness

Already during 1963 Palmer and Yeo [95] discussed the possibility of what they called a “dead metal zone” at the tip of round nosed cutting tools. In later publications this area is commonly referred to as the stagnation zone in analogy to the terminology often used in fluid mechanics. For instance Kazban et al. [96] have used a fluid mechanic approach for analyzing the machining process and in particular the stagnation zone phenomenon. Their results prove that this fluid mechanic approach could be suitable for evaluating at least parts of the machining process. Figure 4.10 illustrate an example of material flow close to the tool edge radius obtained through the use of a so called quick-stop device during orthogonal turning of AISI 1045.

Between the two flows of material forming the chip and the machined surface as exemplified in Figure 4.10, a stagnation zone could be conceived with a stagnation point located at its center. This in turn is generally acknowledged as the reason for the existence of a minimum chip thickness. The minimum chip thickness h_{1min} is defined as the lowest value of the theoretical chip thickness h_1 at which a chip is still being formed by the machining process. Figure 4.11 illustrates examples of the material

deformation close to the cutting edge for the 5 workpiece materials investigated throughout the research presented in this dissertation.

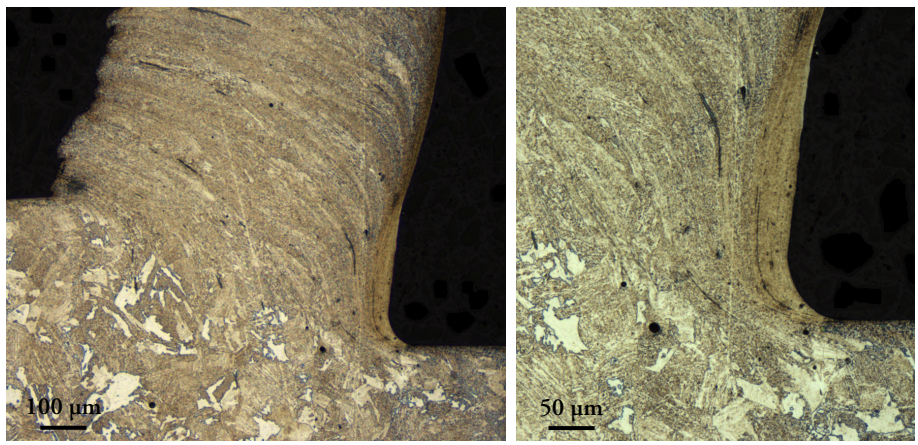

Figure 4.10 Workpiece material flow close to the tool edge radius while orthogonally turning AISI 1045.

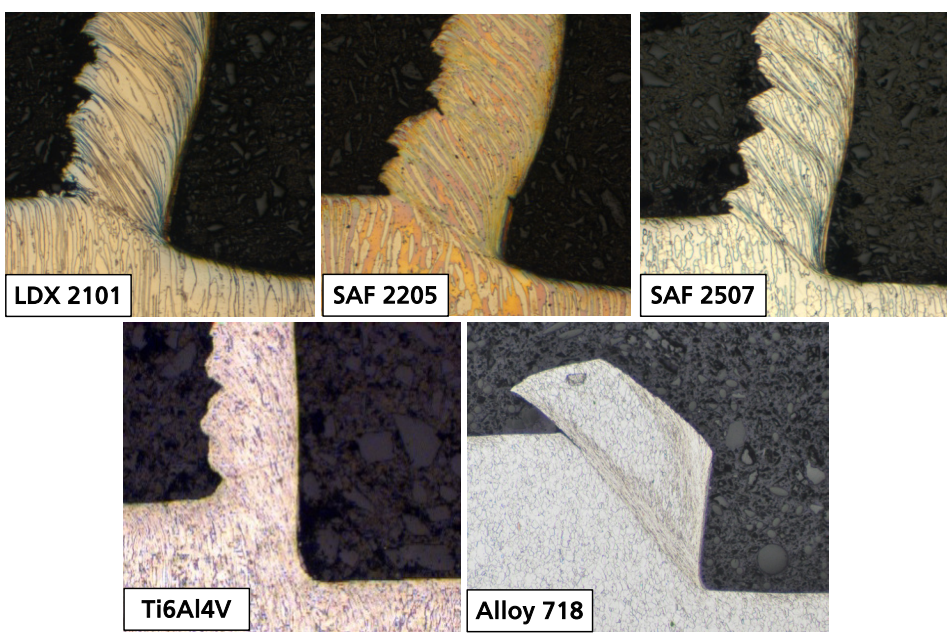

Figure 4.11 Examples of chip formation in selected materials obtained through using a so called quick-stop equipment, modified from [97].

Figure 4.12 illustrates the result from a frozen machining process as obtained by using a quick-stop device seen from the reference plane while turning SAF 2205. As can be

seen in the figure a crack is clearly visible close to the tool nose radius indicating the existence of a minimum chip thickness. It is however not advisable to measure the size of h_{1min} only based on this figure primarily due to the potential risk of tilting of the sample. The three deformation zones, Zone I, Zone II and Zone III, are recognizable in the figure. Also, a side flow may be noticed inside the chip in which the material is deformed after it has been cut.

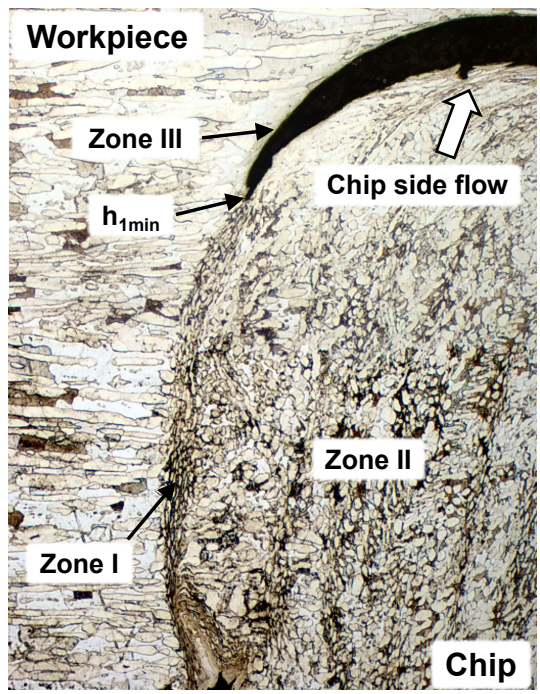

Figure 4.12 Workpiece material close to the tool nose radius as seen from the reference plane while turning SAF 2205 [98].

Several authors have published different methods for determining the size of h_{1min}. Yuan et al. [99] proposed a relationship for determining the value of h_{1min} as based on the obtained cutting forces in combination with the tool edge radius r_β and friction coefficient during the machining process. One of the important conclusions from their research was that the tool edge radius has a significant influence on the value of h_{1min}. Also, Moneim [100] published an equation for calculating the stagnation point as a function of the tool edge radius and the friction coefficient between the workpiece and cutting tool. According to Yen et al. [101] the value of the minimum chip thickness is approximately equal to that of the height of the stagnation point and thus it could be hypothesized that the same process parameters influences both variables. Further, Yen et al. [101] conclude that there exists a strong relationship

between the tool edge geometry and the value of h_{1min}. Theoretical methods for determining the size of h_{1min} has also been presented by among others Son et al. [102]. Their model does however require knowledge of the friction angle which makes it impractical to use while determining the value of h_{1min} for a large amount of different process conditions.

The theoretical chip thickness will vary as a function of the angle δ, Figure 4.13. As can be seen in the figure the minimum chip thickness h_{1min} will be located somewhere along the curve of the tool nose radius and may be described by using the δ angle. Also, note the ploughing area A_{pl} in Figure 4.13. This part of the chip area will only be plastically deformed during the machining process and to a large extent be left on the machined surface. Through assuming that all of this material is left on the machined surface the theoretical chip width b_1 could be compared to the obtained chip width b_2 obtained from experimental trials. Through using this knowledge the angle δ at the location of h_{1min}, δ_{h1min}, could hypothetically be determined. As previously published by Ståhl [5], through analyzing the theoretical geometry close to the tool nose radius according to Figure 4.13, three geometrical relationships can be distinguished, Equation 4.19.

$$r^2 = (f + x)^2 + (r - R_{\max})^2$$
$$\text{where} \quad x = (r - R_{max}) \cdot \tan(\delta) \quad \text{and} \quad \cos(\delta) = \frac{r - R_{max}}{r - h_1} \qquad 4.19$$

By combining these equations the following solution could be obtained according to Ståhl [5], Equation 4.20.

$$h_1(\delta) = f \cdot \sin\delta + r - \sqrt{f^2 \cdot \sin(\delta)^2 + r^2 - f^2} \qquad 4.20$$

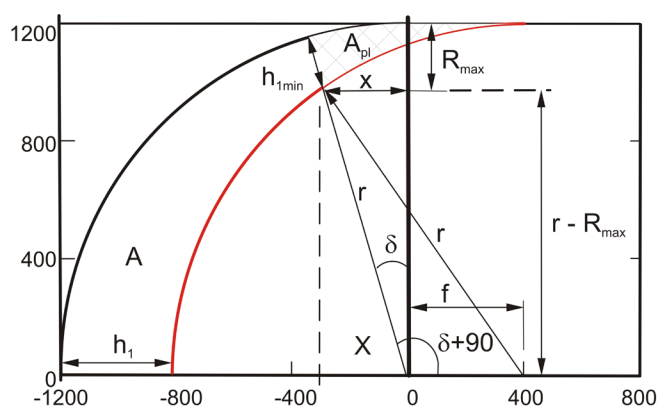

Figure 4.13 Theoretical geometry at the tool nose radius as seen from the reference plane [98].

A possible approach for analyzing the deformation of the obtained chips is through studying their cross-section as seen perpendicular to the chip flow direction, Figure 4.14. The first thing which could be noted in this figure is the difference of the obtained chip area from what theoretically would be expected. This is most obvious in the left part of the chips which is generated by the tool nose radius. The circular arc which would theoretically be expected according to earlier descriptions is hard to discern. Thus, a tension force must be acting on this part of the chip during the machining process. This force has deformed the chip plastically forming a straighter geometry. The secondary deformation zone, Zone II, where the chip has been deformed against the cutting tool as well the tertiary deformation zone, Zone III, where the machined surface on the workpiece has been deformed may also be seen in the figure. The deformation discernible in Zone III is a part of the machined surface for the previous pass. Thus, this deformation was primarily created by the previous pass of the cutting tool.

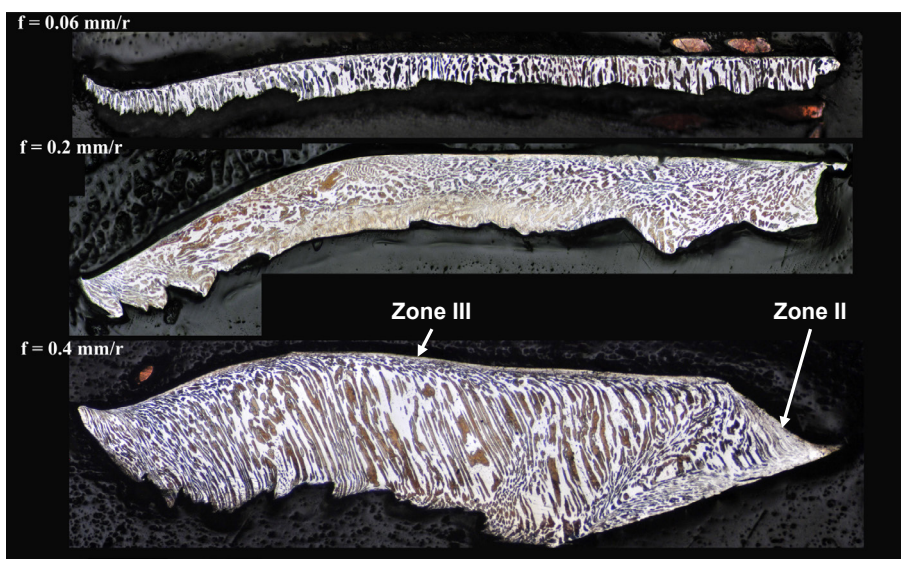

Figure 4.14 Cross-section of obtained chips as seen perpendicular to the chip flow direction while longitudinally turning SAF 2205 [98].

In order to analyze the influence of some selected process parameters on the size of h_{1min} experiments were performed through longitudinally turning a variety of different workpiece materials at varying process parameters, Paper III. The experiments were performed for three different types of duplex stainless steels (LDX 2101, SAF 2205 and SAF 2507) as well as Ti6Al4V and Alloy 718. All of the machined materials were supplied as round bars having an initial diameter ranging from about 100 mm to 150 mm depending on the material. The three duplex stainless steel grades were

machined by coated cemented carbide CNMG120412 cutting tools and Ti6Al4V and Alloy 718 were machined by coated cemented carbide CNMG120408 cutting tools. Also, during some of these experiments the tool nose radius was varied while all other process parameters remained constant. During all of these experiments the inserts were mounted in a DCLNR2525M12 tool holder giving an major cutting edge angle of $\kappa = 95°$. No cutting fluid was used during these experiments.

The obtained chips were measured by using two different measuring techniques, the first of these being optical microscopy. In order to perform these measurements the chips were mounted in transparent epoxy. The reason for using transparent epoxy was to ensure that the chips were mounted as close to perpendicular to the examined surface as possible. The mounted chips were then polished using increasingly finer diamond grit in order to obtain a smooth and even surface. Three to four chips from each set of process parameters were mounted. As a second measurement method the width of the chips were also measured by using a digital micrometer. Through this measurement method a much larger statistical database could be obtained. For all measuring points presented in the following graphs 100 random measurements were performed while using this measurement method. This amount of measurements was assumed as being sufficient for obtaining an acceptable statistical basis for calculating a mean chip width. However, this secondary measurement method has one major disadvantage. The distance measured will no longer be of the sought distance along the chip surface but rather the shortest distance between the two sides. In order to evaluate the size of the potential error this might introduce a comparison between the two different measuring techniques were performed in the case of machining SAF 2205. In this specific case a mean error of roughly 10% could be noted when using the micrometer measurements as compared to distances measured using a microscope. The obtained error is thus too big to neglect. As a result a new parameter, h_{2min}, was introduced to differentiate the results from these simplified chip measurements from those obtained while measuring the actual length along the chip surface. A disadvantage of measuring the chips in order to evaluate the size of h_{1min} or h_{2min} could be that factors such as tool deflection and vibrations will influence the chip geometry and thus also the obtained h_{1min} and h_{2min} values while using these measurement methods. Even though it was attempted to minimize the influence of these parameters during the present research their influence should not be forgotten, potentially attributing to the relatively high h_{2min} values attained during this research. Another potential source of errors is the deformation of the chip which occurs after the minimum chip thickness has been formed. For instance the plastic flow of material inside the chip could be expected to deform the chip to a certain extent after

the formation of h_{1min}. Thus, based on theoretical considerations it could generally be expected that $h_{1min} \leq h_{2min}$.

Several different process parameters could be considered as having an effect on the size of h_{1min} and h_{2min}. The first of these parameters which has been investigated was the influence of different workpiece materials. In Figure 4.15 the variation of h_{2min} for an assortment of different workpiece materials is illustrated. In this figure and all the following in this section the variable h_1 refers to the maximum constant value of the theoretical chip thickness. The graph in Figure 4.15 seems to suggest that h_{2min} is larger for Alloy 718 than for the different kinds of duplex stainless steel and Ti6Al4V and smaller for SAF 2205 than for the other types of duplex stainless steel. However, the significance of these differences could be discussed. Any further conclusions about the differences between materials are hard to make due to the large variations of the obtained values during this analysis. As only small differences were observed between the different workpiece materials it was decided to perform all of the following experiments investigating the influence of different process parameters through longitudinally turning SAF 2205. Even though the use of other workpiece materials may very well influence the obtained results the use of SAF 2205 was seen as a good indicator for the potential influence of varying process parameters on the value of h_{2min}. Further experiments are however needed to fully investigate the validity of the obtained results while using other workpiece materials.

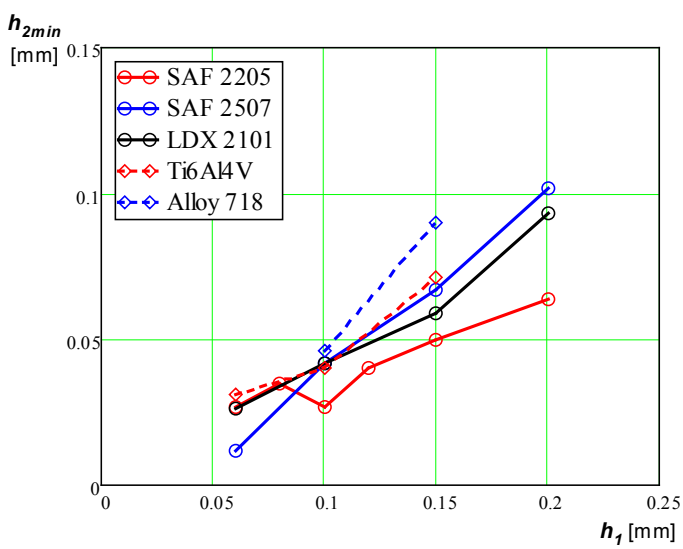

Figure 4.15 Influence of the workpiece material on the value of h_{2min} [98].

If assuming that area of the obtained chips retain their theoretical geometry during a longitudinal turning operation with $\kappa = 90°$ a geometrical comparison between the

two different measured distances could be performed. The theoretical distance along the chip surface, Equation 4.21, could thus be compared with the shortest distance between the two sides of the chip, Equation 4.22.

$$l_{real} = \left(\frac{\pi}{2} + \frac{f}{2 \cdot r} \right) \cdot r + a_p - r \qquad 4.21$$

$$l_{measured} = \left(a_p - \left(r - \sqrt{r^2 - \frac{f^2}{4}} \right)^2 + \left(f + r \right)^2 \right)^{\frac{1}{2}} \qquad 4.22$$

Through calculating the ratio between these two theoretical distances a hypothetical correction factor χ_{corr} may be established, Equation 4.23. Through multiplying the obtained chip widths measured with a micrometer with this correction factor a more accurate value of the distance along the chip surface could potentially be obtained. Thus, a more accurate value of h_{1min} could hypothetically be obtained.

$$\chi_{corr} = \frac{l_{real}}{l_{measured}} = \frac{\left(\frac{\pi}{2} + \frac{f}{2 \cdot r} \right) \cdot r + a_p - r}{\left(a_p - \left(r - \sqrt{r^2 - \frac{f^2}{4}} \right)^2 + \left(f + r \right)^2 \right)^{\frac{1}{2}}} \qquad 4.23$$

Through using this correction factor the following h_{1min} values were obtained for different workpiece materials, Figure 4.16. As can be seen in Figure 4.16 some of the obtained results seem to indicate a negative h_{1min} value which of course is impossible. These incorrect values could to a certain extent be contributed to the influence of chip widening due to plastic deformation of the chip.

Figure 4.17 illustrates the topography of three selected chips obtained during this investigation. Through observing the segmentation lines on each of the chips it could be seen that the flow of workpiece material is not equal throughout the entire chip. The difference is most pronounced close to the tool nose radius which can be found in the lower part of each figure. All three chips also have a certain area close to the location of h_{2min} where no segmentation of the chips may be discerned (see Figure 4.17, right); instead implying plastic deformation of the chip after it has been cut. Although it is difficult to estimate the width of this area from the obtained figure it could be presumed that this plastic deformation of the chip is part of the explanation as to why some machining cases found in Figure 4.16 obtain a negative h_{1min} value as previously discussed.

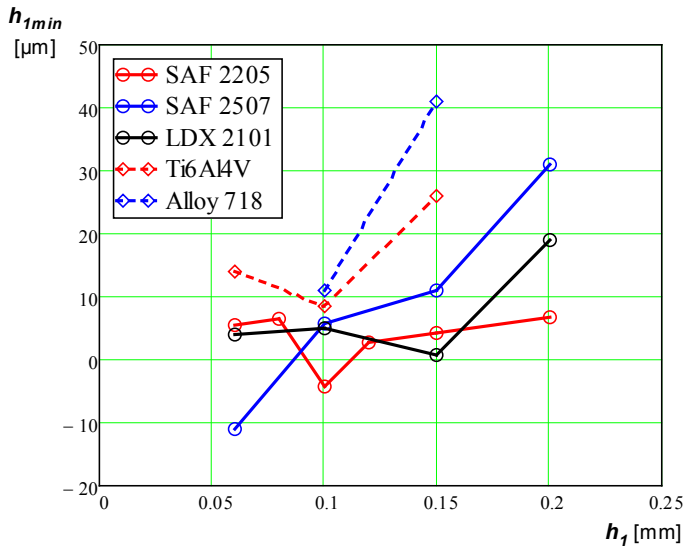

Figure 4.16 h_{1min} values obtained through multiplying the obtained h_{2min} values with the χ_{corr} correction factor.

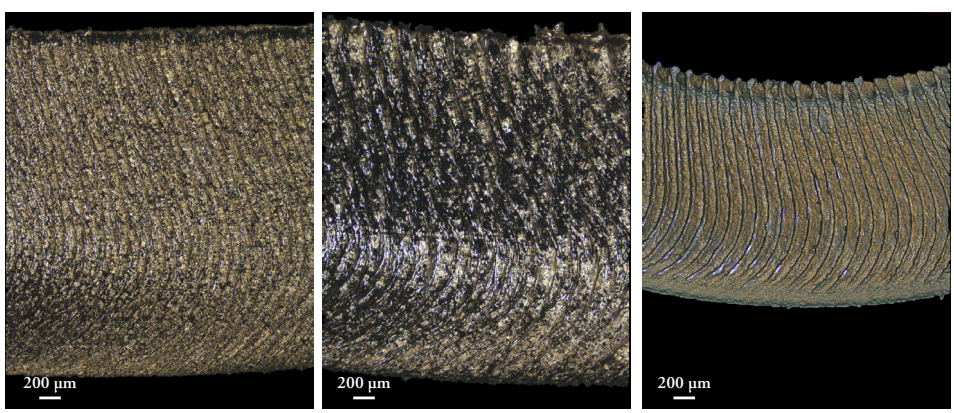

Figure 4.17 Chip topography for SAF 2507 at h_1 = 0.06 mm (left), SAF 2507 at h_1 = 0.15 mm (middle) and Alloy 718 at h_1 = 0.15 mm (right).

The first of the process parameters whose influence on h_{1min} and h_{2min} have been investigated was the tool edge radius r_β. During these experiments the tool edge radius was varied in the range of 20 µm to 100 µm for different values of the theoretical chip thickness. Possibly due to size effect and stochastic variations it was hard to discern any major influence of the tool edge radius for large values of h_1, however, an interesting trend was noted while only studying h_1 = 0.06 mm. For this case it was noted that the value of both h_{2min} and h_{1min} increases as a function of r_β up to r_β = 60 µm. The apparently random behavior of h_{2min} and h_{1min} after this point was

thought to be due to the formation of built-up edges which significantly alter the process characteristics. These results were to a certain extent supported by numerical results obtained through FEM simulations as exemplified in Figure 4.18. The FEM investigation was conducted through using a FEM-model as developed by Agmell et al. [103] utilizing the Johnson-Cook material model [104]. In addition, the Johnson-Cook damage law was used to model the chip separation. The cutting process was simulated through using a fully coupled thermo-mechanical analysis of a 2D model in ABAQUS/Explicit v6.9. During this analysis the Johnson-Cook plasticity model parameters were set to A = 280 MPa, B = 1100 MPa, C = 0.015, n = 0.5, m = 0.7 and $\dot{\varepsilon}_0$ = 1.0 s^{-1} as based on a previous research by Xu and Li [105].

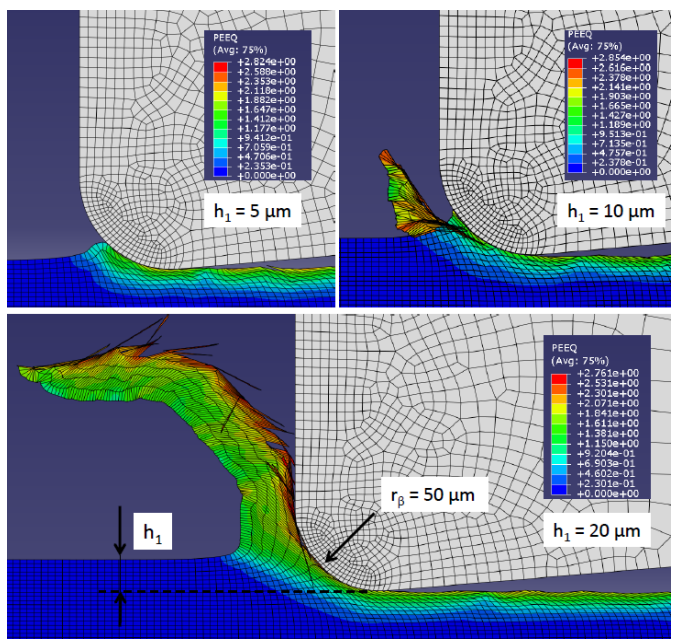

Figure 4.18 Example of results obtained from a 2D FEM-simulation while evaluating the size of h_{1min} during machining of SAF 2205 [98].

Even though significant differences exist between the experimentally obtained and numerically calculated results they both show a clear dependency on the tool edge radius. The difference between the two sets of results could to a certain extent be due to that the FEM-analysis was only performed as a two dimensional simulation and thus only simulating orthogonal turning. This implies that the simulation neglects any influence of the tool nose radius which might be part of the reason for the significant difference between the obtained results. Figure 4.19 and Figure 4.20 illustrate the obtained results while using each of the two methods for h_1 = 0.06 mm for h_{2min} and h_{1min} respectively.

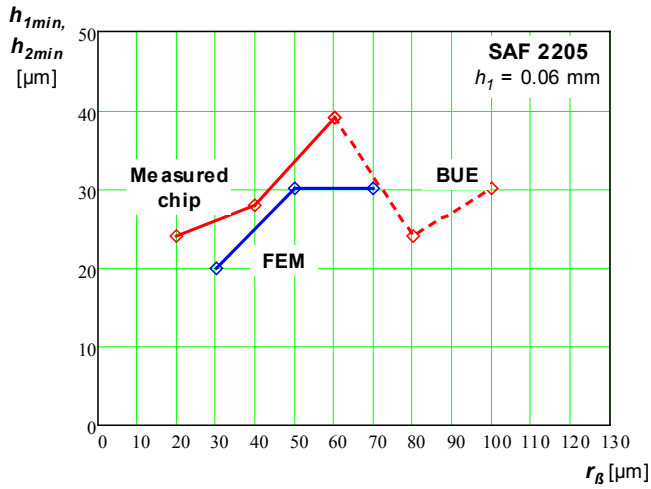

Figure 4.19 Influence of the tool edge radius on h_{2min} at h_1 = 0.06 mm while turning SAF 2205 as compared to values of h_{1min} obtained through FEM simulations [98].

If instead comparing the simulated results with the compensated h_{1min} value the following results were obtained, Figure 4.20. As can be seen in this figure the compensated value of h_{1min} appears to underestimate the true value of h_{1min} as compared to the results obtained from the FEM simulations. Part of this could be due to the limited validity of the assumption that the chips approximately retain their theoretical width even after they have been machined. Thus, it could be expected that the true value of h_{1min} is somewhere in between the compensated h_{1min} value and measured h_{2min} value obtained during this research.

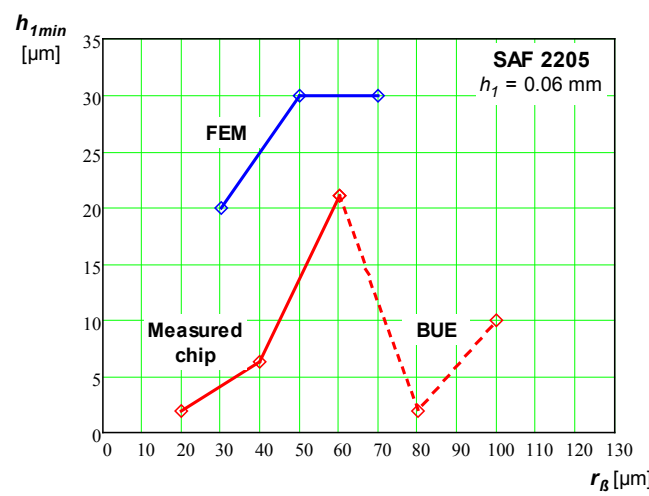

Figure 4.20 Influence of the tool edge radius on the h_{1min} value at h_1 = 0.06 mm while turning SAF 2205 as compared to results obtained through FEM simulations.

The next process parameter whose influence was investigated was the tool nose radius r. This parameter was varied from r = 0.4 mm to r = 1.6 mm under equivalent machining conditions. However, to achieve a larger minor cutting edge angle a different tool configuration was used for the smallest nose radius (DNMG150604 insert in a DDJNR3225P15 tool holder). The reason for this was that the previously presented model limitation while calculating h_{1min} which also applies to h_{2min}, Equation 4.10. According to Equation 4.10 the maximum feed is limited by the combination of tool nose radius and minor cutting edge angle. Thus, an increased minor cutting edge angle is required for this low value of the tool nose radius in order to allow for reasonable feed values. The results obtained during these experiments can be found in Figure 4.21.

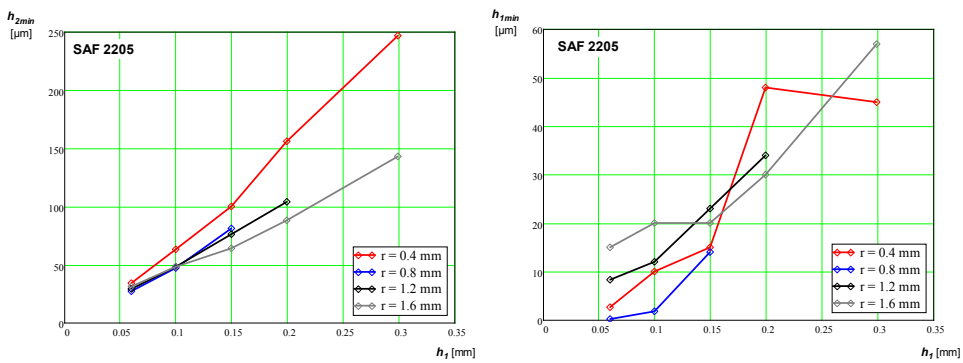

Figure 4.21 Influence of the tool nose radius r on h_{2min} (left) and h_{1min} (right) at varying values of h_1, modified from [98].

As can be seen in Figure 4.21, h_{2min} appear to be dependent upon the tool nose radius were a smaller radius will imply a larger value. However, the difference at low h_1 values appears insignificant in this comparison. A possible explanation for this h_{2min} phenomenon could be the influence of the chip flow angle v_{ch}. The chip flow angle v_{ch} describes the direction of the plastic flow of material in the chip during a machining process and is defined as obtaining the value zero when the flow is parallel to the cut surface. In comparison the behavior of h_{1min} appears more uncertain. Although clear differences between the h_{1min} values obtained for the four investigated tool nose radii can be discerned in the graph their apparently random behavior in relation to each other inhibits any further conclusions.

A previous investigation by Liu et al. [106] found that the plastic side flow has a large influence on the discrepancy between the theoretical and measured surface roughness. Since this discrepancy to a certain extent could be assumed as linked to the minimum chip thickness this conclusion could be thought of as supporting the notion that the

chip flow angle influences the value of h_{2min}. Several equations for calculating v_{ch} have been published through the years, one of the more famous by Spaans [45]. Spaans equation is based on empirical measurements and does not take into account the influence of different parts of the chip having different chip thicknesses. The theoretical chip thickness varies along the tool nose radius. It appears plausible that the part of the chip which has a small theoretical chip thickness should have a lower influence on the chip flow direction as compared to the part of the chip having a constant, maximum value of h_1. To solve this problem two new equations, Equation 4.24 and Equation 4.25, for calculating v_{ch} was proposed by Ståhl [5].

$$v_{ch,I} = \frac{\pi}{2} - \frac{1}{\delta_{ap} + \frac{\delta_c}{2}} \int_{\delta_{h1min}}^{\delta_{ap}+\frac{\delta_c}{2}} G \cdot \delta d\delta$$

$$where \quad G = \frac{h_1(\delta)}{h_1(\delta_f)} \cdot \frac{\delta_{ap} + \frac{\delta_c}{2}}{\int_{\delta_{h1min}}^{\delta_{ap}+\frac{\delta_c}{2}} \frac{h_1(\delta)}{h_1\left(\delta_{ap} + \frac{\delta_c}{2}\right)} d\delta} \qquad 4.24$$

Equation 4.24 is only valid for a depth of cut $a_p \le r \cdot (1 - \cos\kappa)$. For $a_p > r \cdot (1 - \cos\kappa)$ Equation 4.24 needs to be rewritten according to Equation 4.25.

$$v_{ch,II} = \frac{\pi}{2} - \left(\frac{r}{a_p} \cdot v_{ch,I}\Big|_{a_p = r} + \frac{(a_p - r) \cdot \kappa}{a_p} \right) \qquad 4.25$$

In Equation 4.24 δ_{h1min} is the value of the angle δ at $h_1(\delta) = h_{1min}$, Equation 4.26. The two angles δ_{ap} and δ_c are both defined according to Figure 4.22.

$$\delta_{h1min} = -\sin^{-1}\left(\frac{f^2 - 2 \cdot r \cdot h_{1min} + h_{1min}^{\ 2}}{2 \cdot f \cdot (r - h_{1min})} \right) \qquad 4.26$$

It could be speculated that the value of h_{2min} in some way is related to the value of the chip flow angle. Since a variation of the chip flow angle will influence the direction of the forces acting close to the position of the minim chip thickness. However, the sought influence of the chip flow angle is only locally occurring, close to the position of the minimum chip thickness. Thus, it was considered that calculations for the chip flow direction for the whole chip may not be appropriate for analyzing the current problem. Consequently, a hypothesis was formed that by using the value of the maximum surface deviation R_{max} as the depth of cut during this analysis more significant results would be obtained. In this comparison the R_{max} value was calculated

according to Equation 4.27 derived from Equation 4.19 and Equation 4.20 through assuming that $h_1(\delta) = h_{1\min}$.

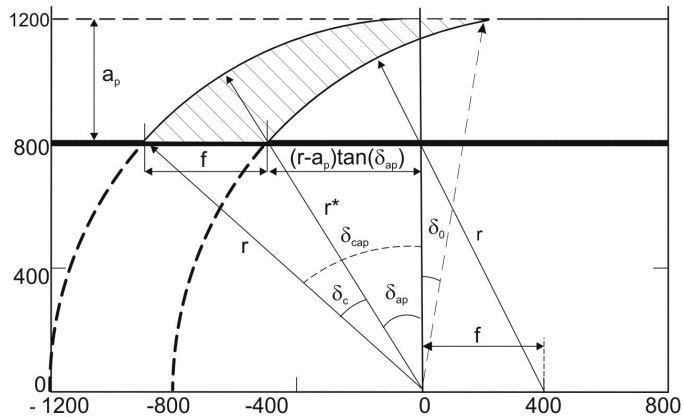

Figure 4.22 Principle illustration of the chip area when $a_p < r$ [5].

$$R_{max} = r + \frac{1}{2 \cdot f} \cdot \sqrt{\left(h_{1\min}{}^2 - f^2\right) \cdot \left(f^2 - \left(h_{1\min} - 2 \cdot r\right)^2\right)} \qquad 4.27$$

Several previous authors have published alternative relationships for calculating R_{max}. For instance Brammertz [107] has published an equation giving almost equal values to those obtained through using Equation 4.27. Further, both Grzesik [108] and Knüfermann [109] have published refined versions of Brammertz equation. However, during the current analysis the proposed relationship according to Equation 4.27 was used as this equation builds on the same foundation as the previously presented equations, Equation 4.19 and Equation 4.20, and was thus thought as suitable for the current investigation. The R_{max} value obtained from Equation 4.27 was thus used as the depth of cut while calculating the chip flow angle according to Equation 4.24 during this investigation. When comparing the obtained h_{2min} value as a function of the chip flow angle a trend was noticed whereas the h_{2min} values appear to be independent of v_{ch} until a certain threshold value is attained, Figure 4.23. After this threshold value has been attained, however, the h_{2min} value increases significantly as a function of v_{ch}. This behavior is however not clear for the compensated h_{1min} value which only displays a minor, if any, correlation with the v_{ch} value. This behavior could possibly be explained through the notion that h_{1min} is conventionally defined as being independent of the chip deformation after h_{1min} has been formed. Since v_{ch} primarily will influence the deformation of the chip after the formation of h_{1min} it could theoretically be expected that only h_{2min} will be dependent upon the v_{ch} value.

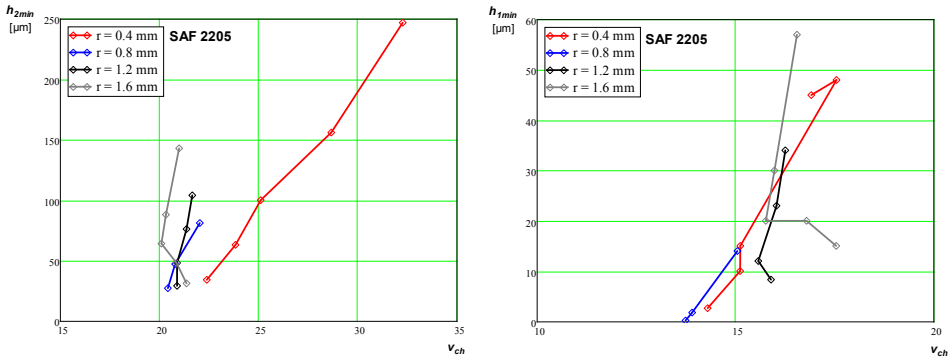

Figure 4.23 Influence of the chip flow angle on the value of h_{2min} (left) and h_{1min} (right).

Through analyzing these results in combination with those obtained on the influence of the tool edge radius the value of h_{2min} was presumed to vary according to the schematic relationship found in Figure 4.24. In Figure 4.24 the influence of v_{ch} on the value of h_{2min} is divided into two regions, the r_β-region and the v_{ch}-region. In the r_β-region the tool edge radius has the primary influence on the value of h_{2min}. However, when the value of the chip flow angle increases the value of h_{2min} will at some point become more influenced by the v_{ch} value, possibly to the exclusion of any influence of the tool edge radius. Thus, a second v_{ch}-region may be considered. As based on this presumed relationship a model for calculating the value of h_{2min} was proposed according to Equation 4.28. In this equation the variable $h_{2min,0}$ is used for describing the minimum chip thickness h_{2min} at $h_1 < h_{1,0}$. In turn the $h_{1,0}$ variable describes the h_1 value at the breakpoint between the r_β-region and the v_{ch}-region. In the equation g_1 and g_2 are model constants used for numerically adapting the equation to experimental obtained data.

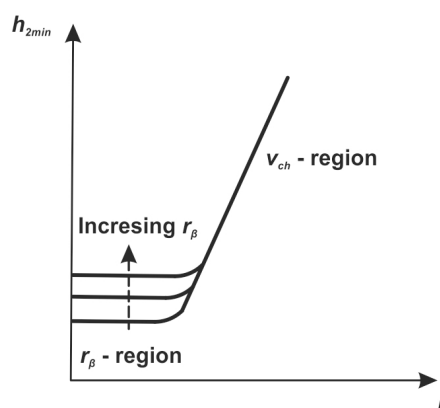

Figure 4.24 Presumed influence of the chip flow angle v_{ch} and tool edge radius r_β on the value h_{2min}, modified from [98].

$$h_{2min} = h_{2min,0} \cdot \left[1 + \left(\frac{h_1}{h_{1,0}} \right)^{g_1} \right]^{\frac{g_2}{g_1}} \qquad 4.28$$

It is well known that different factors such as built-up edges, tool wear, chatter etc. influence the obtained surface roughness which frequently deviate from analytical predictions [110]. In order to investigate the influence of the minimum chip thickness on the obtained surface roughness further experiments were performed. These machining experiments were performed as longitudinal turning operations while using CNMG120404, CNMG120408, CNMG120412 and CNMG120416 cemented carbide cutting tools, respectively, all of which were placed in a DCLNR2525M12 or DCLNL3225P12 tool holder depending on the workpiece material investigated. An exception was made for A48-40B where CNMA120404, CNMA120408, CNMA120412 and CNMA120416 cemented carbide cutting tools were used in order to be suitable for the workpiece material. In order to obtain as reliable data as possible, machining of 7 different workpiece materials were investigated, these being: AlSi9Mg0.3 – 20% vol. SiC_p, A48-40B, AISI 1045, AISI 4140, AISI 420, AISI 316L and Ti6Al4V. Due to the large diversity of workpiece materials it was not possible to use the same tool grade and chip breaker geometry for all machining cases. Thus, it was decided that the optimum tool grade and chip breaker geometry as proposed by the tool manufacturer should be selected for each workpiece material.

For each of the workpiece materials investigated 4 different nose radii were used (r = 0.4, 0.8, 1.2 and 1.6 mm) at up to 4 different feeds (f = 0.06, 0.10, 0.15 and 0.20 mm/rev). The depth of cut remained constant at a_p = 1.5 mm for all machining experiments except for the lowest nose radius while machining Ti6Al4V at which a_p = 1.0 mm was used due to practical reasons. The tools used during these additional experiments had a nose radius of r = 0.8 mm. For each of the experimental machining cases the obtained chips were collected and their widths were measured by using a digital micrometer. The measurements were repeated 100 times at random locations on several different chips for each combination of process parameters in order to gain a sufficient statistical distribution. In addition, the obtained surface roughness was also measured on the machined surface for each of the machining cases by using a conventional digital perthometer. These measurements were also repeated 100 times for each machining case at random locations on the machined surface. Selected surfaces were also investigated more thoroughly through using optical surface profilometry.

An example of an obtained surface while turning ASIS 1045 can be seen in Figure 4.25. Note the distortion from the theoretically expected pattern on the machined surface. Part of this deviation could be attributed to side-flow on the machined surface, a phenomenon with strong connections to the minimum chip thickness.

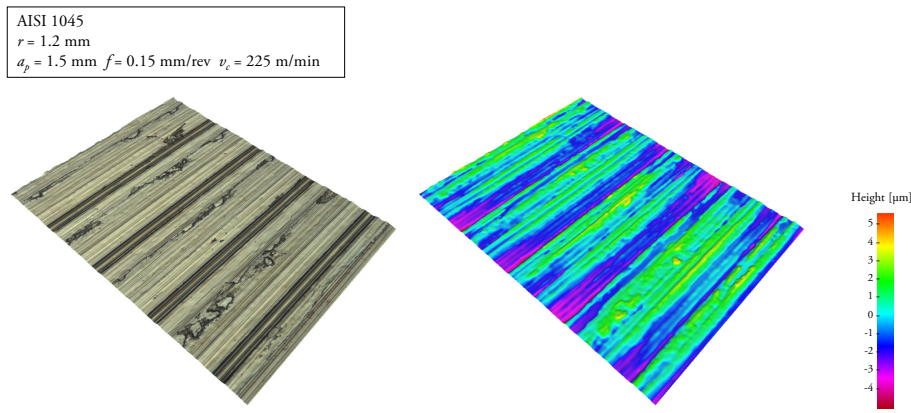

Figure 4.25 Obtained surface micro topography while turning AISI 1045.

Due to the large number of measurements it was inevitable that some recorded values would be faulty due to problems during the measurement process. In order to minimize the influence of these errors it was decided that the 5 largest and lowest measured values, respectively, should be removed for each machining case. These measurements were thus not included in the analysis of the obtained results. It is also important to note that any vibration of the workpiece during the machining process could significantly influence the obtained results. During these experiments vibrations was a great concern and even though it was attempted to minimize any vibrations to the fullest extent possible it should be recognized that even minute vibrations could have a significant influence on the obtained results.

As a first step it was attempted to analyze how the obtained h_{2min} values varies as a function of the workpiece material properties. It was found that the product of the elongation at rupture ε_b and the strain hardening D_n has a significant influence on the h_{2min} value. The main reason for choosing these material properties were primarily the previously described polar diagrams for evaluating the potential machinability of a workpiece material. Out of the five material properties used in these polar diagrams it was hypothesized that predominantly the elongation at rupture and the strain hardening could be thought to influenced the value of the minimum chip thickness. This correlation was believed to be due to the fact that an increase in ε_b or D_n could result in that the formation of a crack between the chip and machined surface appears closer to the tool edge radius. Thus, larger values of ε_b and D_n would theoretichally

result in a decrease of the minimum chip thickness. The obtained results obtained during this comparison is presented below in Figure 4.26. As can be seen in the figure, at low values of $\varepsilon_b \cdot D_n$ the value of h_{2min} decreases as a function of the product of the material properties. However, for large values of $\varepsilon_b \cdot D_n$ the size of h_{2min} appears to remain constant or even increase in some case.

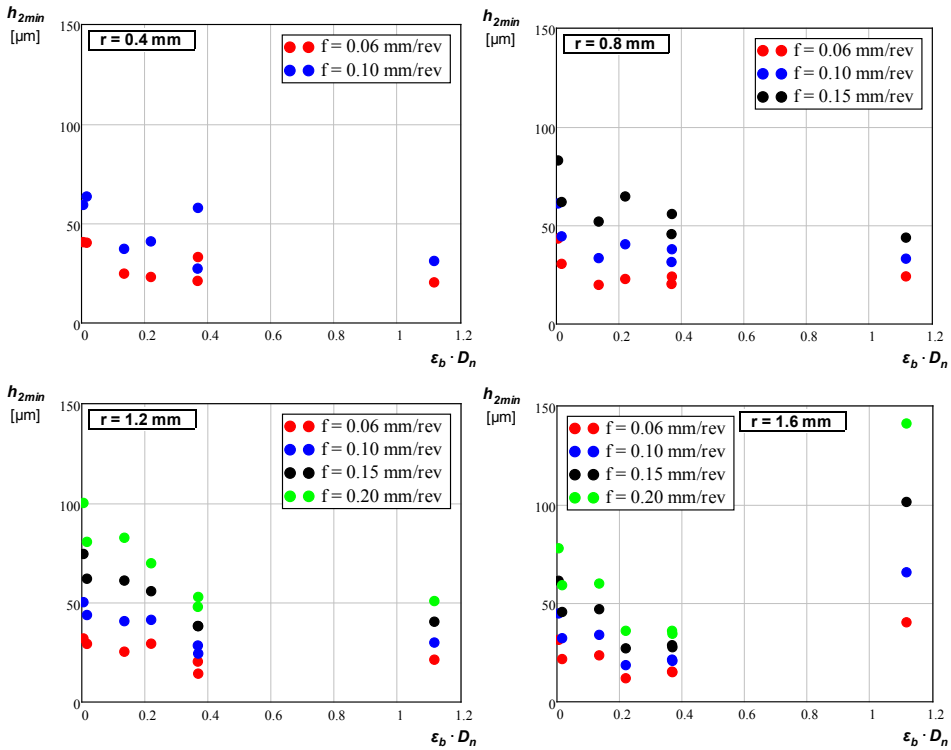

Figure 4.26 Value of h_{2min} as a function of the product between ε_b and D_n for each combination of tool nose radius r and workpiece material investigated.

The results obtained during this experimental evaluation could in turn be used while calculating the model constant used in Equation 4.28. The obtained results from these calculations as well as the mean error for each machining case can be found in Table 4.6 and Table 4.7. As can be found in Table 4.7 the modeling error is comparatively small for most cases even though significant errors might be obtained. Figure 4.27 illustrate the case of machining AISI 1045 using varying tool nose radii as an example of obtainable results.

Table 4.6 Obtained model constants while modeling h_{2min} for different workpiece materials and tool nose radii.

r [mm]	Var.	Al-SiC$_p$ MMC	A48-40B	AISI 1045	AISI 4140	AISI 420	AISI 316L	Ti6Al4V
0.4	h_{2min0} [µm]	4	7	6	0.4	0.9	2	3
	h_{10} [µm]	22	41	90	4	6	23	29
	g_1	0.59	0.58	0.50	0.58	0.59	0.54	0.55
	g_2	1.32	1.26	1.05	1.34	1.34	1.27	1.27
0.8	h_{2min0} [µm]	5	9	2	0.3	2	5	1
	h_{10} [µm]	38	51	22	3	17	59	11
	g_1	0.56	0.57	0.56	0.56	0.57	0.52	0.60
	g_2	1.24	1.21	1.28	1.31	1.27	1.17	1.35
1.2	h_{2min0} [µm]	4	4	4	4	0.4	4	2
	h_{10} [µm]	31	28	54	46	6	49	17
	g_1	0.57	0.63	0.54	0.54	0.57	0.54	0.59
	g_2	1.26	1.36	1.21	1.21	1.31	1.20	1.32
1.6	h_{2min0} [µm]	3	6	3	1	3	4	4
	h_{10} [µm]	31	47	54	18	56	61	43
	g_1	0.57	0.57	0.54	0.56	0.53	0.54	0.56
	g_2	1.25	1.23	1.21	1.27	1.19	1.81	1.25

Table 4.7 Obtained model errors [%] while modeling h_{2min} for different workpiece materials and tool nose radii.

r [mm]	Al-SiC$_p$ MMC	A48-40B	AISI 1045	AISI 4140	AISI 420	AISI 316L	Ti6Al4V
0.4	7.65	8.41	12.12	10.63	6.66	6.00	11.62
0.8	8.37	6.23	6.44	8.67	15.04	5.03	8.86
1.2	7.81	14.74	10.60	6.75	15.86	5.53	5.99
1.6	8.28	6.44	11.36	6.24	7.43	9.25	6.55

The next step was then to take the plastically deformed material on the machined surface into consideration while modeling the R_a surface roughness. This was practically achieved through dividing the ploughing area, A_{pl}, according to Figure 4.13 over the whole machined surface. The A_{pl} area may be calculated according to Equation 4.29.

$$A_{pl} = \int_{\delta_0}^{\delta_{h1min}} h_1(\delta) \cdot \left(r - \frac{h_1(\delta)}{2} \right) d\delta \qquad 4.29$$

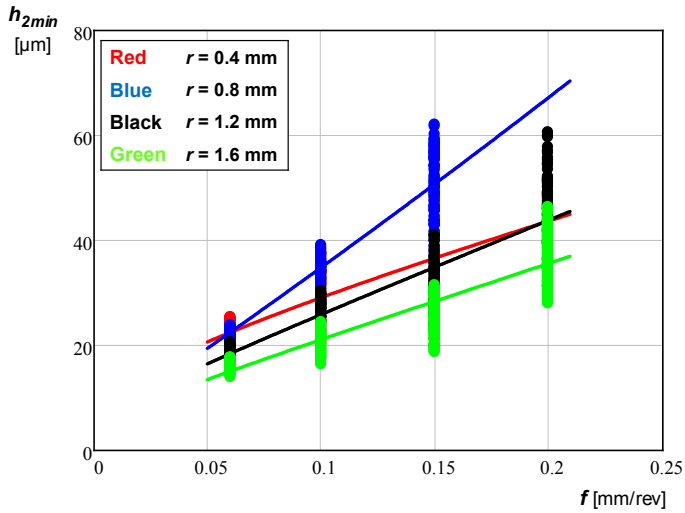

Figure 4.27 Obtained values of h_{2min} while machining AISI 1045 using four different tool nose radii. The circles and the solid lines indicate measured and modeled values, respectively.

In Equation 4.29 the two angles δ_0 and δ_{h1min} are defined according to Equation 4.12 and Equation 4.26 respectively. A_{pl} may either increase or decrease the surface roughness depending on where on the machined surface the material is deposited. A possible solution could be to use the R_{h1min} variable according to Equation 4.30. This variable could be interpreted as the average influence of the plastically deformed workpiece material on the obtained surface roughness.

$$R_{h1min} = \frac{A_{pl}}{f} \tag{4.30}$$

Through using the R_{h1min} variable a new model for calculating the obtained arithmetic mean surface roughness could be obtained according to Equation 4.31. In this equation "theoretical" indicates the R_a value as obtained through using the analytical model according to Equation 4.18. R_0 and χ are both model constants which need to be determined experimentally. The χ model constant is intended to describe the amount of A_{pl} which sticks to the machined surface and thus contributes to the surface roughness. R_0, in turn, is used to compensate the proposed empirical model in regards to factors which, in addition to h_{1min}, might have an influence on the obtained surface roughness. Finnaly, ϖ is a variation factor intended to describe the variation of the obtained surface roughness under seemingly equivalent machining conditions.

$$R_a = \varpi \cdot \left(R_{a,theoretical} + R_0 + \chi \cdot R_{h1\min} \right) \tag{4.31}$$

Stochastic variations of the surface roughness will always appear during any machining process. As previously published by Petropoulos [111] the surface roughness may vary under what appears to be similar conditions due several different factors. Petropoulos [111] divides these factors into four different categories.

1. Chance.
2. Progressive tool wear and effects associated with the cutting edge, e.g. built-up edges.
3. Rigidity and stability of the machining process.
4. Reproducibility of the experimental results.

Regarding item 1 on this list, "chance" might to a certain extent be related to the stochastic distribution of the ploughing material over the machined surface. In terms of items 2 and 3 on the list, it was attempted to minimize these effects during the preformed experiments. This was primarily done through using suitable process parameters for each workpiece material as proposed by the tool manufacturer as well as attempting to clamp the workpiece as rigidly as possible during the machining process. In addition, a new cutting edge was used for each machining trial. Each engagement only lasted a few seconds in order to minimizie the influence of any obtained tool wear. Both of these items, 2 and 3, should however be remembered while analyzing the obtained results as they might be a potential sources of error. As for item 4, this influence is difficult to distinguish from the pure chance according to item 1. Even though it was attempted to perform the experiments through using the same procedure during all machining cases, small variations are inevitable. Thus, this factor could contribute to the variation of the obtained results. Due to the possible variation of the obtained surface roughness a variation factor, ϖ, was introduced into Equation 4.31. This variation factor was used for modeling the variation of obtained results. If no variation occurs during the machining process this variation factor will obtain a value equal to 1.0. However, since this is commonly not the case, the variation factor will obtain two different values, larger and smaller than one, for describing the range of possible surface roughnesses.

Through using the proposed R_a surface roughness model it was attempted to model the experimentally obtained results. Further, the value of h_{2min}, which was used for calculating A_{pl} for each machining case, was based on experimentally obtained values modeled through Equation 4.28. An example of the obtained surface roughnesses while machining AISI 1045 is illustrated in Figure 4.28. These can be seen as typical for all results obtained during this analysis even though some variations did exist.

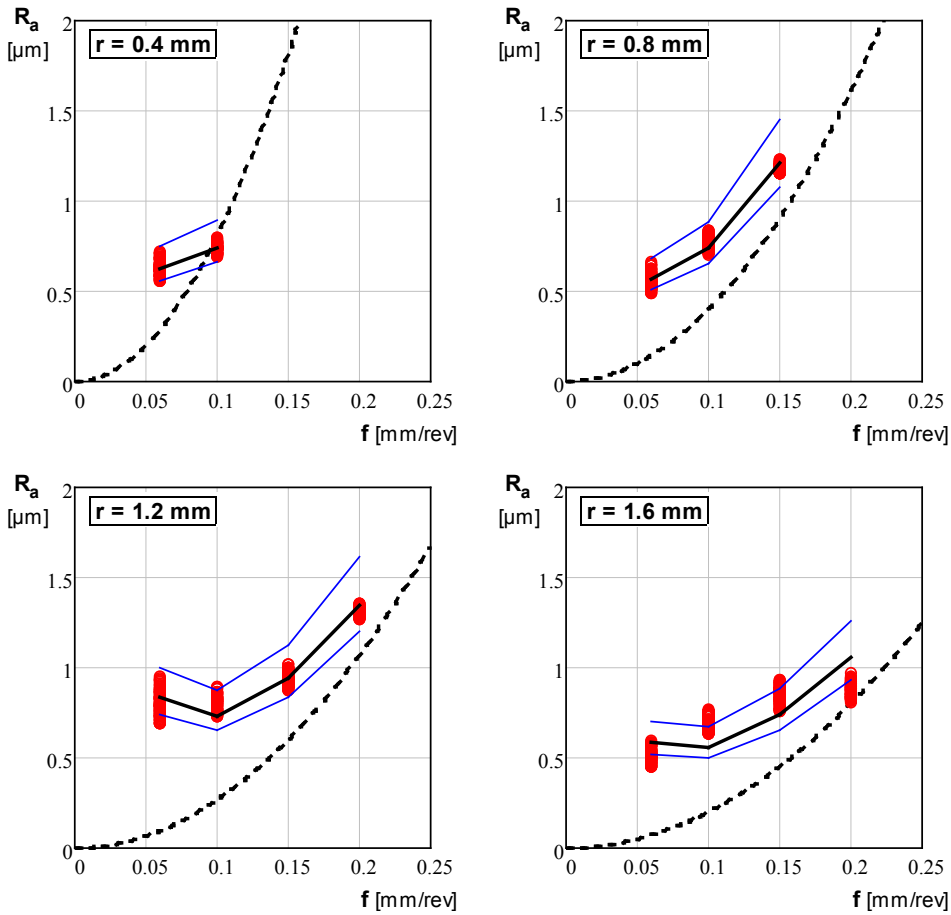

Figure 4.28 Obtained R_a surface roughnesses while machining AISI 1045 illustrated as red circles in the graphs. The thick solid- and interrupted curves indicate the modeled values according to Equation 4.31 and Equation 4.18, respectively. The thin blue solid curves illustrate the possible variation while using the overall average variation factor ϖ.

In general it was found that the R_a surface roughness decreased as a function of the tool nose radius as expected. More interesting, however, was that the influence of the feed on the surface roughness appeared to be significantly larger for small values of f. It was also noted that for the smallest nose radius the theoretical model according to Equation 4.18 appeared to overestimate the obtained surface roughness. The opposite appeared to be true for the larger tool nose radii. Similar results were obtained for all materials investigated even though some local differences were observed. A large amount of different machining cases were tested in order to investigate the validity of the proposed model to the fullest extent practically possible. Table 4.8 and Table 4.9 illustrate the obtained model constants as well as the average error obtained for all

investigated machining cases. As can be seen in Table 4.9 the obtained error is small for most cases even though some are worse than others. Further, in Table 4.8 it can be seen how the two constants vary depending on machining case. Even though the constants appear to obtain values in roughly the same range for all machining cases investigated no conclusive trend was found during this study.

Table 4.8 Obtained model constants while modeling R_a for different workpiece materials and tool nose radii.

r [mm]	Var.	AlSi9Mg0.3 – 20% vol. SiC_p	A48-40B	AISI 1045	AISI 4140	AISI 420	AISI 316L	Ti6Al4V
0.4	R_0 [µm]	-2.63	-1.18	-0.63	2.94	5.37	-1.32	-2.31
	χ [%]	3.74	1.68	3.41	-6.10	-9.50	5.62	5.81
0.8	R_0 [µm]	-0.72	-0.14	-0.19	1.74	-0.87	-0.32	2.42
	χ [%]	0.92	0.30	1.07	-2.91	1.65	1.33	-2.48
1.2	R_0 [µm]	-0.42	-3.05	-0.18	-0.06	5.73	-0.31	0.24
	χ [%]	0.66	2.82	1.61	0.96	-13.05	1.11	-0.04
1.6	R_0 [µm]	0.41	-0.94	-0.007	-2.41	-0.29	-0.18	0.02
	χ [%]	0.07	0.99	1.03	5.71	3.02	1.41	0.30

Table 4.9 Obtained model errors [%] while modeling R_a for different workpiece materials and tool nose radii.

r [mm]	AlSi9Mg0.3 – 20% vol. SiC_p	A48-40B	AISI 1045	AISI 4140	AISI 420	AISI 316L	Ti6Al4V
0.4	0.21	0.00	0.00	0.25	7.28	0.00	0.00
0.8	0.08	1.49	2.78	7.88	5.72	1.61	4.01
1.2	16.50	15.48	3.86	15.51	7.19	13.38	13.89
1.6	4.08	11.31	16.63	14.08	12.75	1.31	9.48

The next step in the investigative process was then to analyze the variation factor ϖ. In order to obtain complete insight into the whole range of values the maximum and minimum value of the variation factor for each machining case was calculated, thus describing the maximum and minimum measured value, respectively. Mathematically it is possible to calculate the variation factor for each of the machining cases investigated. This is however not a practical solution from an engineering perspective. This solution was thus discarded during this investigation. Also, it could be speculated whether the value of the variation factor varies as a function of the feed or the tool nose radius. However, no clear indications of this were observed during this

study. Thus, for simplicity reasons an average maximum and minimum value for the variation factor was calculated for each workpiece material investigated. When doing these calculations it was noted that the maximum and minimum value of the average variation factor varied only slightly from one workpiece material to the other. Thus, it was considered that there might exist a global value for these two parameters which is applicable for all workpiece materials. Due to this an average maximum and minimum value for the variation factor was calculated for all machining cases investigated. The obtained result from these calculations can be found in Table 4.10.

Table 4.10 Average value of the variation factor ϖ.

ϖ	AlSi9Mg0.3 – 20% vol. SiC_p	A48-40B	AISI 1045	AISI 4140	AISI 420	AISI 316L	Ti6Al4V	Average
Maximum	1.38	1.19	1.12	1.13	1.18	1.20	1.17	1.20
Minimum	0.80	0.89	0.92	0.90	0.86	0.91	0.92	0.89

Even though some obtained values were insignificantly outside of the obtained average interval this solution was thought of as beneficial from an engineering perspective due to its simplicity. If only a maximum and minimum value of the variation factor is required independently of workpiece material the use of the proposed model will be considerably simplified. However, the user should be aware of this simplification and possibly a safety factor could be added for certain machining operations, especially while finishing critical surfaces. Figure 4.29 illustrates the sequence of factors influencing the R_a surface roughness as described throughout this section.

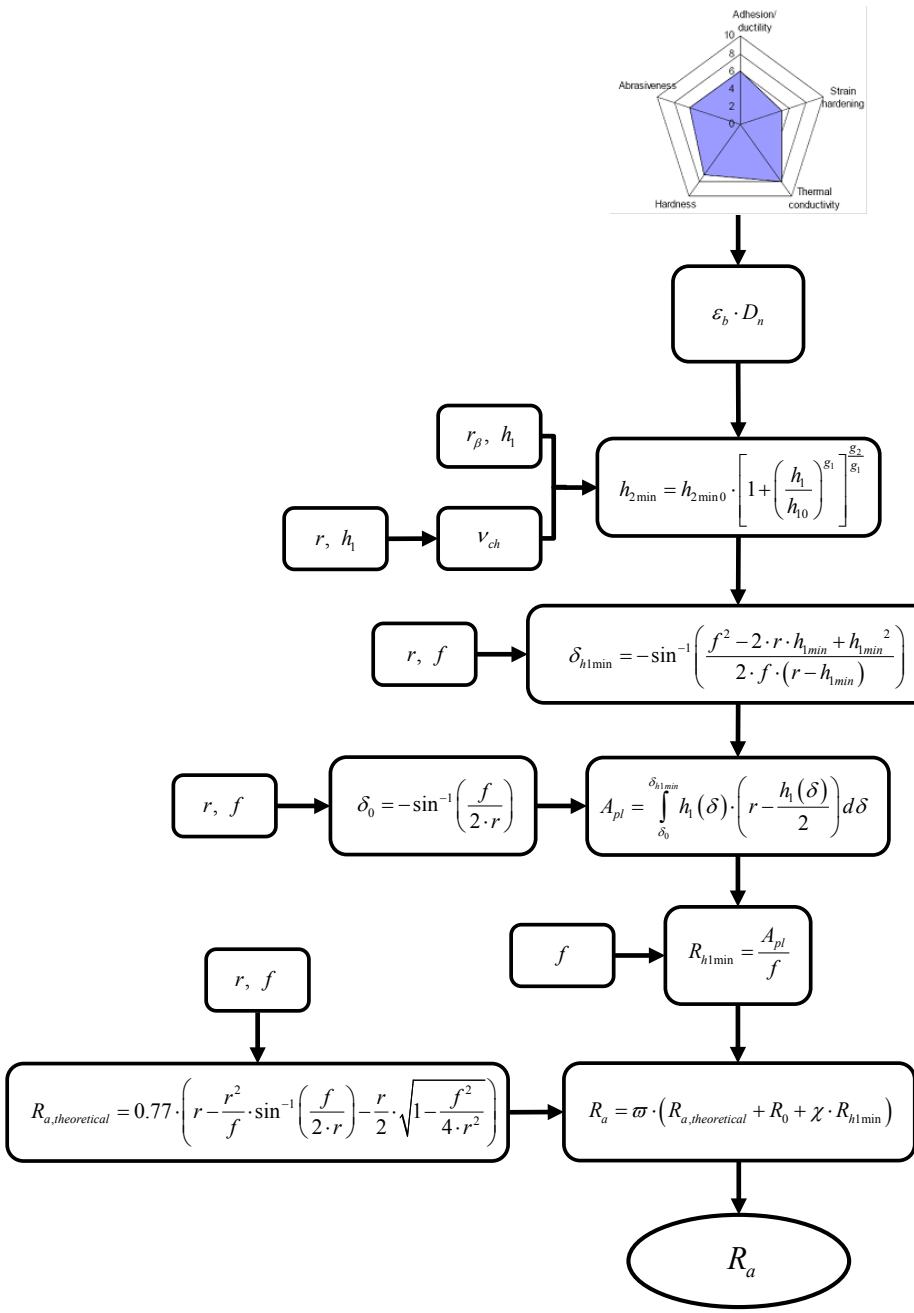

Figure 4.29 Sequence of factors influencing the obtained R_a surface roughness.

4.3 Influence of the Tool Surface Topography

For conventional machining operations the influence of parameters such as cutting data and workpiece material has been widely investigated. In comparison fairly few studies focusing on the influence of the tool surface micro topography on the machining process has thus far been published [5, 112-114]. Adequate knowledge of the contact conditions acting between the cutting tool and workpiece material is essential while modeling and analyzing any machining process. For instance the contact condition is commonly used as an input variable when modeling the machining process using finite element simulations. By using an inadequate contact condition the simulations may produce ambiguous or even faulty results.

During conventional metal cutting operations the contact conditions between the tool surface and chip/workpiece material varies significantly and the rake and clearance surfaces are generally subjected to different contact pressures and temperatures during the machining process [112, 115-117]. The contact surfaces at both interaction zones are commonly divided into three parts as a result of their different contact behavior. These three contact zones generally include: A) sticking, B) adhesion and C) sliding as schematically illustrated in Figure 4.30 [115, 118-120]. Subzone B "adhesion" is a transition zone between subzone A and C where both sliding and adhesion between the workpiece and cutting tool may occur. This implies that a friction coefficient according to the conventional definition primarily may be calculated for subzone C as opposite to the contact condition which is intended to take all three zones into consideration. For simplicity reasons several previous authors have only consider sliding contact [121], sticking contact [122] or a fixed combination of these phenomena [123]. The coatings ability to improve and stabilize the adhesion zone is of vital importance for the function of the coating. As such the coating contributes to the minimization of the sliding zone [5].

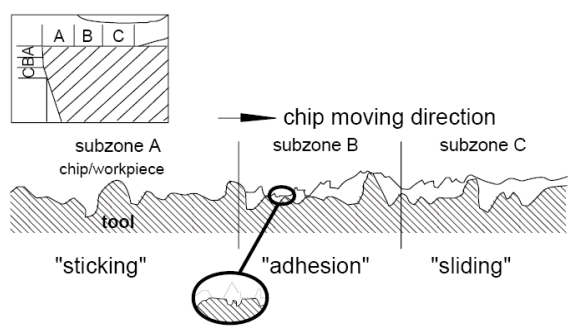

Figure 4.30 Schematic illustration of the division of the contact zone into three discrete regions, adapted from Höglund [118].

The tribological behavior of the tool-workpiece interface can be further understood through analyzing the friction acting between the two active surfaces. Son et al. [102] has previously concluded that the size of the friction coefficient has a significant influence on the deformation and thus the quality of the machined surface. Gekonde et al. [124] further emphasizes that the tool wear is strongly dependent upon the local tribological situation at the tool-workpiece contact surface. As the contact is a mixture of both sticking and sliding behavior it could be considered as inappropriate to use the conventional term "friction coefficient" during these applications. Instead it was decided to refer to this surface interaction as "contact condition" and this terminology will be used for the rest of this dissertation.

Several authors have investigated the contact condition acting between the tool and workpiece during metal cutting. Previously, Childs [112] have stated that the tool-workpiece contact on the rake face near the cutting edge reaches 100%. He also states that local thermal softening of the chip takes place at relatively high cutting speeds resulting in what he describes as a kind of self-lubrication of the machining process. In addition, Özel and Altan [125] stress that the prevalent conditions at the chip-rake face interface constrain the use of a friction coefficient obtained from ordinary sliding tests. Currently, little is known on how the tool surface micro topography influence the machining process. Thus, an investigation was launched on the tribological characteristics during metal cutting operations with special focus on the contact conditions as a function of the tool surface micro topography, Paper IV and V.

In order to investigate the influence of the tool micro topography on contact conditions during machining operations, experiments were performed while using commercially available Al_2O_3 coated cemented carbide inserts (TPUN160308) with a substrate composition of 93.5 wt.% WC, 0.5 wt.% (Nb,Ta)C and 6 wt.% Co. The tools were CVD coated with a 5 µm thick Ti(C,N) layer at a temperature of 860°C before depositing a 3 µm thick α-Al_2O_3 layer at 1020°C, Figure 4.31.

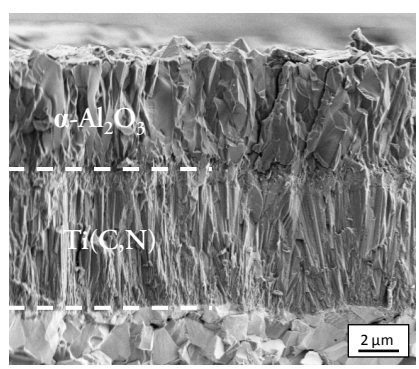

Figure 4.31 Cross-section of the as-deposited coating [126].

After coating deposition, the inserts were polished using three different commercially available surface polishing treatments in order to remove the crystalline facets of the α-Al_2O_3 layer and thus obtain three distinctly different surface micro topographies as exemplified in Figure 4.32. The thickness of each polished coating was controlled via SEM and EDX, where any insert with a α-Al_2O_3 coating less than 2 µm thick was discarded.

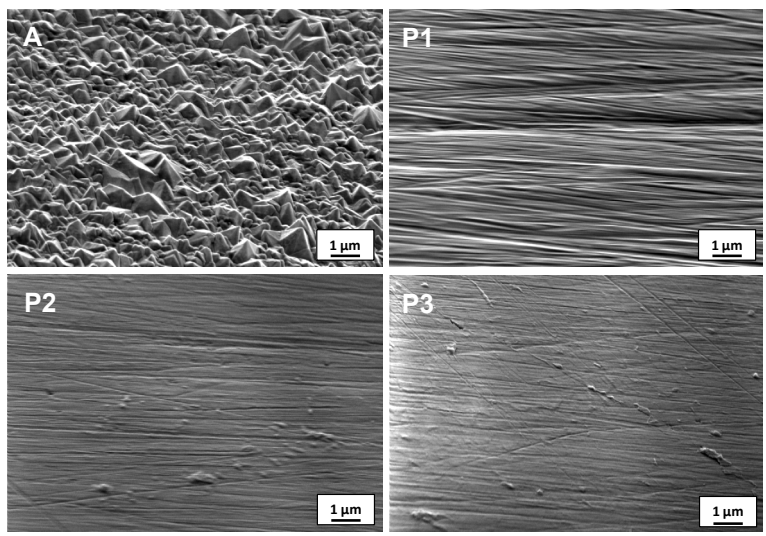

Figure 4.32 Morphology of the four investigated tool surfaces [126].

Also, two different tool edge geometries were used during these experiments; one conventional with a circular tool edge radius of approximately 20 µm (denoted "Standard insert") and one with a 200 µm wide synthetic wear land VB_s (denoted "SWL insert"), Figure 4.33. The surface micro topography and edge radius for each of the different inserts tested can be found in Table 4.11.

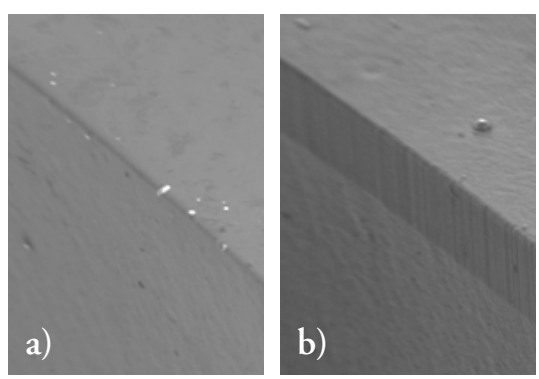

Figure 4.33 Insert geometries used: a) Standard insert and b) SWL insert [126].

Table 4.11 Tool surface micro topography and edge radius for the different types of inserts investigated.

Coating	Standard insert			SWL insert				
	Rake face		Edge radius [µm]	Rake face		Clearance face		Edge radius [µm]
	R_a [nm]	R_z [µm]		R_a [nm]	R_z [µm]	R_a [nm]	R_z [µm]	
A	360±16	4.5±0.4	25±2	360±20	5±0.5	370±19	7±0.8	15±1.5
P1	111±6	1.5±0.3	23±2	109±6	1.6±0.2	109±7	1.5±0.2	15±1.3
P2	54±3	0.7±0.1	21±1.9	55±2	0.7±0.1	55±3	0.6±0.1	13±1
P3	23±2	0.4±0.03	21±1.5	24±2	0.3±0.04	26±2	0.2±0.02	12±1

In order to evaluate the influence of the tool surface micro topography on the obtained contact conditions during machining operations orthogonal turning experiments of AISI 4140 tempered steel were performed using each of the previously described types of cutting tools. During these tests the cutting forces were measured through using a standard piezoelectric dynamometer. All turning experiments were carried out without any cutting fluid while using the following cutting data: cutting speed v_c = 240 m/min, depth of cut a_p = 3 mm and feed f = 0.025, 0.050, 0.075, 0.100, 0.200 and 0.300 mm/rev. Each of the machining experiments was run for an engagement time corresponding to a machined volume of 10 mm^3. In order to evaluate the subsurface plastic deformation hardness indentations were performed both on the chip as well as on the cross-section of the machined surface. These hardness indentations were performed by using a Vickers indentor at a load of 5 g. The hardness was calculated through analyzing the obtained indentation curves (load vs. displacement) according to Oliver-Pharr [127].

4.3.1 Rake face characteristics

Figure 4.34 illustrates a view of the rake face of one of the inserts used during these machining experiments. Three different contact zones can be distinguished in the figure: a) sticking, b) adhesion and c) sliding. Through investigating zones b) and c) more carefully superficial plastic deformation as well as ridge formation can be distinguished in both contact zones, Figure 4.35. While the as-deposited coating (A) displays a significant amount of adhered workpiece material the fine polished coating (P3) is relatively free from adhered material.

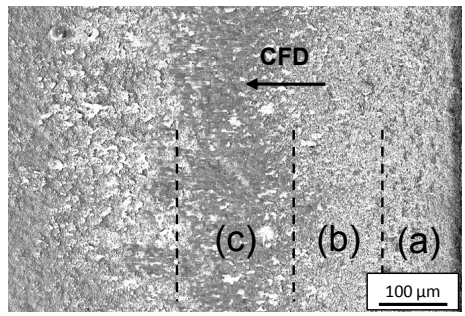

Figure 4.34 View of the rake face after machining showing the three contact zones: a) sticking, b) adhesion and c) sliding. The chip flow direction (CFD) is indicated with an arrow [126].

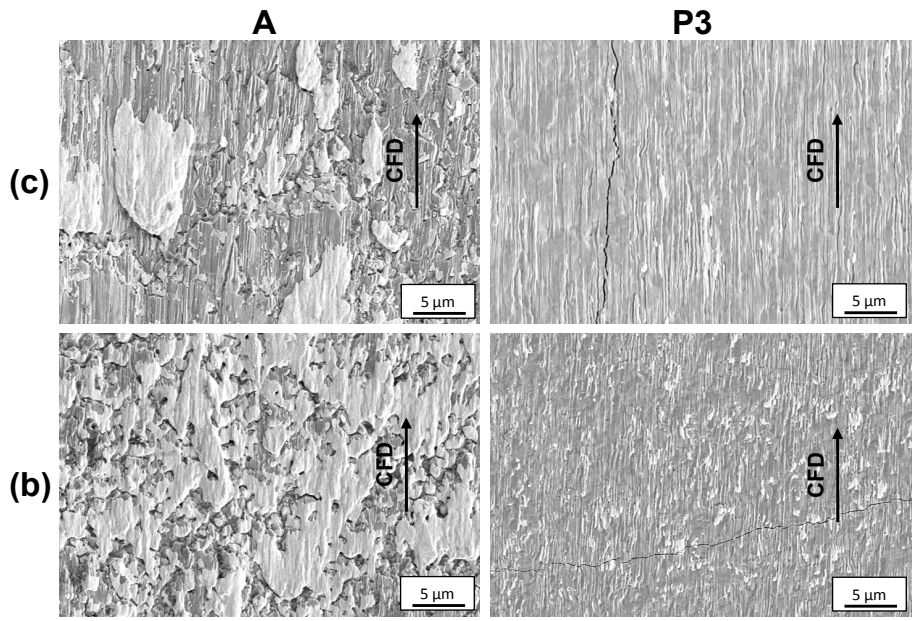

Figure 4.35 Detailed view of contact zones b) and c) on the rake face for coating A and P3 at f = 0.300 mm/rev. The chip flow direction (CFD) is indicated with an arrow [126].

The tool surface micro topography was found to have a significant influence on the length of contact zones a), b) and c), Table 4.12. As can be seen in this table a decrease of the tool surface roughness results in an increase of the length of the contact zones a) and b) by more than 30% while the length of contact zone c) decreases by approximately 15%.

Table 4.12 Estimated length of the contact zones a), b) and c) acting on the rake face.

Coating	Feed 0.050 mm/rev Contact length [µm]			Feed 0.300 mm/rev Contact length [µm]		
	a)	b)	c)	a)	b)	c)
A	50±9	36±5	79±8	157±8	200±14	229±15
P3	57±4	43±2	64±3	214±11	221±9	200±8

Figure 4.36 illustrates the cross-section of some selected chips obtained after using coatings A and P3 (R_a = 360 nm and R_a = 23 nm), respectively. Note the significant difference in the width of the secondary deformation zone, ε_{II}, in the figure. As can be seen in the figure a smoother polished coating will result in a reduction in the width of this deformation zone as compared to the rougher as-deposited coating, 7 and 20 µm, respectively.

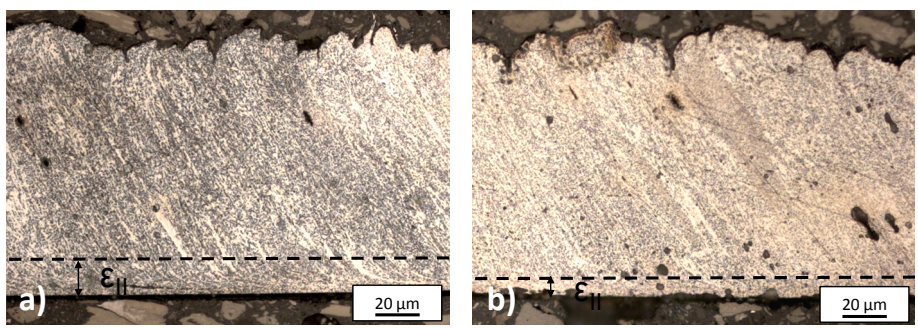

Figure 4.36 Cross-section of obtained chips at f = 0.050 mm/rev as seen parallel to the chip flow direction for a) coating A and b) coating P3 [126].

Apart from optically examining the obtained chips the subsurface hardness gradient was also measured as a function of the distance from the tool contact into the chip, Figure 4.37. Note that there is a significant difference in subsurface hardness for chips sliding against the two different coatings. While comparing the obtained chip surfaces after sliding against the tool surfaces a clear difference was also noted, Figure 4.38. A significant difference can be observed between the obtained results where significant scratches are evident on the chip surface sliding against the rough cutting tool. In comparison, no significant scratches can be observed on the chips sliding along the smoother tool surface.

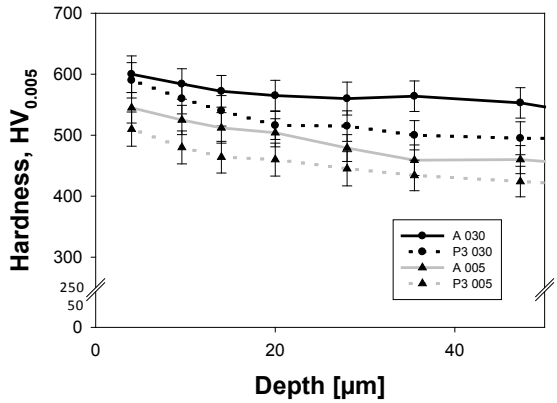

Figure 4.37 Micro hardness profile in the obtained chips as a function of the distance from the tool contact for coatings A and P3 at feeds 0.050 and 0.300 mm/rev [126].

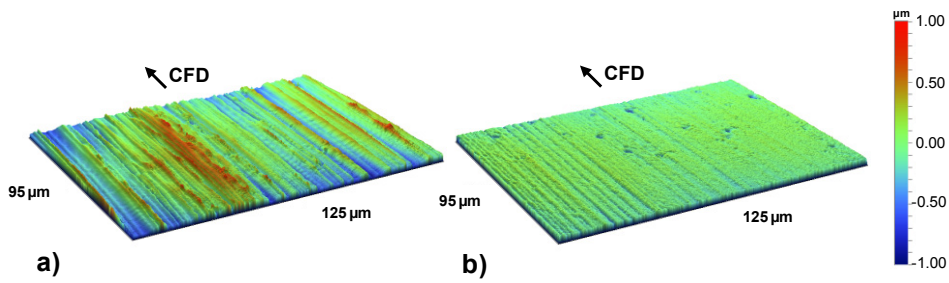

Figure 4.38 Surface topographies of chips sliding against a) coating A and b) coating P3 at f = 0.05 mm/rev. The chip flow direction (CFD) is indicated with an arrow [126].

Through knowing the shear angle it is possible to calculate the contact condition acting on the rake face during a machining process. Considerable effort by the scientific community has been put into defining an equation for calculating the shear angle during a general machining operation. Bayard [128] presents about 50 different equations which have been published from 1893 until 1990 on this subject. One of the more commonly used equations was published by Ernst and Merchant [129]. Their shear angle equation, Equation 4.32, is based on finding the shear angle which minimizes the amount of energy needed by the machining processes. The result is an equation where the shear angle, ϕ, is a function of the friction angle, ρ_r, and the rake angle, γ, according to Equation 4.32.

$$2\phi + \rho_r - \gamma = \frac{\pi}{2} \qquad 4.32$$

Through geometrically analyzing the machining process it can be found that there exists a relationship between the shear angle, the rake angle and the chip compression ratio, λ_h, Equation 4.33 [5].

$$\phi = \tan^{-1}\left(\frac{\cos\gamma}{\lambda_h - \sin\gamma}\right) \qquad 4.33$$

Through combining the two previous equations, Equation 4.32 and Equation 4.33, a new relationship for calculating the friction angle may be established, Equation 4.34.

$$\rho_r = \frac{\pi}{2} - 2\cdot\tan^{-1}\left(\frac{\cos\gamma}{\lambda_h - \sin\gamma}\right) + \gamma \qquad 4.34$$

The chip compression ratio λ_h is defined as the ratio between the theoretical chip thickness h_1 and the obtained chip thickness h_2, Equation 4.35.

$$\lambda_h = \frac{h_2}{h_1} \qquad 4.35$$

The contact condition on the rake face, μ_r, is the relationship between the mean shear stress and mean normal stress. Through using the shear angle equation as published by Ernst and Merchant it is possible to analyticaly calculate the contact condition according to Equation 4.36 [5]. The contact condition calculated through using this equation is denoted $\mu_{r,EM}$ in this dissertation in order to avoid potential misinterpretation.

$$\mu_{r,EM} = \tan(\rho_r) \qquad 4.36$$

Thus, by knowing γ and h_1 as well as measuring h_2 the contact condition may be calculated. The results obtained while using this method during the current experimental investigation is illustrated in Figure 4.39.

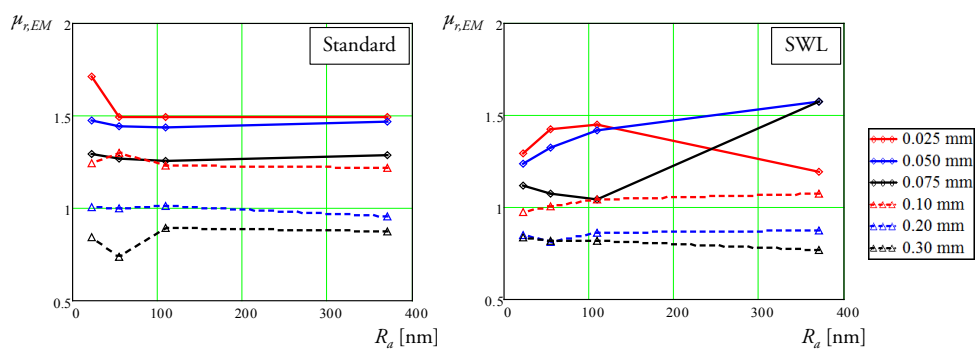

Figure 4.39 Contact condition $\mu_{r,EM}$ of the Standard and SWL inserts calculated for each of the different tool surface micro topographies and feeds investigated [130].

As can be seen in Figure 4.39, the influence of the tool surface micro topography on the contact condition appears insignificant while using the current analysis method.

There are some variations between the obtained results for the Standard and SWL inserts but the significance of these results could be disputed due to the small variations of the obtained values.

An alternative method for calculating the contact condition could be based on the measured cutting forces. As previously stated the cutting forces may be considered as linearly dependent upon h_1, Equation 4.5. However, some problems arise while using these forces for calculating the contact condition. The value of the contact condition on the rake face should only be based on the forces acting on the rake face of the cutting tool while at the same time taking the force direction into consideration, Figure 4.40. During these calculations it is important to take the stagnation zone into consideration. The y_s distance in the figure is the distance to the stagnation point from the theoretically extension of the machined surface. The tangential and radial force acting on the rake face, T_r and A_r, may be divided into two parts acting on opposite sides of the stagnation point acting in a positive (*pos*) and negative (*neg*) direction in relation to the stagnation point, Figure 4.40.

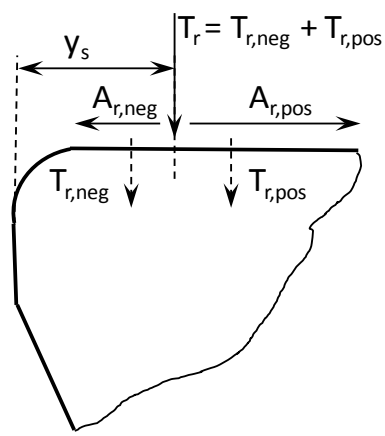

Figure 4.40 Cutting forces acting on the rake face with respect to the location of the stagnation point [130].

It might be noted that the feed force acting in a negative direction on the rake face, $A_{r,neg}$, will reduce the value of the measured contact condition. Thus, the measured contact condition on the rake face, $\mu_{r,measured}$, may be calculated according to Equation 4.37.

$$\mu_{r,measured} = \frac{A_{r,pos} - \left|A_{r,neg}\right|}{T_r} = \frac{A_{r,pos} - \left|A_{r,neg}\right|}{T_{r,pos} + T_{r,neg}} \qquad 4.37$$

For a given value of the rake angle γ the measured contact condition on the rake face may be calculated according to Equation 4.38.

$$\mu_{r,measured} = \frac{\frac{F_f - D_2}{F_c - C_2} + \tan\gamma}{1 - \frac{F_f - D_2}{F_c - C_2}\tan\gamma} \qquad 4.38$$

If considering a hypothetical scenario where the entire force acting in the axial direction on the rake face of the cutting tool a hypothetical maximum value of the contact condition acting on the rake face, $\mu_{r,max}$, could be obtained, Equation 4.39.

$$\mu_{r,\max} = \frac{A_{r,pos} + \left|A_{r,neg}\right|}{T_r} = \frac{A_{r,pos} + \left|A_{r,neg}\right|}{T_{r,pos} + T_{r,neg}} \qquad 4.39$$

If it is assumed that the distance to the stagnation point y_s is smaller than the tool edge radius r_β the force component $A_{r,neg}$ could be thought of as being negligible and thus a new contact condition $\mu_{r,pos}$ could be calculated, Equation 4.40.

$$\mu_{r,pos} = \frac{A_{r,pos}}{T_{r,pos}} \qquad 4.40$$

With respect to the previous variations of potential solutions for calculating the contact condition on the rake face the following comparison could be made, Equation 4.41. In this equation $\mu_{r,true}$ denotes the true value of the contact condition on the rake face. Even though some definitions of the contact condition on the rake face might be expected to produce a more accurate value from a theoretical perspective no solutions on how to solve this dilemma has thus far been envisioned.

$$\mu_{r,measured} \le \mu_{r,true} \le \mu_{r,pos} = \mu_{r,EM} \le \mu_{r,\max} \qquad 4.41$$

Based on this knowledge of the influence of the perceived cutting forces a first step in the analysis process could be to evaluate the obtained cutting forces for different tool surface micro topographies, Figure 4.41.

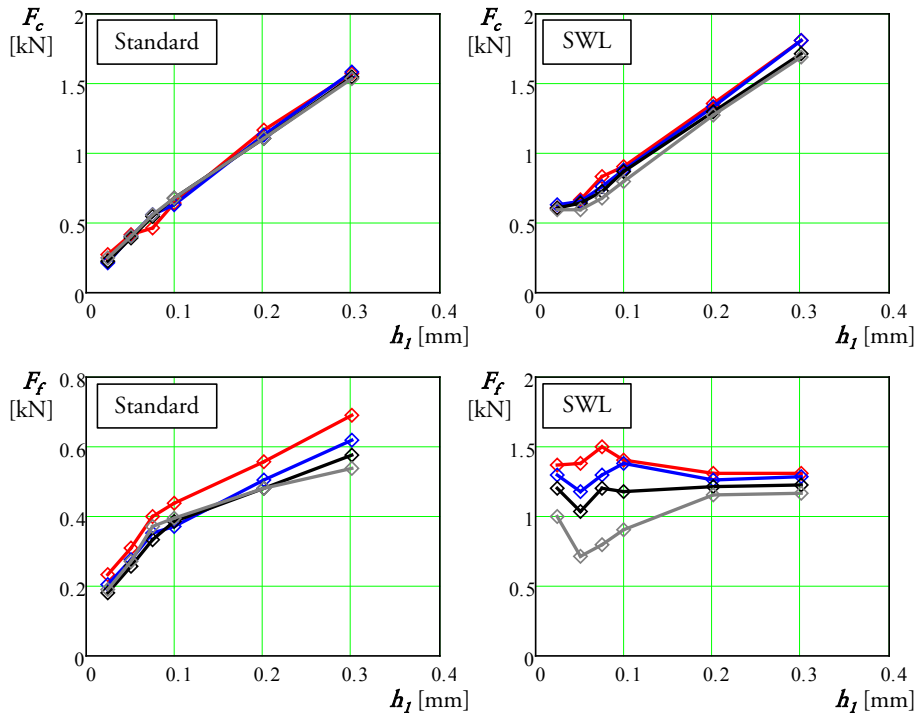

Figure 4.41 Obtained cutting forces for coatings A (red), P1 (blue), P2 (black) and P3 (gray) [130].

As can be seen in Figure 4.41 the difference in the main cutting force for the different coatings appears to be negligible for both types of inserts. However, a difference between the investigated coatings could potential be discern while examining the feed forces in the lower part of the figure. For the Standard insert this difference is possibly more pronounced for the roughest coating, coating A. However, it is questionable whether the size of this difference is significant enough to validate any further conclusions. Conversely, for the SWL insert the difference is pronounced and particularly obvious at $h_1 > 0.2$ mm. As the size of the synthetic flank wear for this insert was 200 µm it could be speculated that this size could be connected to the break-point observed for the measured feed force. No additional experiments were however performed to validate this hypothesis.

Through using the linearized cutting forces it is possible to calculate the contact condition on the rake face through using for example Equation 4.38. While using this equation for the forces obtained during this study the following results were obtained, Figure 4.42.

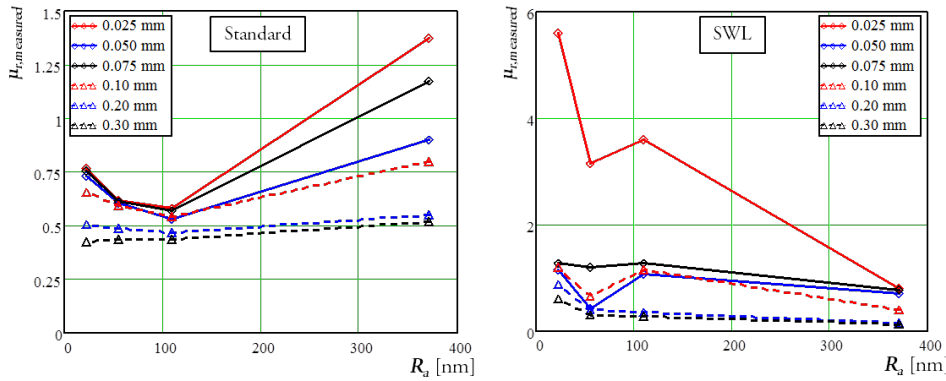

Figure 4.42 Experimentally derived values of $\mu_{r,measured}$ [130].

In Figure 4.42 it can be noted that the value of $\mu_{r,measured}$ for the SWL insert at h_1 = 0.025 mm differs significantly from the other obtained results. A potential reason for this difference could be the occurrence of built-up edges which significantly alter the fundamentals of the machining process. It could thus be argued that these values should be ignored in order to not distort the obtained results. It could also be argued that the tool edge radius will have a more distinguishable effect on the obtained results at low values of h_1 due to the influence of the stagnation zone which could distort the obtained results even further.

4.3.2 Clearance face characteristics

The contact conditions on the clearance face of the cutting tool could be calculated in a similar manner to its equivalent on the rake face. For instance the same type of contact zones can be distinguished on both surfaces, Figure 4.43. Examples of the width of contact zones a) and b) can be found in Table 4.13. As can be noted in Table 4.13 a rougher coating appears to decrease the sticking contact zone a) while increasing the adhesion contact zone b).

Table 4.13 Estimated length of the contact zones a) sticking and b) adhesion acting on the clearance face.

Coating	Feed 0.050 mm/rev Contact length [µm]		Feed 0.300 mm/rev Contact length [µm]	
	a)	b)	a)	b)
A	145±6	45±3	131±9	59±5
P3	158±8	32±2	149±11	42±5

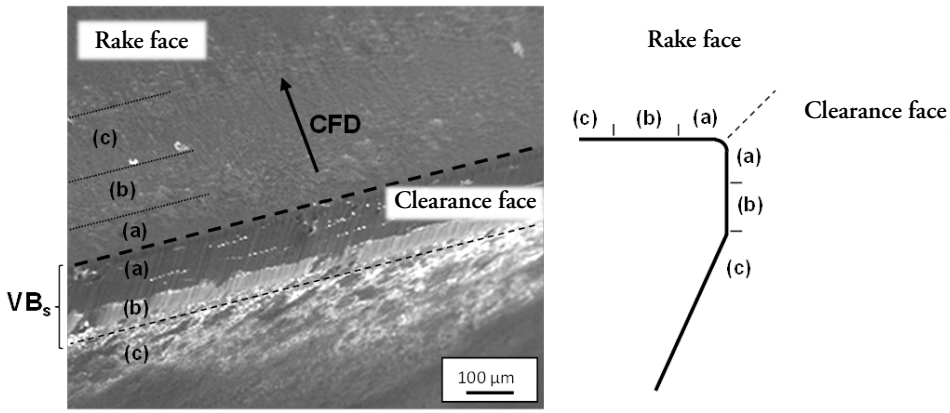

Figure 4.43 View of a used SWL insert illustrating the contact zones a) sticking, b) adhesion and c) sliding on both the rake and clearance face. The chip flow direction (CFD) is indicated with an arrow [126].

Through knowing the obtained cutting forces it is possible to calculate the contact condition on the clearance face, $\mu_{cl,measured}$, according to Equation 4.42.

$$\mu_{cl,measured} = \frac{\frac{C_2}{F_c}}{\frac{D_2}{F_f} \cdot \frac{F_f}{F_c}} \qquad 4.42$$

While using this equation for evaluating the results obtained during this experimental study the following results were obtained, Figure 4.44. The results found in Figure 4.44 seem to imply that the contact condition on the clearance face decreases rapidly as a function of h_1 until it obtains a asymptotic value at which it stabilizes, significantly decreasing the relation between $\mu_{cl,measured}$ and h_1. As expected it is possible to observe a significant difference between the two types of inserts investigated at low values of h_1. This is attributed to the influence of the synthetic wear land on the SWL inserts which could be presumed as having a more significant effect at these low values of h_1. It is also of interest to consider the difference between the four different tool coatings. Even though the obtained results are limited they seem to imply a decreasing influence of the synthetic wear land for incereasing values of the theoretical chip thickness.

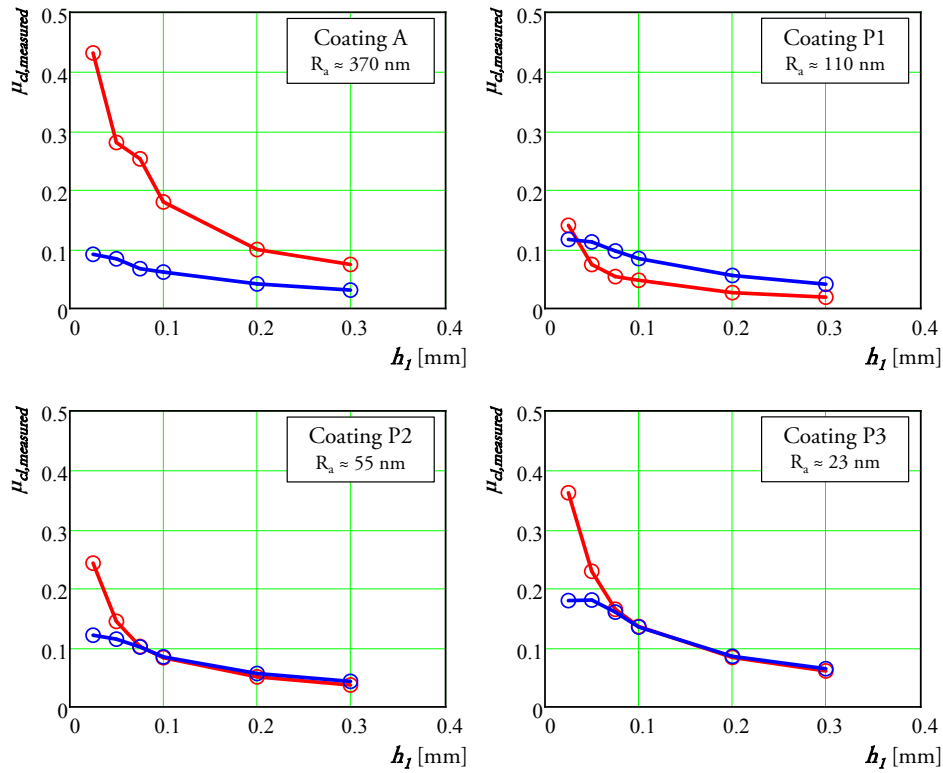

Figure 4.44 Contact conditions on the clearance face for the Standard (red) and SWL insert (blue) [130].

Through subtracting the obtained cutting forces for the Standard insert from those obtained for the SWL insert, the differences ΔF_c and ΔF_f may be obtained, Figure 4.45.

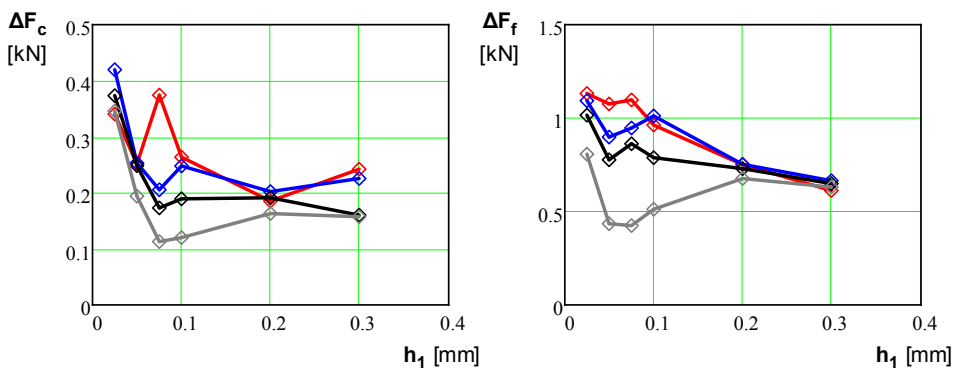

Figure 4.45 Experimentally obtained values of ΔF_c and ΔF_f for coatings A (red), P1 (blue), P2 (black) and P3 (gray) [130].

Figure 4.45 clearly illustrate a significant difference for the four coatings investigated. This difference is especially pronounced for ΔF_f at low values h_1. Through using this information it is possible to assess the average size of the stresses acting on the clearance face in the normal, $\bar{\sigma}_{N,cl}$, and tangential, $\bar{\tau}_{cl}$, direction for the SWL insert, Equation 4.43 and 4.44.

$$\bar{\sigma}_{N,cl} = \frac{\Delta F_f}{\left(VB_s - r_\beta\right) \cdot b_1} \qquad 4.43$$

$$\bar{\tau}_{cl} = \frac{\Delta F_c}{\left(VB_s - r_\beta\right) \cdot b_1} \qquad 4.44$$

The results obtained while using these equations are illustrated in Figure 4.46. As can be seen in the figure both the normal and tangential stresses appear to decrease as a function of h_1. Significant differences may also be noted for the different coatings investigated, especially for $\bar{\sigma}_{N,cl}$ at $h_1 < VB_s$.

When calculating the mean values of the stresses for each of the four coatings investigated, an interesting trend may be distinguished, Figure 4.47. For both the normal and shear stress the trend appear to be that a rougher tool surface micro topography will correspond to an increase of the stresses acting on the clearance face of the SWL cutting tool.

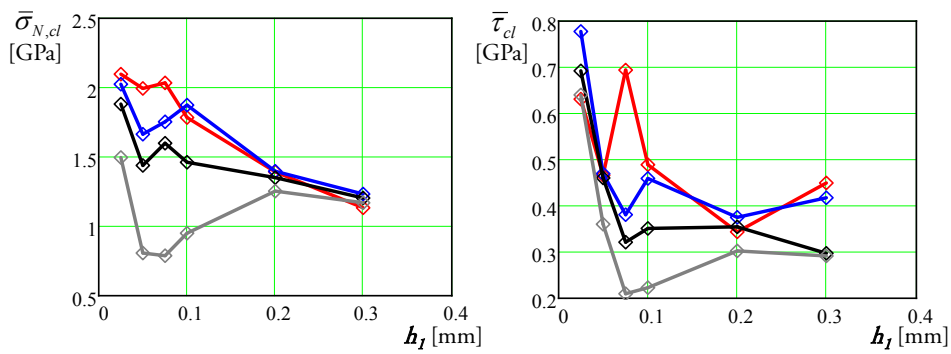

Figure 4.46 Stresses acting on the clearance face of the SWL cutting tool for coatings A (red), P1 (blue), P2 (black) and P3 (gray) [130].

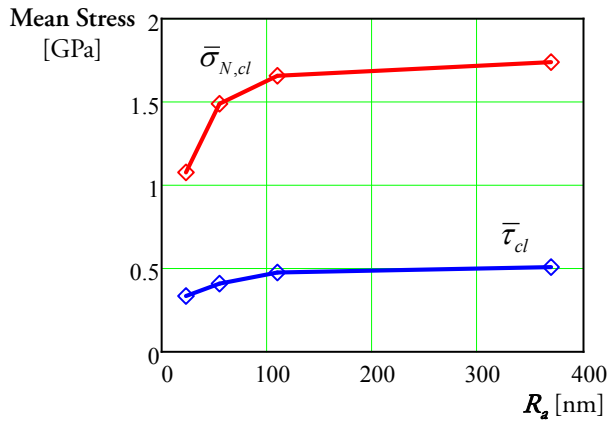

Figure 4.47 Mean values of the normal and shear stresses acting on the clearance face of the SWL inserts as a function of the tool surface micro topography [126].

4.4 Investigations of the Obtained Tool Wear

The obtained tool wear and in extension the obtained tool life are important factors for evaluating the machinability of a workpiece material in any machining process. Significant efforts by the scientific community have been devoted into modeling the tool wear and predicting the tool life during machining operations resulting in a substantial amount of knowledge and scientific publications. One of the pioneers in this field was Taylor who published his by now famous tool life equation 1906 [10]. He was consequently followed on the same subject by several other authors. One of the more famous of these was Colding [51, 52] who published a tool life model based on the use of an equivalent chip thickness h_e. A commonly used definition of h_e has been published by Woxén [131]. However, the accuracy of this equations at $a_p < r$ could be debated as presented in section 4.4.1. This inaccuracy in the major input parameter could potentially influence the precision of any tool life model based on the obtained results.

In general the model according to Colding only considers the wear gradually developing over time such as flank and notch wear. For many practical applications this may be enough but due to the increasing trend of using new, difficult to machine materials in different applications the importance of understanding other types of tool wear is also increasing. Large arrays of different types of tool wear might occur during varying machining processes while machining these new materials. For instance when discussing the machining of high performance materials such as duplex stainless steel,

Ti6Al4V and Alloy 718 deformation of the cutting edge due to for example plastic deformation is a concern during machining operations using cemented carbide inserts, not least due to the low thermal conductivity of the workpiece material in combination with a high strength at elevated temperatures. Machining situations resulting in plastic deformation of the cutting edge should be avoided to the fullest extent possible due to the rapid deterioration of the cutting edge during these conditions, possibly resulting in unacceptable product quality or tool failure. In order to avoid these conditions knowledge of when they occur must first be established. A new model for analyzing plastic deformation of the cutting tool has thus been developed and experimentally evaluated while machining Ti6Al4V (Paper VI) as presented in section 4.4.2.

4.4.1 Calculation of the equivalent chip thickness

Based on experience from industry it is very hard to predict tool life in finishing operations. There are several reasons why rough machining may easier be described in tool life models than finishing operations. One of these is how the value of the theoretical chip thickness h_1 varies during different process conditions. The theoretichal chip thickness could be considered as approximately constant when rough machining with large values of a_p as compared to the significant variation of h_1 during finishing operations at $a_p < r$. In Colding's tool life model the equivalent chip thickness h_e is used for evaluating the tool wear [51, 52]. In these publications the equivalent chip thickness was defined as previously published by Woxén [131], Equation 4.45. If studied closely, it can be concluded that Woxén's equivalent chip thickness has numerical deficiencies for $a_p < r$. Figure 4.48 principally illustrates how the active cutting length is divided into three segments while calculating the equivalent chip thickness according to Woxén's definition.

$$h_{eW} = \frac{a_p \cdot f}{\frac{a_p - r \cdot (1 - \cos\kappa)}{\sin\kappa} + \kappa \cdot r + \frac{f}{2}} \qquad 4.45$$

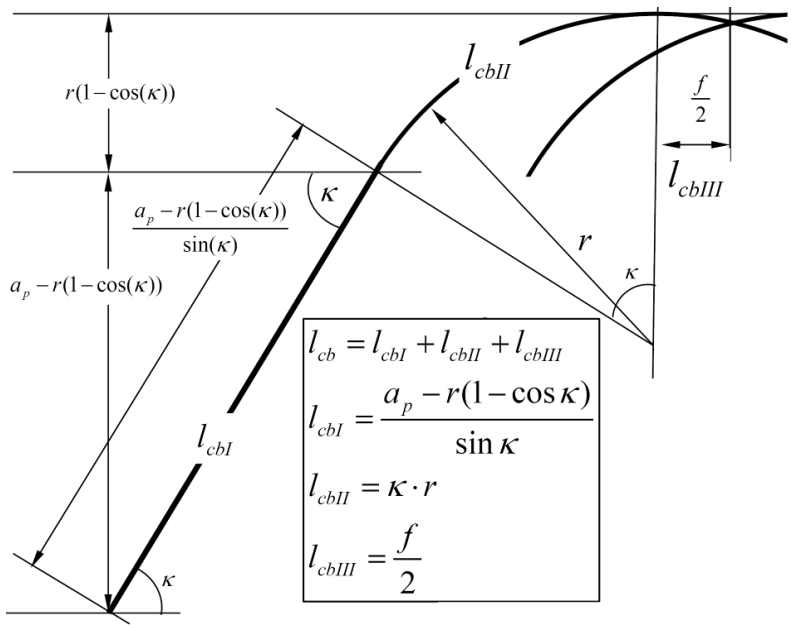

Figure 4.48 Principle illustration of the division of the active cutting length into three separate regions as proposed by Woxén [5].

Equation 4.45 is obtained by approximating the chip area as a rectangle obtained by straightening out the chip area at the tool nose radius. This is principally illustrated in Figure 4.49. Additional relationships for calculating the equivalent chip thickness has since then also been published by Bus et al. [92], Hodgson and Trendler [132], Carlsson and Stjernstoft [133] and Hägglund [134]. In addition to the tool life model as presented by Colding [51, 52], Kals and Hijink [135] used the equivalent chip thickness while developing a method for optimizing turning conditions. Also, Choi [136] used the equivalent chip thickness while analyzing chip breaker design. A problem with the definition of the equivalent chip thickness according to Woxén is that it contains a simplification while calculating the chip area at the tool nose radius which produces a significant error when using small depths of cut as compared to the tool nose radius. Since this scenario is not uncommon while machining difficult to machine materials a more accurate description of the equivalent chip thickness was sought for.

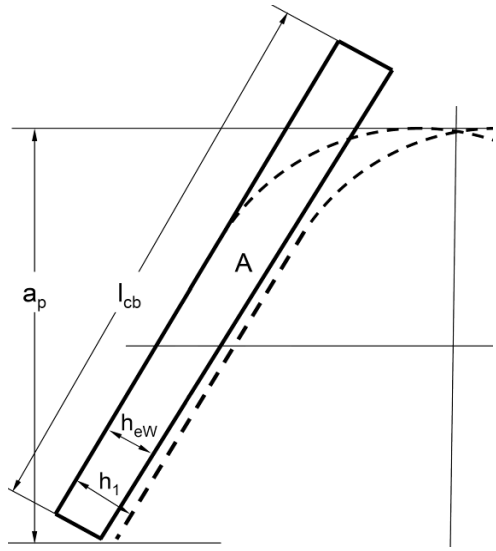

Figure 4.49 Principle illustration of Woxéns chip area and related equivalent chip thickness h_{eW} [5].

As previously presented, the value of the theoretical chip thickness h_1 will vary along the tool nose radius. Through geometrical observation as presented by among others Brammertz [107] a theoretical relationship between the different significant parameters could be identified. A relationship between the theoretical chip thickness h_1, feed f, and nose radius r can be identified and calculated according to Equation 4.20. The case of $a_p < r$ is principally illustrated in Figure 4.22 and Figure 4.50. The angular position δ_0 is used for describing the value of δ at $h_1 = 0$ and may be calculated according to Equation 4.46.

$$\delta_0 = -\sin^{-1}\left(\frac{f}{2 \cdot r}\right) \qquad 4.46$$

Three additional angular positions, δ_{ap}, δ_{cap} and δ_c, could be identified and defined according to Figure 4.22 and Figure 4.50. The value of each of these can be determined according to Equation 4.47 to Equation 4.49.

$$\delta_{ap} = \tan^{-1}\left(\frac{-f + \sqrt{2 \cdot r \cdot a_p - a_p^2}}{r - a_p}\right) \qquad 4.47$$

$$\delta_{cap} = \cos^{-1}\left(\frac{r - a_p}{r}\right) \qquad 4.48$$

$$\delta_c = \delta_{cap} - \delta_{ap} \qquad 4.49$$

As can be seen in Figure 4.50 the chip area can be identified as the sum of 3 different surface elements, Equation 4.50. These surfaces are the surface A_n with integration limits (δ_0, δ_{ap}), the triangular surface A_t, and the segmental surface A_c which can be calculated through using the chord formula. Equations for calculating each of these areas can be found in Equation 4.51 to 4.53.

$$A = A_n + A_t + A_c \tag{4.50}$$

$$A_n = \int_{\delta_0}^{\delta_{ap}} h_1(\delta) \cdot (r - \frac{h_1}{2}) d\delta \tag{4.51}$$

$$A_t = \frac{f \cdot h_{1\max} \cdot \cos(\delta_{ap})}{2} \tag{4.52}$$

$$A_c = \frac{r^2}{2}\left(\delta_c - \sin\left(\delta_c\right)\right) \tag{4.53}$$

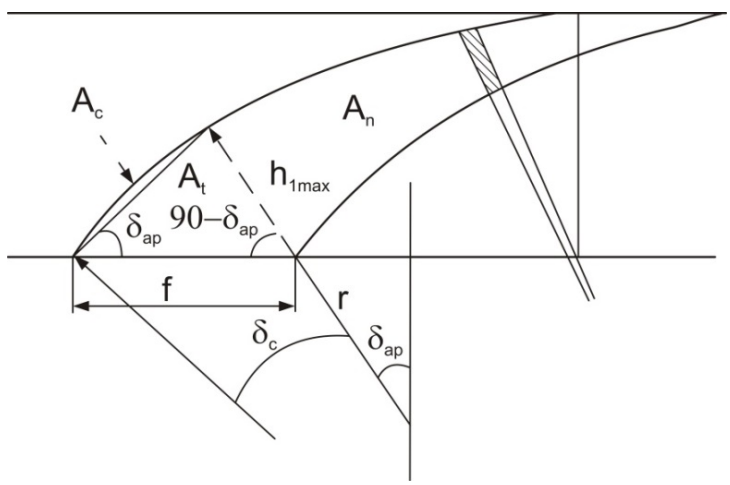

Figure 4.50 Principle division of the chip area into three separet areas for $a_p < r$ [137].

The surfaces A_n and A_t are dominant in size while the contribution of the A_c surface could be considered as insignificant for most practical machining cases. Unfortunately, Equation 4.51 does not have any analytical solution due to that the derivate of the chip area as a function of the angular coordinate lacks a primitive function. For $a_p > r$ the addition to the equivalent chip thickness h_e can be calculated by adding the area corresponding to the major cutting edge, $f \cdot (a_p - r) \cdot \sin(\kappa)$ [5]. The proposed model allows h_e to be calculated for any arbitrary value of the major cutting edge angle κ by setting the upper integration limit to κ in Equation 4.51. For $a_p < r$ the length of the active cutting edge, l_c, is composed by 3 parts, Equation 4.54.

$$l_c = r \cdot (|\delta_0| + \delta_{ap} + \delta_c) \qquad 4.54$$

The equivalent chip thickness h_e can be calculated as the ratio between the chip area A and the active cutting length l_c. Thus, the equivalent chip thickness may be calculated according to Equation 4.55.

$$h_e = \frac{A}{l_c} = \frac{\int_{\delta_0}^{\delta_{ap}} h_1(\delta) \cdot (r - \frac{h_1}{2}) d\delta + \frac{f \cdot h_{1\max} \cdot \cos(\delta_{ap})}{2} + \frac{r^2}{2}\left(\delta_c - \sin(\delta_c)\right)}{r \cdot \left(\sin^{-1}\left(\frac{f}{2 \cdot r}\right) + \tan^{-1}\left(\frac{-f + \sqrt{2 \cdot r \cdot a_p - a_p^2}}{r - a_p}\right) + \left(\delta_{cap} - \delta_{ap}\right)\right)} \qquad 4.55$$

If comparing the new equation for calculating h_e with the simplified expression according to Woxén, h_{eW}, the following difference could be discerned for a selected range of cases, Figure 4.51. As can be seen in Figure 4.51, significant differences may be discerned at low values of a_p. However, while increasing a_p these differences will decrease and become insignificant from a practical perspective at a certain value of a_p which still will be smaller than the tool nose radius r. It is also of interest to note that the difference between the two different models is indistinguishable for large values of a_p possibly indicating that the proposed model is valid for all values of a_p.

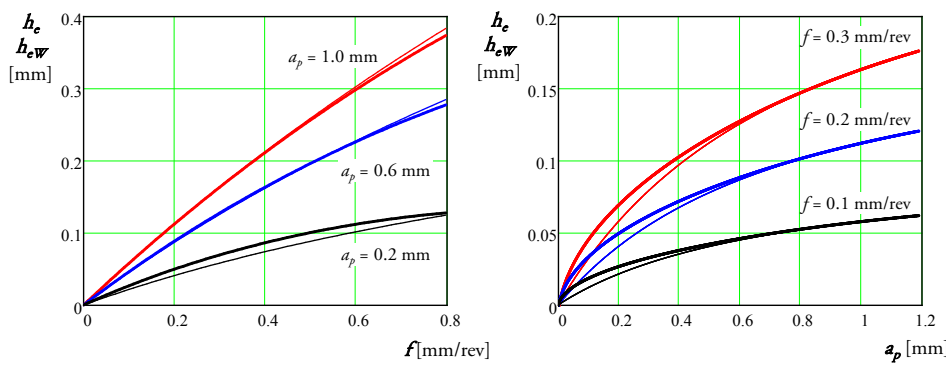

Figure 4.51 Comparison between h_e (thick lines) and h_{eW} (thin lines) as a function of feed f and depth of cut a_p for r = 1.2 mm.

4.4.2 Evaluation of geometrical deformations of the tool

Cutting tools often encounter high thermal and mechanical loads during machining operations. This is especially true while machining difficult to machine materials such as nickel- and titanium alloys as well as duplex stainless steel. Commonly, high

mechanical loads and elevated temperatures results in plastic deformation of the cutting tool. According to Astakhov [138] plastic deformation of the cutting tool is the predominant cause for premature tool failure when machining difficult to machine materials. Ideally any machining conditions resulting in large scale deformation of the cutting tool should be avoided. If however it is impossible to avoid plastic deformation of the cutting tool Kuljanic [139] suggests a series of steps to maximize the tool utilization:

1. The cutting data for a given workpiece material and cutting tool should be determined during rough machining at which plastic deformation of the cutting tool occurs. This should be done through using cutting force sensors and/or acoustic emission sensors.
2. The cutting speed should be decreased gradually until no plastic deformation of the cutting tool occurs.
3. If plastic deformation of the cutting tool is still present at low cutting speeds the feed should gradually be decreased until no plastic deformation of the cutting tool occurs.
4. As a last resort the depth of cut could be decreased until no plastic deformation of the cutting tool occurs.

To achieve the goal of avoiding plastic deformation a reliable method for determining at which conditions deformation of the cutting tool occurs is thus required. As a result a new method for experimental identification of geometrical changes of the cutting tool during machining was developed, Paper VI. The proposed method was validated for the case of machining Ti6Al4V with coated cemented carbide tools. However, the intention was to create a method suitable for all workpiece materials and thus the general format of the whole model was created in order to be possible to implement during other machining scenarios at a later stage.

Today, machining of titanium alloys is a topic of great interest for industrial production and scientific research worldwide [140]. The reason for choosing Ti6Al4V during this study was due to the previously reported rapid tool wear during machining which has been reported as being due to the following reasons [62, 65, 141, 142]:

- Variations of the mechanical stresses acting on the cutting tool due to the formation of segmented chips.
- High temperature concentration at the edge of the cutting tool primarily due to the low thermal conductivity of the workpiece material.
- Enhanced chemical reactivity between the workpiece material and the cutting tool at elevated temperatures.

Out of these three factors primarily the high temperature during machining could be thought as having a pronounced effect on the plastic deformation of the cutting tool. Several different approaches for decreasing the temperature while machining Ti6Al4V have previously been published, for instance by using a high-pressure coolant [143] or liquid nitrogen [144]. Through reducing the process temperature these methods could be expected to reduce the risk of plastic deformation of the cutting tool during machining operations. Jawaid et al. [145] investigated the different types of tool wear occurring during face milling of Ti6Al4V. They found that although several different types of wear mechanisms could be identified, plastic deformation of the cutting tool occurred during most of the investigated cutting conditions. Meng et al. [146] attempted to predict the cutting conditions resulting in plastic deformation of the cutting tool. Their model does however contain several limitations which decrease the usefulness for the current application. For a general machining operation a change in tool geometry will result in a change of the load distribution acting on the cutting tool. Thus, in theory it might be possible to evaluate the change of tool geometry by comparing the load distribution of the unworn tool with the current load on the worn tool. Thus, a hypothesis was formed that it could be possible to conclude whether or not a change of the tool geometry has occurred through analyzing the variation of the load distribution acting on the cutting tool.

The load on the clearance face of the cutting tool changes when plastic deformation occurs or after a certain level of progressive tool wear has been attained. Through analyzing the load ratio between the unworn and worn tool a deterioration factor φ_{DF} may be calculated which in turn could be used to determine the degree of geometrical change of the cutting tool. Ståhl [147] has previously introduced 5 load functions. Two of these load functions are used for describing the value of the cutting forces acting in the feed- and passive directions in relationship to the main cutting force acting in the tangential direction, Equation 4.56 and Equation 4.57.

$$\varphi_{AT} = \frac{F_f}{F_c} = \frac{D_2 + D_1 \cdot h_1}{C_2 + C_1 \cdot h_1} \qquad 4.56$$

$$\varphi_{RT} = \frac{F_p}{F_c} = \frac{E_2 + E_1 \cdot h_1}{C_2 + C_1 \cdot h_1} \qquad 4.57$$

The three other load functions are intended to describe the load ratio between forces acting on the clearance face and the total cutting force in each direction, Equation 4.58 to 4.60.

$$\varphi_T = \frac{C_{22} + C_{21} \cdot VB}{C_{22} + C_{21} \cdot VB + C_1 \cdot h_1} \qquad 4.58$$

$$\varphi_A = \frac{D_{22} + D_{21} \cdot VB}{D_{22} + D_{21} \cdot VB + D_1 \cdot h_1} \quad 4.59$$

$$\varphi_R = \frac{E_{22} + E_{21} \cdot VB}{E_{22} + E_{21} \cdot VB + E_1 \cdot h_1} \quad 4.60$$

Progressive tool wear, tool deformation or other types of damage on the clearance face of the cutting tool will increase the relative ratio of the force on the clearance face of the cutting tool as compared to the rake face. Through using experimentally measured cutting forces all cutting force coefficients may be determined for an unworn cutting tool. If assuming that the geometrical change of a specific cutting tool is only associated with the clearance face the coefficients D_1, E_1 and C_1 will remain constant. Further, the changes of the cutting forces acting on the tool may then be directly related to the coefficients D_2, E_2 and C_2 and calculated according to Equation 4.61 [5].

$$\begin{aligned} C_{2z} &= F_{cz} - C_1 \cdot h_1 \\ D_{2x} &= F_{fx} - D_1 \cdot h_1 \\ E_{2y} &= F_{py} - E_1 \cdot h_1 \end{aligned} \quad 4.61$$

In this equation x, y and z denotes the measured data where the variables were measured in different directions in relationship to the workpiece. Based on Equation 4.61 the load functions may be rewritten according to Equation 4.62.

$$\begin{aligned} \varphi_{Ax} &= \frac{F_{fx} - D_1 \cdot h_1}{F_{fx}} \\ \varphi_{Ry} &= \frac{F_{py} - E_1 \cdot h_1}{F_{py}} \\ \varphi_{Tz} &= \frac{F_{cz} - C_1 \cdot h_1}{F_{cz}} \end{aligned} \quad 4.62$$

Any changes of the normal forces acting on the clearance face of the tool (related to coefficients D_2 and E_2) have a strong correlation to geometrical changes of the cutting tool. If considering that the D_2 and E_2 constants are contributing to normal forces on the clearance face these forces can be considered as significantly stronger indicators than the coefficient C_2 contributing to a shear force on the clearance face. Through calculating the ratio between the normal force measured at any given cutting situation and the normal forces acting on a new tool the relative load change on the clearance face can be determined. This ratio is referred to as the cutting tool deterioration factor, φ_{DF}. The deterioration factor can be calculated in either the axial or radial

direction, or in the horizontal plane as based on the vector sum of D_2 and E_2. The deterioration factor φ_{DF}^{A} in the axial direction may be calculated as follows, Equation 4.63.

$$\varphi_{DF}^{A} = \frac{\varphi_{Ax} \cdot \varphi_{ATxz} \cdot F_{cz}}{\varphi_{A} \cdot \varphi_{AT} \cdot F_{c}} \qquad 4.63$$

The corresponding equation for the horizontal plane can be defined according to Equation 4.64.

$$\varphi_{DF}^{H} = \frac{\sqrt{\left(\varphi_{Ax} \cdot \varphi_{ATxz}\right)^2 + \left(\varphi_{Ry} \cdot \varphi_{RTyz}\right)^2} \cdot F_{cz}}{\sqrt{\left(\varphi_{A} \cdot \varphi_{AT}\right)^2 + \left(\varphi_{R} \cdot \varphi_{RT}\right)^2} \cdot F_{c}} \qquad 4.64$$

A difficulty while using the proposed method is that the cutting forces are dependent upon the value of the cutting speed. As a result the deterioration factor must be compensated for the general decrease of cutting forces attributed to increased cutting speeds. An approximate compensation factor can be defined according to Equation 4.65 which describes the ratio between the main cutting force at the current cutting speed $F_c(v_c)$ and the main cutting force at a reference cutting speed $F_c(v_{c,ref})$.

$$\chi_{vc,comp} = \frac{F_c\left(v_c\right)}{F_c\left(v_{c,ref}\right)} \qquad 4.65$$

By multiplying the deterioration factor with this compensation factor an approximate compensation can be performed. In order to achieve a good compensation the calculations of the compensation factor should be done at the highest feasible value of the theoretical chip thickness h_1 while still allowing for an undamaged cutting tool. For any cutting data combinations resulting in instantaneous deformation of the cutting tool the modeled cutting forces should be used. Even though this implies an approximation of the true value this operation will still produce a better result than the alternative of neglecting the compensation factor altogether.

As an initial step towards validating the proposed method, experiments were performed by longitudinall turning Ti6Al4V while stepwise increasing the feed value. These experiments were performed by using a CNMG120408 coated cemented carbide cutting tools set at a major cutting edge angle of κ = 90°. During all these experiments the depth of cut was held constant at a_p = 2 mm and a new tool was used for each cutting speed in order to minimize the potential influence of any tool wear. Further, two different tool grades denoted “Grade A” and “Grade B” were evaluated and compared. Grade A is slightly harder than Grade B which in turn has a higher ductility. The static cutting force values were measured during all experiments

through using a standard piezoelectric dynamometer. The measured signals were low pass filtered; reducing the amplitude of frequencies above 10 Hz. Figure 4.52 below illustrated an example of the obtained results. In this case no visible tool deformation was present on the cutting tool and thus these results were possible to use while calculating the reference parameters for an undamaged cutting tool.

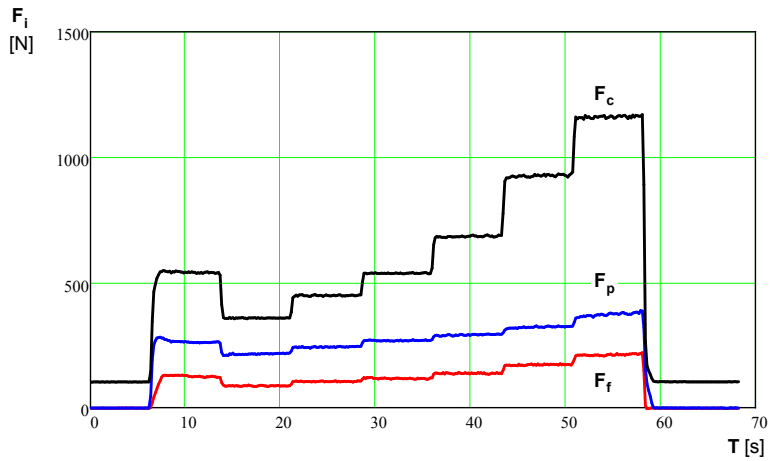

Figure 4.52 Measured cutting forces for Grade A at v_c = 70 m/min with no visible tool deformation [148].

As can be seen in Figure 4.52 the measured cutting forces are approximately constant for each combination of cutting data. This is however not true for a machining case where the cutting tool is deformed, Figure 4.53.

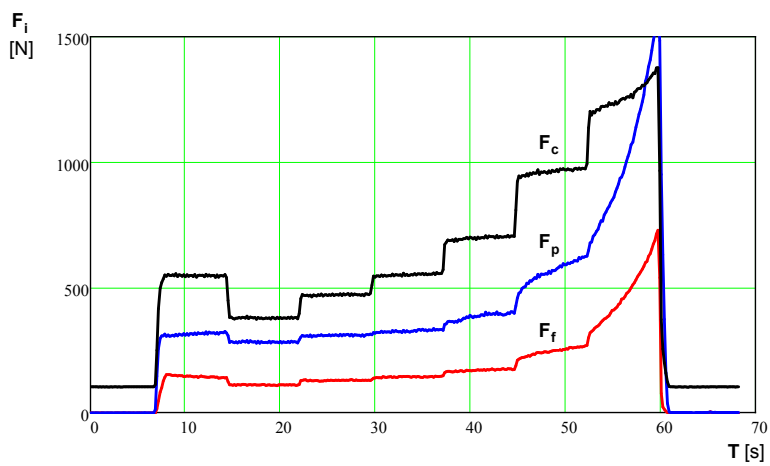

Figure 4.53 Measured cutting forces for Grade B at v_c = 110 m/min resulting in significant deformation of the cutting tool [148].

The obtained results for each machining case are summarized in Table 4.14 and Table 4.15 below. In these tables any plastic deformation, or similar geometrical tool changes that produce a significant increase of the deterioration factor $\varphi_{DF}^{A} \geq 1.5$, are marked in red. In both cases the obtained results have been compensated for the increased cutting speed according to Equation 4.65. Also, the denotation "1^{M}" specifies that the data has been used to calculate the model coefficients for an unworn cutting tool.

Table 4.14 Calculated deterioration factors for Grade A based on experimentally obtained results.

v_c [m/min]	φ_{DF}^{A} at varying h_1 [mm]					
	0.050	**0.075**	**0.10**	**0.15**	**0.25**	**0.35**
70	1^{M}	1^{M}	1^{M}	0.9	0.6	0.2
80	1	0.9	0.9	0.8	0.4	-1.2
90	1.1	1.1	1.1	1.3	1.8	4.4
100	1.1	1.2	1.2	1.4	2.8	9.0
110	1.1	1.1	1.1	1.1	1.5	3.9
120	1.0	1.0	1.0	1.1	1.8	6.4
130	0.8	0.9	0.9	1.1	2.2	7.3

As can be seen in Table 4.14, 10 different investigated machining cases resulted in a deformation of the cutting tool increasing the normal load on the tool clearance face by up to more than 700%. Equivalent results were also obtained for Grade B as illustrated in Table 4.15. Note the difference in cutting data resulting in deformation of the cutting tool for these two cases.

Table 4.15 Calculated deterioration factors for Grade B based on experimentally obtained results.

v_c [m/min]	φ_{DF}^{A} at varying h_1 [mm]					
	0.050	**0.075**	**0.10**	**0.15**	**0.25**	**0.35**
60	1^{M}	1^{M}	1^{M}	1.0	0.5	0.3
70	1.1	1.0	1.0	1.0	1.3	2.2
80	1.1	1.0	1.1	1.1	1.6	3.5
90	1.0	0.9	0.9	0.8	1.0	2.6
100	0.9	0.9	0.9	0.9	1.6	4.6
110	1.2	1.2	1.2	1.2	2.9	17.5
120	1.3	1.2	1.2	1.4	4.4	17.8

From these results it is evident that Grade B will be deformed at a lower cutting speed than Grade A given that a sufficiently large feed is used. From the obtained results it

is also evident that φ_{DF}^{A} is dependent upon the h_1 value. However, no clear difference between the two grades investigated was found in this respect.

Figure 4.54 illustrates a comparison of the modeled values as compared to experimentally obtained values of the axial load function φ_A as a function of h_1. In this figure the theoretical values for an undamaged tool is represented by a solid line and the real, measured values are represented by red circles. The values for the undamaged tool are approximately equal to the measured values of φ_A for low values of h_1 and thus indicating that no deformation of the cutting tool has occurred for these values of h_1. However, for large values of h_1 the theoretical values of φ_A for an undamaged tool and the measured values differ significantly, thus indicating that the tool has been deformed.

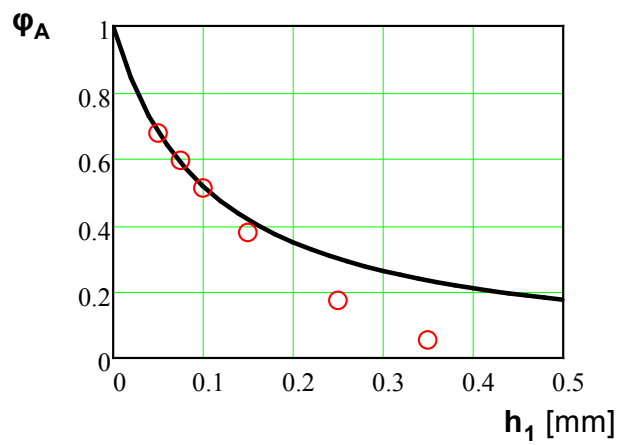

Figure 4.54 Comparison between modeled and measured values of φ_A for tool Grade A at v_c = 70 m/min [148].

A possible way of illustrating the obtained values of φ_{DF}^{A} can be found in Figure 4.55. Note how the values of the deterioration factor increasingly differ from the reference value for high values of h_1. In addition to the force measurments some used tools were evaluated via SEM microscopy in order to observe the attained tool deformation during each machining case, Figure 4.56. As can be seen in Figure 4.56 the type of deformation differes depending on machining case. For the lower of the two cutting speeds it is difficult to visually distinguish any plastic deformation, independently of tool grade. However, for the two cases of high cutting speeds illustrated in the lower part of the figure significant deformation may be discerned which corresponds well to the expected results as obtained while analyzing the deterioration factors. However, the type of deformation varies for the two tool grades. For Grade A chipping of the

cutting edge as well as removal of the coating may be discerned. For Grade B a significant plastic deformation of the cutting tool is instead evident.

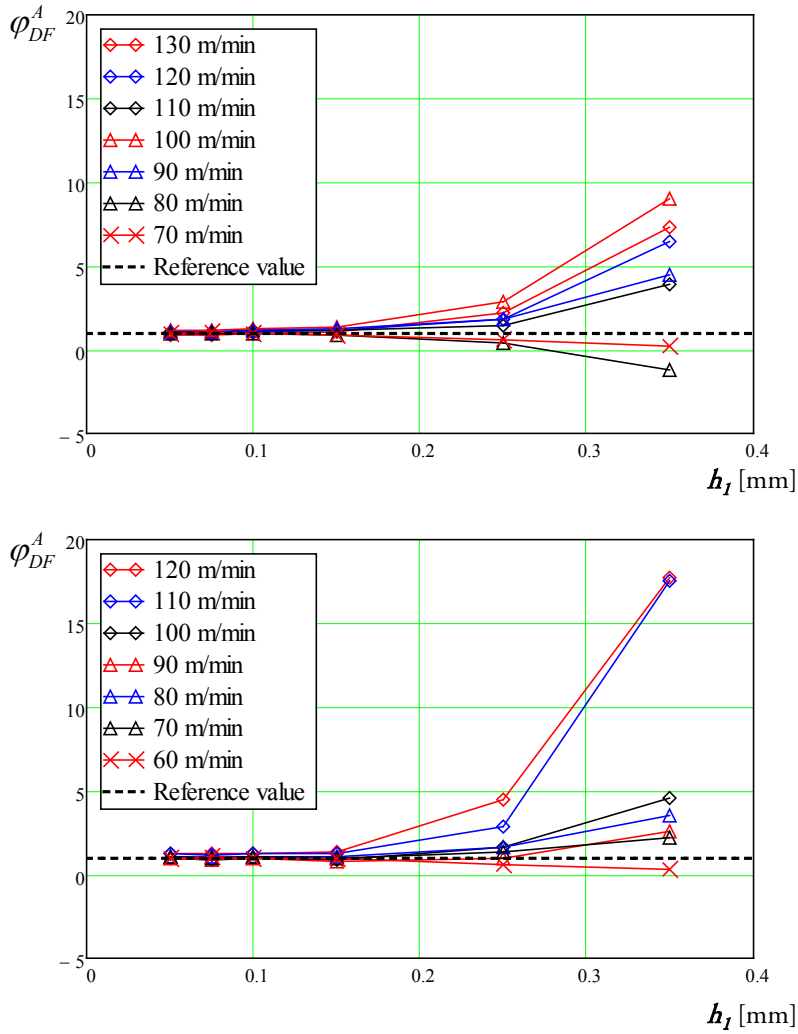

Figure 4.55 Progression of the deterioration factor φ^A_{DF} for different values of h_1 and cutting speeds v_c for Grade A (top) and Grade B (bottom) [148].

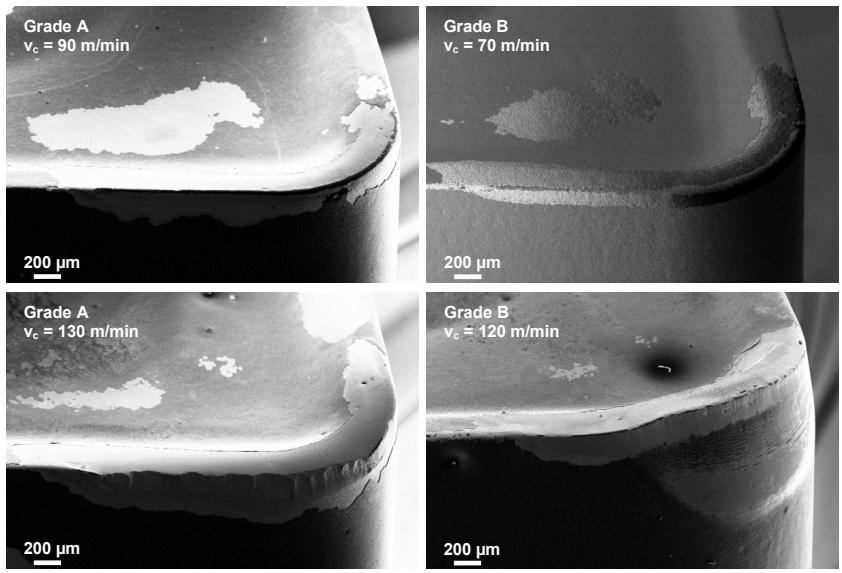

Figure 4.56 Examples of the tool deformation obtained at varying process conditions [148].

It may also be of interest to note that in both of these cases cracks were discernible, running roughly parallell to the edge of the cutting tool along a large part of the active cutting edge as examplified in Figure 4.57. The reason for the formation of these cracks is however currently unknown. It should be mentioned that φ_{DF} can only be used to distinguish wether or not any deformation of the cutting tool has occurred, not which type of deformation the tool has sustained. In order to determine the type of deformation further investigations are required for each machining case.

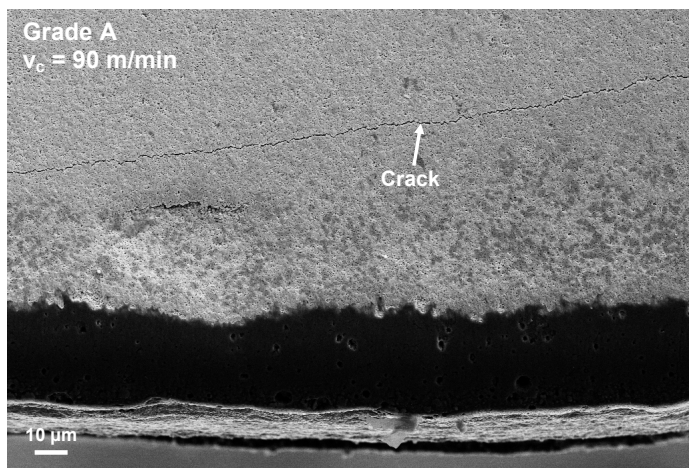

Figure 4.57 Example of a observed crack running roughly parallell to the edge of the cutting tool [148].

While performing these observations an interesting trend in the tool wear was observed. All machining cases investigated resulted in removal of the coating of the cutting tool even though the extent varied from case to case. However, for all machining cases investigated a thin band of coating remained at the active tool edge as exemplified in Figure 4.58. The author's theory is that this is due to the influence of the stagnation zone resulting in significantly different process conditions for this part of the cutting edge.

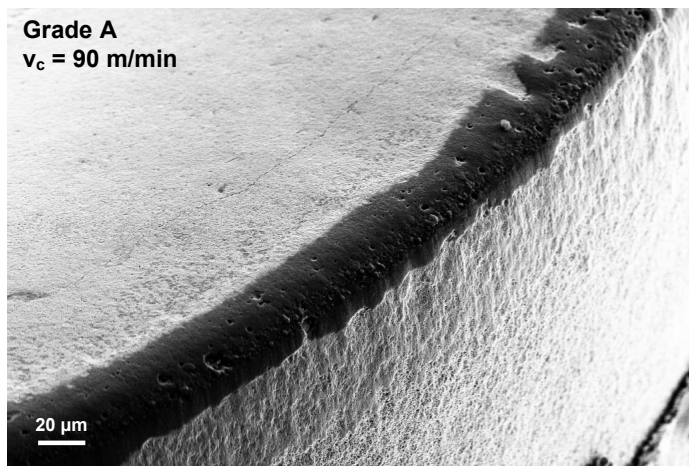

Figure 4.58 Example of obtained tool wear along the active cutting edge [148].

4.5 Optimization of the Machining Process

A machining process may be optimized towards one or more of several different goals. Often the goal is to minimize the production cost or maximize the production rate but it might as well be to increase the product quality or increase the sustainability of the manufacturing process. This section presents a novel approach for incrementally improving the production process during conventional production, section 4.5.1. In addition an innovative method for increasing the cutting tool utilization during both milling and turning operations is presented, section 4.5.2.

4.5.1 Incremental production improvements

A common problem during conventional production is the substantial amount of resources required for improving a production process. Often this results in a very

limited amount of improvements after commencing normal production. Part of the solution to this problem could be so called incremental production improvements. This improvement process, presented in Paper VII, is based on structured variations of predetermined process parameters combined with careful documentation of the obtained results. During these investigations the proposed method was implemented on a conventional machining process but it is plausible that a similar approach could be used for other manufacturing processes, although with minor alterations.

The aim of the incremental production improvement process is to refine a current machining process. Thus, it can be assumed that the workpiece material as well as cutting tool has been predetermined. Some changes to these parameters might be possible even during production, but these changes are commonly complex and resource intensive. Thus, a simpler optimization process can be obtained through only considering variations of the cutting data. During many machining operations performed in industry the depth of cut is predetermined due to the size of the workpiece as compared to the finished part. Thus, out of the three parameters constituting the cutting data only the feed and cutting speed may commonly be varied. Variations of the cutting data will primarily influence the tool life and quality of the machined part. These variations will in turn influence the obtained manufacturing cost for a specific part. Through carefully recording the obtained results for different combinations of cutting data a minimum cost alternative may be recognized. Depending on circumstances these new process parameters may then be used as the starting point for a new incremental improvement process.

Several tool life models have been published through the years by among others Taylor [10], Kronenberg [50] and Colding [51, 52]. The results from the incremental production improvement process could be used for modeling the tool life through using any one of these equations given that an appropriate amount of data has been collected for each case. Often this tool life modeling could even be done while using fewer measuring points than the proposed incremental production improvement process. However, through using the proposed method several other positive characteristics could be attained. The primary of these is the pure simplicity of the proposed process. With minimal training and instructions it is plausible that any operator could manage to collect and analyze the obtained results. Thus, the operators will be able to improve their manufacturing process without involving any other assets at the company. This may also have the positive side-effect that the operators themselves will become more interested in further optimizing their production process and thus other process improvements could be obtained.

Lean Production is a well-known and widespread production philosophy made famous by among others Womack et al. [149]. Lean Production has also been further

described by among others Voss et al. [150], Hay [151] and Monden [152]. The Lean Production philosophy contains several different positive aspects, some of which could be linked to the implementation of the incremental production improvement process. For instance the involvement, participation and motivation of all employees are central parts of the Lean Production philosophy as well as effective use of resources and visualization of problems. In addition to Lean Production the Next Step philosophy as published by Ståhl [9] further emphasizes the importance of using economic indicators as the basis for decisions during industrial production.

As part of the validation procedure the incremental production improvement process was implemented at a small Swedish company while machining a commercial part of solution annealed Alloy 718. This part was primarily manufactured through a series of turning operations as well as some additional drilling operations. In addition to varying the feed f and cutting speed v_c the cutting fluid was also varied through the addition of 5% sulfur. Several different cutting tools were used to manufacture the investigated part, four of which are presented in this dissertation to illustrate the variation of cutting operations used for producing the specific part. A short summary of the four operations as well as their original cutting data can be found in Table 4.16. For all operations used by the company a flank wear criterion, VB_{crit}, was used in order to determine when a specific tool could be considered as worn out. Due to the small diameter of the drill used during Operation D it was thought as unrealistic to use the traditional tool wear criterion of VB = 0.3 mm. Thus, it was decided that for this operation, Operation D, the tool life criterion should be that VB may not exceed 5% of the drill diameter. This decision was based on previous experience about reasonable values of the tool wear during drilling operations. However, the validity of this assumption should be further investigated in the future.

Table 4.16 Examples of the initial cutting data used by the company while producing a part of solution annealed Alloy 718.

Operation	Description	a_p [mm]	f [mm/rev]	v_c [m/min]	VB_{crit} [mm]
A	General turning	0.2	0.06	87	0.3
B	Facing	0.2	0.06	87	0.3
C	Grooving	0.8	0.04	28	0.6
D	Drilling	1.05	0.022	14	0.105

Through varying both the feed and the cutting speed ±10% of their original value, it was possible to observe a varying tool life as a function of the cutting data used. In addition to the tool life the scrap rate q_Q was monitored during all machining cases. The cutting data was varied according to Table 4.17 during this investigation.

Table 4.17 Variation of the cutting data used during this investigation as a function of the original cutting data used by the company.

Machining case nr.	0	1	2	3	4	5	6	7	8
Variation of f [%]	0	-10	+10	0	0	-10	+10	-10	+10
Variation of v_c [%]	0	0	0	-10	+10	-10	-10	+10	+10
V_{rel} [%]	100	90	110	90	110	81	99	99	121

The obtained results were evaluated through calculating the part cost by using the part cost equation as proposed by Ståhl et al. [153] and then further improved by Jönsson et al. [154], Equation 4.66. In this equation knowledge of the hourly cost for machines during production k_{cp}, Equation 4.67, as well the hourly cost for machines during downtime and setup k_{cs}, Equation 4.68, is required. In turn both of these variables are a function of the annuity factor a, Equation 4.69, as previously described by Ståhl [8]. All variables used in Equation 4.66 to Equation 4.69 are defined according to Table 4.18. Due to lack of input data the used model was simplified from the original version through assuming that the production equipment was in use 100% of the available production time.

$$k = \frac{k_B}{\left(1-q_Q\right)} + \frac{k_{CP}}{60N_0}\cdot\frac{t_0 N_0}{\left(1-q_Q\right)\left(1-q_P\right)} + \frac{k_{CS}}{60N_0}\left(\frac{t_0 N_0}{\left(1-q_Q\right)\left(1-q_P\right)}\cdot\frac{q_S}{\left(1-q_S\right)} + T_{su}\right) + \frac{k_D}{60N_0}\left(\frac{t_0 N_0}{\left(1-q_Q\right)\left(1-q_S\right)\left(1-q_P\right)} + T_{su}\right) \quad 4.66$$

$$k_{CP} = \frac{a\cdot K_0 + k_{UH}}{T_{plan}} + \frac{k_A}{t_0}\cdot 60 \quad 4.67$$

$$k_{CS} = \frac{a\cdot K_0}{T_{plan}} \quad 4.68$$

$$a = \frac{p\cdot\left(1+p\right)^n}{\left(1+p\right)^n - 1} \quad 4.69$$

Table 4.18 Definition of variables used for economic calculations according to Equation 4.66 to Equation 4.69.

Variable	Description
a	Annuity factor
k	Part cost
K_0	Basic investment in production equipment
k_A	Tool cost
k_B	Material cost per part including scrap
k_{CP}	Hourly cost for machines during production
k_{CS}	Hourly cost for machines during downtime and setup
k_D	Worker salary
k_{UH}	Maintenance cost
n	Economic lifetime of production equipment
N_0	Nominal batch size
p	Interest rate
q_P	Production rate
q_Q	Scrap rate
q_S	Downtime rate
t_0	Nominal cycle time per part
T_{plan}	Scheduled production time per year
T_{su}	Setup time for a single batch

In order to be able to compare the obtained results the relative chip flow volume, V_{rel}, was defined, Equation 4.70. In this equation "*0*" indicates the original machining conditions and "*i*" indicates the current machining conditions. Note that during all of these experiments the depth of cut a_p remained constant.

$$V_{rel} = \frac{f_i \cdot v_{c,i} \cdot a_{p,i}}{f_0 \cdot v_{c,0} \cdot a_{p,0}} \qquad 4.70$$

The following results were obtained for the investigated machining scenario, Figure 4.59. As may be discerned in the figure it is possible to lower the part cost by approximately 5% through using the incremental production improvement process. Further research is however needed in order to scrutinize any potential limitations attributed to the use of the process. Even though the use of this method may result in local optimization of the part cost this improvement is still better than none at all. A major advantage of the incremental production improvement process is also the involvement of the operators in the improvement process. With proper training and software it is feasible that the operators could handle these optimizations by themselves without involvement of any senior staff. This could in turn be seen as a motivation for all staff to continuously evaluate and improve their part of the production process.

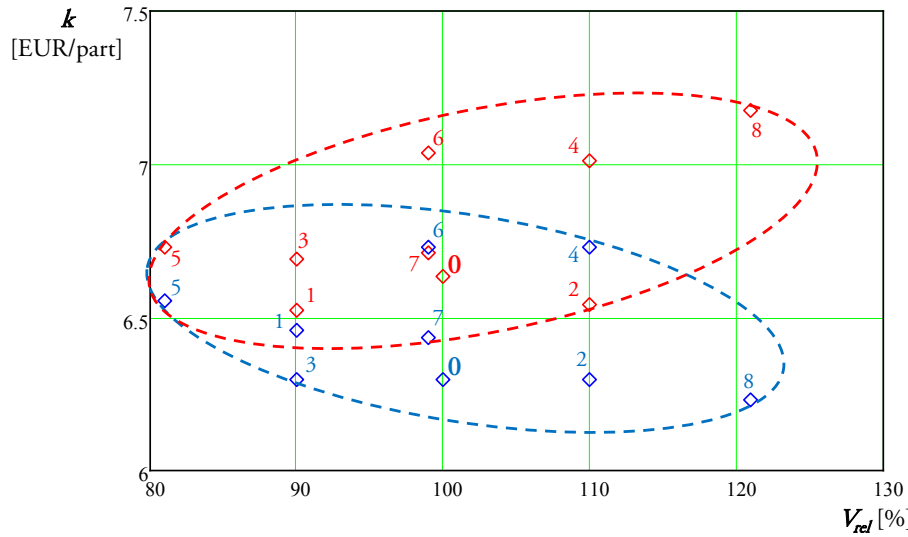

Figure 4.59 Obtained part costs for the different combinations of process parameters investigated at the participating company (Red – Original cutting fluid, Blue – Modified cutting fluid) [155].

4.5.2 Increasing the cutting tool utilization

During 1987 sustainable development was defined by the United Nations as "development that meets the needs of the present without compromising the ability of future generations to meet their own needs" [53]. The sustainable production concept emerged during the United Nations Conference on Environment and Development UNCED 1992 [54]. As has previously been stated by Jovane et al. [55], enabling of sustainable production is an important step for achieving sustainable development. Smith and Ball [156] emphasizes the need for a holistic view of the whole manufacturing process in order to identify potential strategies for improving the sustainability during any production process. For instance Duflou et al. [157] stress the importance of choosing an appropriate manufacturing process as a crucial measure for achieving sustainable production. While choosing production process it is important to evaluate the process sustainability in addition to the more traditional technical and economical limitations. As expressed by Ståhl [9] it is important to establish a clear link between technology and economy in order to achieve a sustainable production process. In addition, it is imperative that sustainable development goes hand in hand with technological development. This could possibly be aided by the use of standards and norms as conveyed by Garetti and Taisch [158].

Despeisse et al. [159] presents a set of tactics for achieving sustainable production which could be summarized as the following:

- Prevention (avoid usage).
- Waste reduction.
- Resource use reduction.
- Reuse (waste as a resource).
- Substitution (new resource or technology).

Dieter [2] has estimated that more than 80% of all manufactured parts has undergone one or more machining operations before they are finished. It is thus likely that improvement of a machining process could have a significant influence on the sustainability during production. Currently there is no universally accepted definition for sustainable machining [160]. However, it is conceivable that sustainable machining could be defined as any procedure improving the sustainability during a machining process. As stated by Pusavec et al. [161] there exists several different approaches for improving the sustainability during machining operations. For example, in many cases the use of cutting fluid is described as one of the primary environmental hazards during machining operations [162]. However, another problem from a sustainability perspective is the quick wear of cutting tools. Through improving the cutting tool utilization and thus the tool life, significant improvements could be made from a sustainability perspective. As possible techniques for increasing the cutting tool utilization new methods have been presented for both milling and turning operations, Paper VIII.

4.5.2.1 Proposed method for milling

Common practice during milling operations is to rotate the milling cutter in only one direction. Then when the tool wear reaches a predetermined value the inserts are considered as worn out and scrapped. However, this procedure implies that only part of the cutting edge is used for the actual machining. In general the obtained tool wear will be concentrated to the major cutting edge as well as to a certain extent the tool nose radius. However, the minor cutting edge is often only slightly worn, if worn at all. Thus, by using this minor cutting edge as a "new" major cutting edge during a secondary machining operation the overall tool utilization could be significantly increased. Practically this could be achieved through changing the rotational direction of the milling cutter, given that a suitable milling head is available. A principle illustration of the proposed method can be found in Figure 4.60.

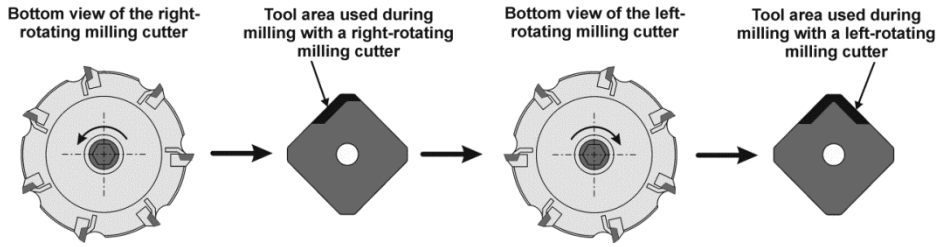

Figure 4.60 Principle illustration of the proposed method for milling [163].

In order to investigate the validity of the proposed method milling experiments were conducted while machining SAF 2304 duplex stainless steel. During these experiments SEEX09T3AFTN inserts were used in an R220.53-0100-09-7A and L220.53-0100-09-7A milling head respectively. Slabs of the workpiece material measuring approximately 42 mm in width and 405 mm in length were used and the milling cutter was centered in relation to the workpiece during all milling experiments. No cutting fluid was used during these experiments. During the whole experimental procedure the tool wear was measured through using optical microscopy and the surface roughness was measured through using a conventional digital perthometer. During these milling experiments the cutting data remained constant with a cutting speed v_c = 80 m/min, depth of cut a_p = 2 mm and feed per tooth f_z = 0.15 mm/tooth. The experiments were performed by first using the right-rotating milling head and then when the flank wear approached VB = 300 µm the inserts were shifted into the left-rotating milling head. In both cases great care was taken to position the inserts as accurately as possible to minimize the relative positional variation between individual inserts in the milling cutter.

The wear on the major cutting edge observed during these experiments was not only limited to flank wear. Chipping was also observed, in some cases severe. It is however of interest to note that the obtained wear on the wiper edge primarily was limited to flank wear, possibly in combination with some minor chipping. Thus, it is feasible that the proposed method for milling could be considered as only having a minor influence on the obtained surface roughness during face milling operations. Figure 4.61 illustrates the measured flank wear on the major cutting edge for all 7 inserts while using both the right- as well as the following left-rotating milling head. Note how the flank wear displays an almost identical pattern for both the right- as well as the following left-rotating milling head. Some measuring points appear to indicate a negative tool wear which of course is impossible. This should be seen as a result of potential measuring errors, partially due to the decision to measure the obtained tool wear with the inserts in situ in the milling head. This decision was taken in order to minimize the variation of the relative position of the inserts. Adhered workpiece

material on the cutting tools may also have resulted in additional measuring errors. A solution to this problem could have been to use an etchant to remove the adhered material before measuring. This would however have influenced the adhesive wear of the cutting tool and thus maybe result in a larger measuring error. Also, depending on the relation between the insert material and the etchants used, chemical wear of the cutting tool could be introduced. Thus, it was decided to measure the obtained tool wear "as is" after each test cycle.

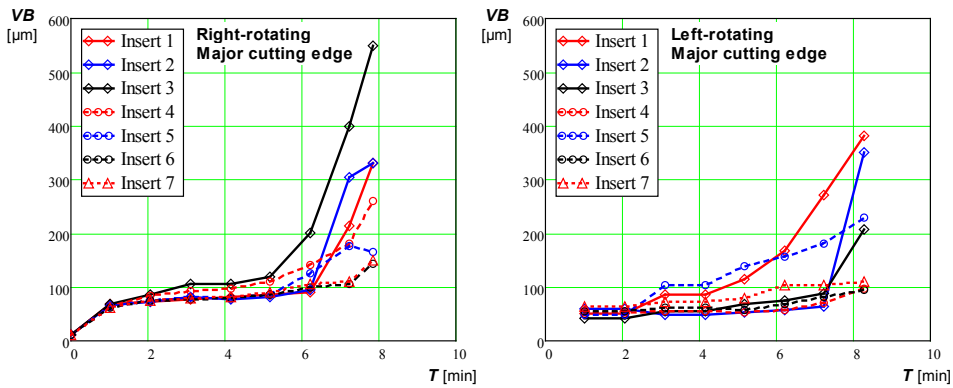

Figure 4.61 Flank wear *VB* on the major cutting edge as a function of the machining time *T* for each of the 7 inserts for the right- and left-rotating milling head [163].

The flank wear on the wiper edge was also measured during the whole test cycle, Figure 4.62. Note that this wear is considerably smaller than on the major cutting edge. None of the 7 inserts obtained flank wear on the wiper edge close to the limit of *VB* = 300 µm used during these machining experiments.

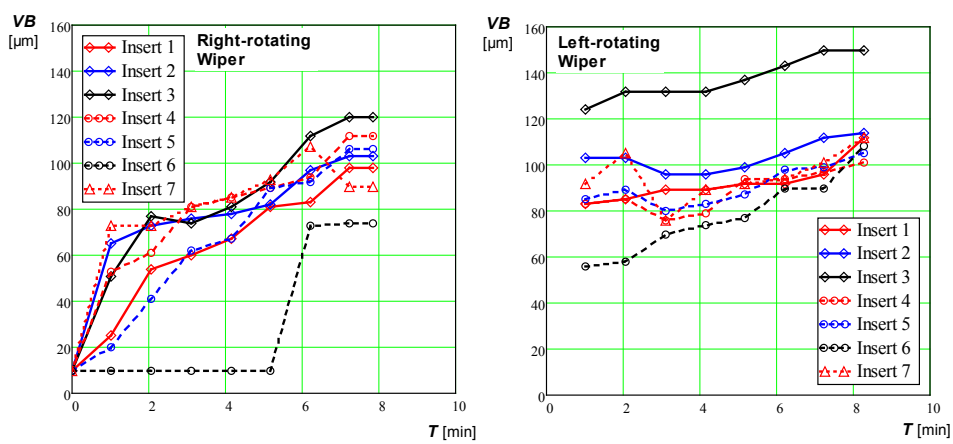

Figure 4.62 Flank wear *VB* on the wiper face as a function of the machining time *T* for each of the 7 inserts for the right- and left-rotating milling head [163].

A general concern while initially using the proposed method was that it would have an adverse influence on the quality of the machined surface. In order to investigate validity of this concern the surface roughness was measured throughout this test cycle. Even though the surface roughness does not describe all essential parts of the surface integrity it was still considered as a substantial first step towards better understanding the influence on the obtained surface quality while implementing the proposed method. Figure 4.63 illustrates the obtained surface roughness for both the right- as well as the following left-rotating milling head. As can be seen in this figure the surface roughness varies as a function of the machining time. The worst surface roughness is obtained at the end of the test cycle while using the right-rotating milling head as well as at the beginning of the test cycle using the left-rotating milling head. It is also of interest to note that the obtained surface roughness at the end of the complete test differs only slightly from the values obtained during the initial milling stages with a right-rotating milling head. These results appear to indicate that the proposed method for milling does not have any major adverse influence on the obtained surface roughness for the machining case investigated. More research is however needed on the general validity of the proposed method while implemented for other milling operations and workpiece materials.

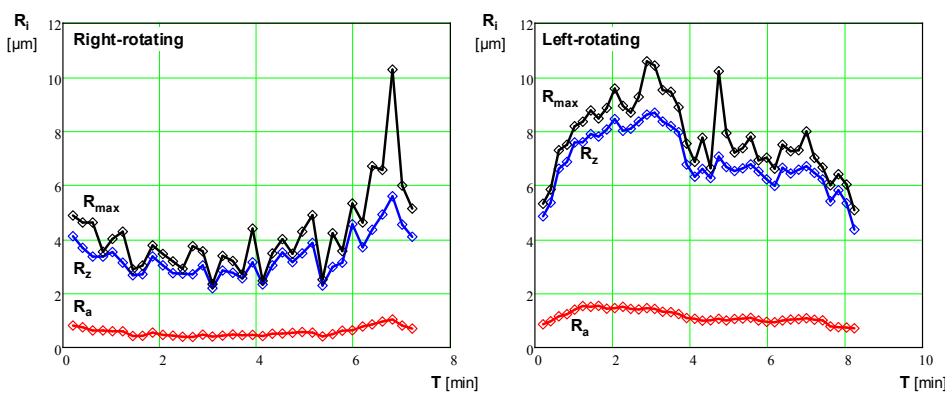

Figure 4.63 Surface roughness as a function of the machining time T [163].

4.5.2.2 Proposed method for turning

A common problem during conventional turning is principally depicted in Figure 4.64. This figure illustrates a facing operation followed by a longitudinal turning operation. This operation can be performed by using two different cutting tools, one for each operation. However, significantly larger tool utilization could be obtained if the same tool is used for both operations. The location and size of the tool wear might vary somewhat depending on the major cutting edge angle but in general the

use of the same cutting tool for both operations will result in tool wear on both sides of the nose radius and thus a better tool utilization.

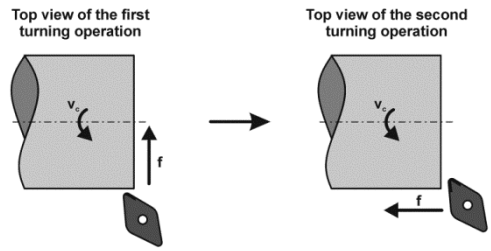

Figure 4.64 Principle illustration of a common turning process involving two individual operations [163].

The scenario illustrated in Figure 4.64 might be problematic to evaluate experimentally. An experimental procedure according to Figure 4.65 was instead used during this investigation. If accurately implemented, this procedure will create a tool wear closely resembling that of the previously described operation. However, any potential variations due to for instance changing from radial to longitudinal feed direction will be diminished. Even though this procedure primarily is intended to mimic the previously described turning situation it could also be implemented by itself as a method for increasing the tool utilization during longitudinal turning given that a suitable workpiece and tool holder is used.

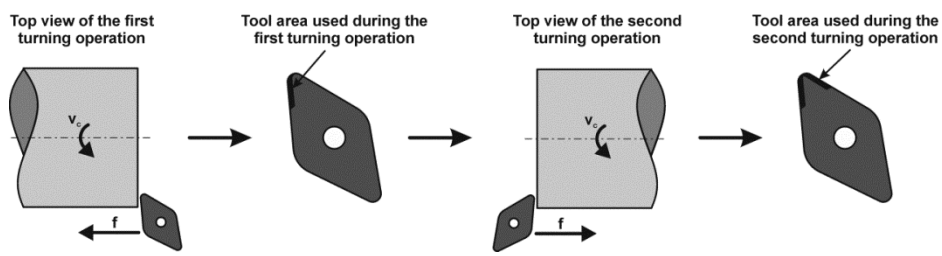

Figure 4.65 Principle illustration of the proposed method for turning [163].

In order to validate the proposed method for turning, experiments were performed by longitudinal turning AISI 4340 according to the method depicted in Figure 4.65. The experiments were performed by initially having a feed direction towards the chuck of the lathe (referred to as "left feed direction") as is commonly the scenario during conventional turning. Then when the cutting tool had sustained a sufficient amount of flank wear the feed direction was reversed (referred to as "right feed direction"). This was practically achieved through machining several groves close to the chuck in order to allow space for the tool holder during the secondary operation. During these experiments a bar of AISI 4340 having an initial diameter of 168 mm

and a length of 960 mm was used. Since the workpiece was comparatively long a center hole and tailstock was used during all turning experiments. However, no cutting fluid was used during any experiment. For all turning experiments commercially available CNMG120412 coated cemented carbide inserts were used in a DCLNL3225P12 or DCLNR3225P12 tool holder depending on feed direction. The depth of cut a_p = 2.5 mm during all these experiments while the feed f and cutting speed v_c varied according to Table 4.19.

Table 4.19 Cutting data used during the turning experiments.

Experiment	v_c [m/min]	f [mm/rev]	a_p [mm]
1	200	0.25	2.5
2	260	0.25	2.5
3	170	0.30	2.5
4	270	0.30	2.5
5	220	0.40	2.5

Primarily flank wear of the cutting tools was observed during these experiments. In addition, no significant change of the type of tool wear was observed while changing from the left to the right feed direction. Examples of the tool wear obtained during these experiments are illustrated in Figure 4.66. As may be discerned in the figure, primarily flank wear of the cutting tool was obtained during these experiments. The primary difference observed between the two feed directions was that the secondary operation resulted in an increased flank wear at the tool nose radius. Thus, while implementing the proposed method the user should be vigilant of the tool wear obtained on all parts of the active cutting edge in order not to risk excessive tool wear.

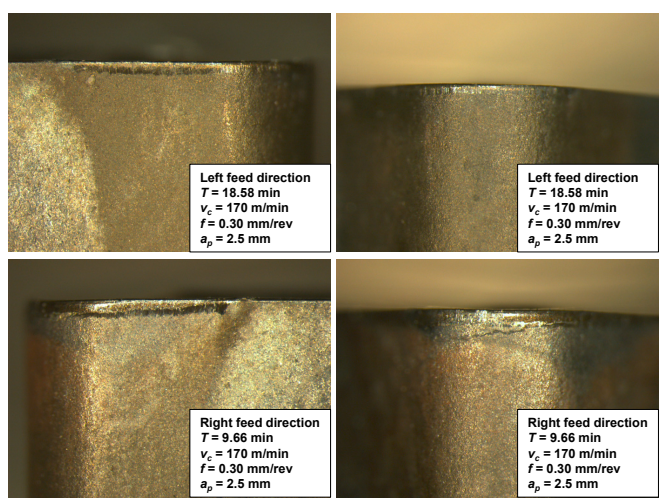

Figure 4.66 Flank wear as seen on the flank face (left) and at the tool nose (right) for both feed directions [163].

As for the previously described milling scenario the flank wear *VB* was measured as a function of the machining time *T* for all investigated turning cases. The obtained results are displayed in Figure 4.67. As previously discussed, some measurements appear to indicate negative tool wear which of course is impossible. This measuring error was thought to be due to the problem of accurately measuring the flank wear at an equivalent position as well as due to the existence of adhered workpiece material on the cutting tool.

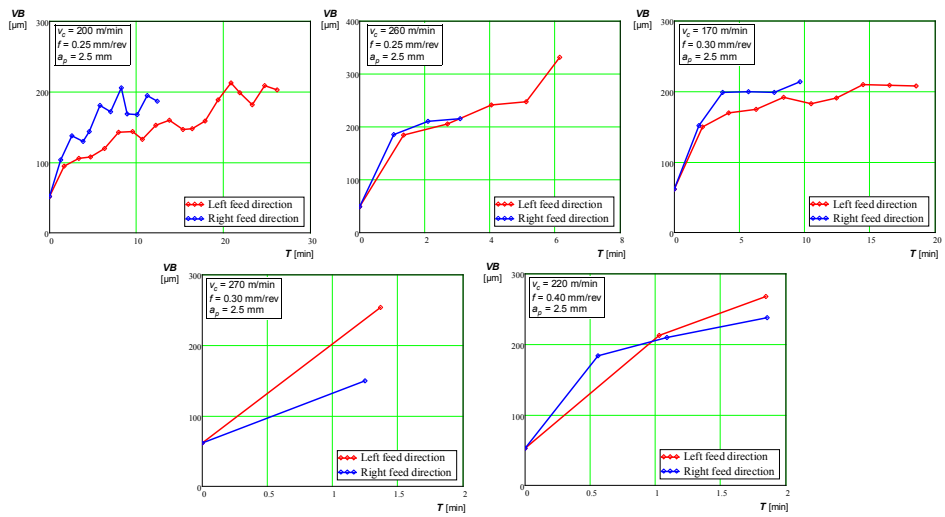

Figure 4.67 Obtained flank wear *VB* as a function of the machining time *T* for different sets of process parameters [163].

Some variations of the obtained surface roughness were obtained while changing from one feed direction to the other as exemplified in Figure 4.68. Whether these variations could be considered as significant may vary from one machining case to the other. However, as the proposed method mainly is intended for rough and semi-finish machining it is the author's impression that these variations generally could be seen as insignificant.

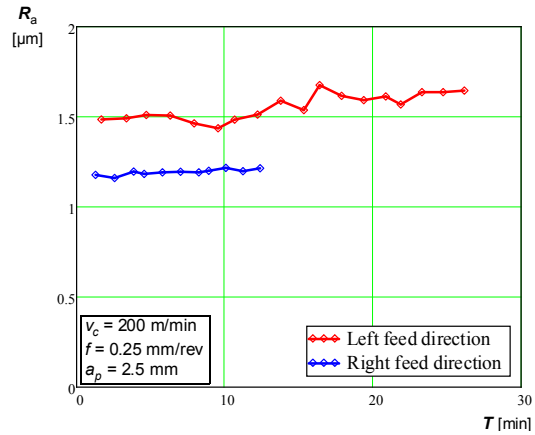

Figure 4.68 Example of obtained R_a surface roughness for both feed directions [163].

The results obtained from this study can be used for modeling the tool life. Several applicable tool life models have been presented, one of the more famous by Colding [51, 52] and further evaluated by Hägglund [134, 164], Equation 4.71.

$$v_c = e^{\left[K - \frac{(\ln(h_e) - H)^2}{4 \cdot M} - (N_0 - L \cdot \ln(h_e)) \cdot \ln(T)\right]} \qquad 4.71$$

In this equation h_e is the equivalent chip thickness and T is the tool life. K, H, M, N_0 and L are all model constants. Several different equations for calculating the equivalent chip thickness does exist as published by among others Hägglund [134] and Bus et al. [92]. The author has also published a revised model intended for low depths of cut as previously described in section 4.4.1. One of the more common and widespread models was however published by Woxen [131, 165] and it was thus decided to use this definition during the current comparison, Equation 4.45.

During modern research a flank wear criteria of VB = 300 µm is commonly used. If it is assumed that the tool life increases linearly as a function of the machining time the following tool life would be obtained for each machining case investigated, Table 4.20. Through using these measurements the following model constants could be attained as part of Colding's tool life equation, Table 4.21.

Table 4.20 Tool life obtained for each feed direction at varying cutting data if the criteria *VB* = 300 µm is used.

Experiment	v_c [m/min]	f [mm/rev]	a_p [mm]	h_e [mm]	Left T [min]	Right T [min]
1	200	0.25	2.5	0.19	38.75	19.93
2	260	0.25	2.5	0.19	5.56	4.29
3	170	0.30	2.5	0.22	26.80	13.54
4	270	0.30	2.5	0.22	1.62	2.50
5	220	0.40	2.5	0.29	2.07	2.35

Table 4.21 Model constants attained through evaluating the experimentally obtained data.

Feed direction	K	H	M	N_0	L
Left	5.9534	-2.5256	1.0259	0.4789	-0.2081
Right	6.0315	-2.3855	0.8608	0.5554	-0.2089

A model error may be calculated as the relative difference between the experimentally obtained values and those predicted by the model, Table 4.22. As can be seen in the table the obtained errors are in some cases significant and thus careful scrutiny of the obtained results is required before drawing any further conclusions.

Table 4.22 Modeling error for the different turning cases investigated.

Experiment	v_c [m/min]	f [mm/rev]	a_p [mm]	h_e [mm]	Left feed direction Error [%]	Left feed direction Mean Error [%]	Right feed direction Error [%]	Right feed direction Mean Error [%]
1	200	0.25	2.5	0.19	1.26		16.35	
2	260	0.25	2.5	0.19	7.56		-10.49	
3	170	0.30	2.5	0.22	-5.49	6.24	-13.23	10.18
4	270	0.30	2.5	0.22	-9.51		7.84	
5	220	0.40	2.5	0.29	7.38		3.00	

In general it was found that the wear at the tool nose radius was significantly smaller than the flank wear on the major cutting edge for both feed directions. From a theoretical standpoint it could be argued that if only the wear on the major cutting edge is investigated for each feed direction the two operations should have an equivalent tool life with some statistical variation. This since the two operations could be considered as two separate machining operations not influencing each other. This is however an oversimplification of the investigated problem. Even though the tool wear is smaller at the tool nose radius this tool wear will result in an increased temperature during the machining process. This increase in temperature will affect the whole cutting tool resulting in a more rapid wear of the major cutting edge. The significance of this effect will increase during the secondary machining operation since the wear at the tool nose radius is larger for this operation. It is thus theoretically plausible that the tool life will be slightly shorter for the secondary machining

operation. This notion could to some extent be corroborated by the results presented in Figure 4.69.

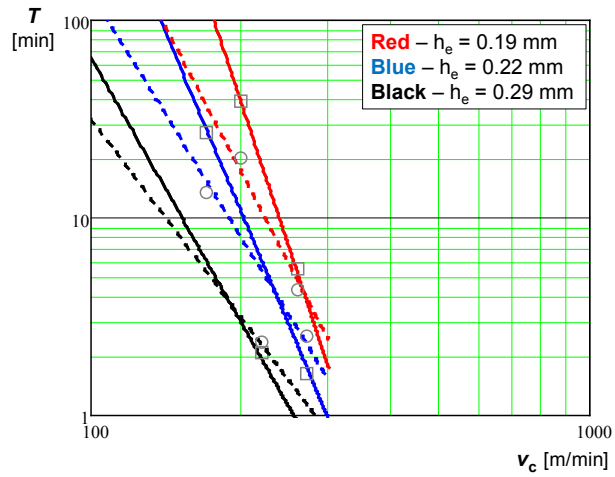

Figure 4.69 Taylor curves as based on Colding's tool life equation. The solid and interrupted lines correspond to the model values for the left- and right feed direction and the squares and circles correspond to the experimental values for the left- and right feed directions [163].

As can be seen in Figure 4.69 the secondary machining operation in the right feed direction generally results in a slightly lower tool life for a specific equivalent chip thickness. This relationship is however reversed at high cutting speeds. Even though this phenomenon could have a physical explanation any further conclusions should be avoided due to the modeling error which might influence the obtained results.

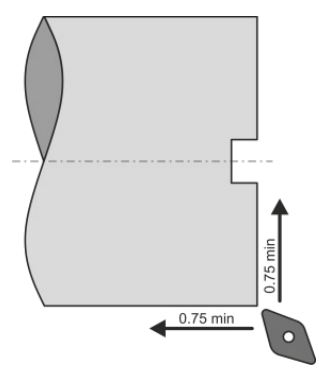

Figure 4.70 Principle illustration of a hypothetical machining scenario [163].

In order to gain a better understanding of the potentials of the proposed method a hypothetical turning case may be considered. Assume that the machining time is 0.75 min for each feed direction as illustrated in Figure 4.70. Also, assume that the tool life

is 15 min and that 20 parts may be produced during a conventional process using one tool for each feed direction. Based on the obtained experimental results it could be estimated that by using the proposed new method 80% of the parts produced with 2 cutting tools during conventional turning could now instead be produced by using a single cutting tool. Further, when using two cutting tools for machining of a single part the cutting tools needs to be indexed during the machining process which is estimated as taking 0.33 min/part. The cutting tool also needs to be transported to the right position before initiating the cutting process which is estimated as taking 0.15 min/part. Replacing a finished part with a new workpiece is estimated as taking 0.33 min/part and changing of the cutting tool due to tool wear is estimated as taking 3 min for a single cutting tool and 5 min for two cutting tools due to the benefits of changing several cutting tools simultaneously. A short summary of the different values used in this hypothetical case can be found in Table 4.23.

Table 4.23 Hypothetical parameters used for comparing the conventional and proposed new process.

Process parameter	Variable	Conventional	Proposed
Number of parts per cutting edge	N	20	16
Machining time per part [min/part]	t_i	1.5	1.5
Tool indexing time per part [min/part]	t_{ind}	0.33	0
Tool transportation without cutting [min/part]	t_{pos}	0.15	0.15
Change of workpiece [min/part]	t_{wch}	0.33	0.33
Change of cutting tool due to tool wear [min]	T_{tch}	5	3

As based on this information the cycle time per part may be calculated and compared for both the conventional machining process as well as the proposed new process. It was found that under these hypothetical conditions a conventional turning process would have a cycle time of approximately 2.56 min as compared to 2.17 min for the new process. Further, the energy requirement per part may be calculated through using Equation 4.72.

$$E_0 = P_m \cdot \left(t_i + \xi \cdot \left(t_{ind} + t_{pos} + t_{wch} + \frac{T_{wch}}{N} \right) \right) \qquad 4.72$$

In this equation ξ is a constant which depicts the relative amount of energy used when not cutting as compared to while machining a workpiece. Even though this is a simplification of the actual conditions this model was considered as sufficient for evaluating the relative difference between the two investigated machining cases. As stated by among others Balogun and Mativenga [166], the machine tool also requires a significant amount of energy even while not cutting. In this hypothetical comparison it was estimated that ξ = 0.70. This estimation was to a certain extent

corroborated by Behrendt et al. [167]. In Equation 4.72 P_m is the engine power used during the machining process. This parameter could be estimated for a specific machining case but as only a relative comparison between the two alternative processes was sought no knowledge of this variable was needed during this comparison. More complex models for calculating the energy requirements do exist if a more accurate value is desired. For instance Balogun and Mativenga [166] investigates the energy requirements during different parts of the machining process in more detail. In addition Li et al. [168] have published an alternative model which uses an empirical approach for modeling the process energy requirement. Even though these more advanced models could be considered as producing a more accurate result the simplified model according to Equation 4.72 was considered as appropriate for this simple comparison of two similar machining processes. It was found that the energy consumption was reduced by approximately 12% while using the proposed new process as compared to a conventional turning process. The difference between the two alternative processes is illustrated in Figure 4.71.

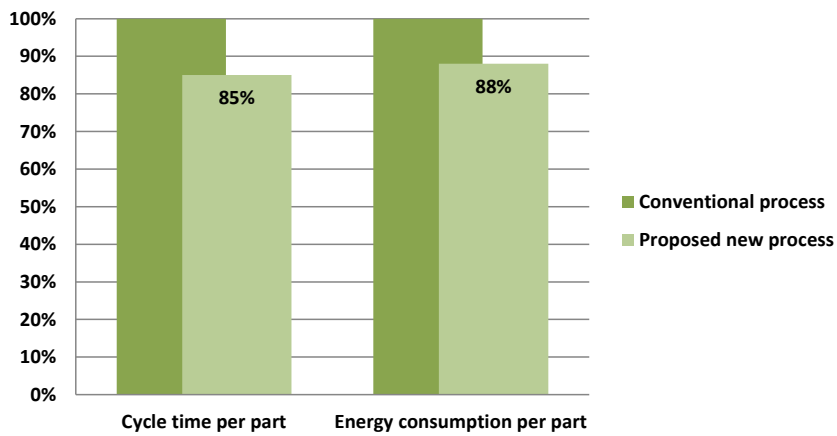

Figure 4.71 Relative cycle time and energy consumption per part for the new process as compared to a conventional turning process [163].

Cutting tools are just a small part of the whole machining process and their influence on sustainability should not be exaggerated. However, while striving towards sustainable production no part of the machining process should be neglected. This does not necessarily imply that increased tool utilization is the most urgent improvement during a machining process but rather one of a whole series of factors which needs to be improved to achieve a truly sustainable process.

4.6 Summary of Appended Publications

This section briefly describes the appended publications with particular focus on the obtained results and derived conclusions.

4.6.1 Paper I

The research presented in this paper evaluates the machinability of duplex stainless steel for some machining cases. Three different types of duplex stainless steel have been investigated; LDX 2101, SAF 2205 and SAF 2507. It was found that these kinds of duplex stainless steel may be considered as having an equivalently low potential machinability as compared to AISI 4140, as indicated by the obtained polar diagrams derived according to previous descriptions in this dissertation. The obtained polar diagrams indicated that this low potential machinability primarily could be attributed to the high ductility and low thermal conductivity of duplex stainless steel as compared to AISI 4140. In general the machining experiments indicated a strong tendency towards adhesive wear resulting in an unpredictable wear of the cutting tool over time. Through the use of so called quick-stop experiments it was found that the phases in the investigated materials displays a ductile behavior which allows for substantial deformation of the workpiece material without shearing of a chip as indicated by the deformation of phases close to the cutting edge.

4.6.2 Paper II

The research presented in this paper introduces the general conception and use of polar diagrams for describing the potential machinability. A problem when describing machinability is the need to discuss a specific workpiece material in combination with a specific machining process. The concept presented in this article introduces the possibility of only using 5 material properties for describing the potential machinability of a specific workpiece material without any prior knowledge about the machining process itself. As based on previous publications it was found that ductility, strain hardening, thermal conductivity, hardness and abrasiveness at room temperature could be sufficient for describing the potential machinability of a material. Two case studies were also presented in the article during which the proposed method appeared to produce plausible results for both a group of common steels as well as a group of stainless steels.

4.6.3 Paper III

The research presented in this paper investigated the influence of different process parameters on the size of the minimum chip thickness. First of all a novel approach for measuring the value of the minimum chip thickness through measuring the width of the obtained chips was presented. Then, this approach was used while evaluating the effect of different process parameters on the size of the minimum chip thickness. It was found that the value of h_{2min} is dependent upon the size of the theoretical chip thickness as well as the tool nose radius. After further investigations it was found that this influence possibly could be attributed to influence of the chip flow angle. Based on these results a new model for estimating the value of the minimum chip thickness was proposed. This model divides the influence into two sections, the tool edge radius region and the chip flow region. According to this theory it was predicted that at low values of h_1 the tool edge radius has a pronounced influence on h_{2min} at which a larger value of the tool edge radius will result in a larger value of h_{2min}. However, after a critical value of h_1 has been attained the chip flow angle will start to have a much more pronounced influence on the value of h_{2min}, possibly rendering the influence of the tool edge radius irrelevant.

4.6.4 Paper IV

The influence of the tool surface micro topography on the tribological characteristics during metal cutting was investigated and presented in this paper. Tools having four different surface roughnesses were initially investigated through using a so called pin-on-disc test. During these tests a significant difference between the varying tool surface roughnesses were observed. In particular it was found that the adhesion between the two surfaces increased for rougher coating surfaces. In addition, while performing machining experiments it was found that the length of the adhesion zone on the both rake and clearance face increased as a function of the tool surface roughness. It was also found that the tool surface micro topography has a pronounced effect on the normal and shear stresses acting on the clearance face of the cutting tool during machining operations. A large surface roughness on the cutting tool will result in a more inhomogeneous deformation of the workpiece material resulting in a larger subsurface deformation layer. Also, an increased amount of workpiece material sliding against the clearance face will result in an increase of the hydrostatic pressure acting between the two surfaces. Thus, as proven by experimentally obtained results, an increase of the tool surface roughness will result in a decreasing contact condition on the clearance face of the cutting tool.

4.6.5 Paper V

The research presented in this paper is a continuation of that presented in the previous paper, Paper IV. It was found that during metal cutting conditions the tool surface roughness does have an influence on the contact conditions acting on the rake face of the cutting tool. However, the value of the contact condition is difficult to determine experimentally and present methods could only be used to obtain approximate results. The contact conditions attained during this study was mainly acquired through evaluating the obtained cutting forces although other potential methods of calculating the contact condition were described in the paper. It was found that the tool surface micro topography influences the contact condition acting on the clearance face. For low values of the theoretical chip thickness large differences were observed between conventional inserts and equivalent tools having a synthetic wear land. While increasing the theoretical chip thickness the values of the contact condition for these two cases appear to approach the same value. Further, it was found that the tool surface roughness does influence the cutting resistance. For conventional inserts the influence of the tool surface roughness on the cutting resistance was insignificant. However, for the tool having a synthetic wear land a clear influence of the tool surface roughness was observed.

4.6.6 Paper VI

As more and more difficult to machine materials are being used during modern production new problems arise while attempting to evaluate the obtained tool wear. This paper presents a new method for evaluating geometrical tool changes during the machining of Ti6Al4V. Through measuring the cutting forces, while incrementally increasing the feed, a deterioration factor can be calculated. When the deterioration factor becomes sufficiently larger than 1.0 it could be concluded that the cutting tool has been deformed. By also varying the cutting speed during the experimental investigation more knowledge on the specific machining operation investigated is obtainable. The model proved valid for the machining cases investigated while turning Ti6Al4V even though no correlation between the value of the deterioration factor and the size of the tool deformation was explicitly determined.

4.6.7 Paper VII

All companies strive towards lowering their production costs and often devote significant resources to achieve this ambition. However, few companies achieve

continuous improvements of the production process after the initial launch of production. This paper presents a novel approach for incrementally improving the production process during the production of a specific product. Through incrementally varying the cutting data and carefully recording the obtained results it is possible to optimize the production process. In addition, if the variations are done carefully the manufactured parts will meet the quality demands and thus could be sold to the customer minimizing the amount of resources needed. Even though this approach could result in a sub-optimization of the machining process this improvement is still better than no improvement at all. Also, since the implementation is based on the the operators it could be seen as a method for getting the operators involved in the overall improvement process at the company. The incremental production improvement process was evaluated as a case study at a small Swedish company. Implementation of this method while machining a part of solution annealed Alloy 718 intended for the offshore industry resulted in a part cost reduction by approximately 5% at the same time as the cycle time was slightly reduced.

4.6.8 Paper VIII

Sustainable development has received an increasing amount of attention during recent years. It has also been recognized that sustainable production is an imperative part for achieving sustainable development. This paper introduces a novel approach for increasing the cutting tool utilization, in some cases resulting in a tool life up to twice that of a conventional machining process. Through using the minor cutting edge as a "new" major cutting edge during a secondary machining operation it has been proven that the tool utilization could be significantly increased in some cases. Even though this approach is limited to certain machining operations which allow for the use of other cutting tools as well as tool paths the suggested method could still be implemented for a substantial amount of all machining operation used today. Through the investigation of a limited amount of machining cases the proposed method proved to be a plausible approach for both turning and milling operations. Further, no significant effects on the obtained surface roughness could be discerned during this investigation. However, it is the author's opinion that the proposed method should only be used for rough- and semi-finish machining since the probability of tool chipping or even tool failure will increase substantially with increasing tool wear. Also, the user should be vigilant of the obtained tool wear as not to obtained excessive tool wear and thus risk discarding the machined part.

5 Conclusions

Machinability investigations are complex and extensive in their nature and as a result it has been impossible to investigate all aspects of machinability during this research even for the limited amount of materials investigated. However, the current research has shown that it is possible to predict and compare the potential machinability of a workpiece material by using material properties commonly available from material certificates. For the materials of primary concern in this dissertation the ductility and strain hardening had a significant influence on the obtained machinability. In addition these materials displayed a relatively low thermal conductivity as compared to more commonly machined materials such as ordinary carbon steels. As a result adhesive wear of the cutting tools was a major concern, sometimes in combination with plastic deformation of the cutting tool, while machining the investigated materials.

A large part of this dissertation has been devoted to the influence of the minimum chip thickness during machining operations. The minimum chip thickness influences all parts of the machining operations but the influence on the obtained surface integrity could be expected to be more pronounced for ductile and strain hardening materials as shown during this research. It has been shown that a complex series of circumstances influence the obtained surface roughness starting with the ductility and strain hardening of the investigated material. These factors in turn influences the size of the minimum chip thickness which determines the amount of material plastically deformed onto the machined surface and thus in turn determines the roughness of the machined surface.

During this study it has been demonstrated how the tool surface micro topography will have a measurable influence on the machining process. The results seem to imply that there exists an optimal value of the tool surface micro topography as decreasing surface roughness tends to decrease the value of the contact condition on the clearance face.

Different aspects of the tool wear while machining these materials have also been investigated. Adhesive tool wear as well as deformation of the cutting tool is a concern while machining ductile and strain hardening materials. Thus, a model for

determining when deformation of the cutting tool has occurred through using the obtained cutting forces was developed. This model showed great potentials even though it was only validate for turning of Ti6Al4V while using a coated cemented carbide cutting tool.

Two different methods for improving the machining process in terms of part cost and sustainability has been developed as part of this research. The first of these was called incremental production improvements and was intended to incrementally improve the production process during conventional production. The advantages obtained through using this method are the limited amount of resources needed in combination with the potential benefit of getting the operators more involved in the improvement process. The second improvement method was aimed at improving the utilization of the cutting tools during both turning and milling operations and thus increasing the sustainability of these operations. Even though cutting tools may have a comparatively small influence on the overall sustainability of a machining process as compared to for example the use of cutting fluid this influence should not be forgotten as all parts of the machining process needs to be optimized in order to achieve a truly sustainable machining process.

Summarizing the research presented throughout the current dissertation the following answers could be given to the previously defined research questions:

RQ1. Can the obtained machinability be attributed to one or more physical phenomena during the machining process and thus be predicted?

As part of the research presented in this dissertation it has been recognized that the stagnation zone and related minimum chip thickness has a fundamental influence on the machining process. The value of the minimum chip thickness has been shown to be related to central parameters during the machining process such as feed, tool edge radius and chip flow direction (Paper III). Further, it has been established that the minimum chip thickness influences the obtained surface roughness either improving or worsening the obtained surface roughness. The current research has also shown that there exists a relationship between the tool/workpiece contact condition and the location of the stagnation point (Papers IV and V). Finally, a new method has been developed on how to measure and evaluate the obtained cutting forces in order to detect any change of the cutting tool geometry (Paper VI).

RQ2. Could any part of the machinability for a specific workpiece material be analyzed without prior knowledge on the machining process?

Five workpiece material properties have been recognized as influential on the potential machinability; these being the ductility, strain hardening, thermal conductivity, hardness and abrasiveness. Through using these material properties it is

possible to analyze the potential machinability for any workpiece material without prior knowledge of the machining process (Paper II). It was also found that the cutting resistance Cr_1 can be modeled as a function of four related workpiece material properties: hardness, yield strength, elongation at rupture and thermal conductivity. Further, it was shown that the ductility and strain hardening of the workpiece material has a significant influence on the obtained surface roughness due to its influence on the minimum chip thickness.

RQ3. How should the machinability of a new machining operation be analyzed in order to aid the choice of appropriate process parameters?

An important first step while evaluating the machinability related to a new machining operation is to consider the properties of the workpiece material. Through comparing workpiece material properties with those for a material with a known machinability, reasonable process parameters, e.g. tool material and cutting data, may be established (Paper II). These process parameters can then be improved through incrementally changing the process parameters, step by step refining the machining process towards a given goal (Paper VII). Common practice in this regard is to optimize the machining process towards a minimum part cost or a maximum output, but in the light of current development parameters related to sustainable production are becoming increasingly important (Paper VIII). Results presented in this dissertation have also shown the importance of monitoring the obtained cutting forces in order to detect any deformation of the cutting tool (Paper VI). An initial attempt to implement the proposed procedure during the current research was performed for the case of machining duplex stainless steel (Paper I).

6 Future Research

The research presented in this dissertation is a step towards better understanding the machinability of ductile and strain hardening materials. Even though a substantial amount of data have been gathered and analyzed as a part of the research presented in this dissertation considerable amount of research still remains to be done on the subject. This section presents some of the author's own thoughts on potential future fields of research related to the present subject.

An initial attempt to investigate the machinability of a group of workpiece materials was presented in Paper I. This paper as well as a substantial amount of other publications by different authors only evaluates the machinability for a specific combination of cutting tool, workpiece material and machining process, thus limiting the potentials for generalizing the obtained results for a broader context. If a procedure for evaluating the machinability of any combination of cutting tool, workpiece material and machining process could be established great advantages could be attained as this would allow the whole scientific community to contribute to a database of comparable machinability data.

Even though much has already been done on the essential physical processes occurring during any machining operation still much remains to be done. The research published in this dissertation has begun to investigate the influence of the stagnation zone on the machining process. An interesting continuation of this research could be to investigate whether it is somehow possible to attain a stable stagnation zone which would protect the tool from wear or improve the surface roughness of a machined surface through filling out the valleys in a systematic fashion.

An initial investigation into the influence of the tool surface micro topography has been presented as a part of this dissertation. These results are however limited by the limited amount of experiments preformed. Thus, the limitations of the validity for the obtained results are to a large extent still unknown. Future research while varying the cutting tool, workpiece material and machining process is needed to broaden the validity of the obtained results as well as further investigate the phenomenon.

The new concept of incremental production improvements has been presented as a part of this dissertation. Further research on this topic is however needed in order to evaluate the validity of the proposed method for different production processes. Also, further research is needed on how incremental production improvements could fit into the existing improvement processes, e.g. Lean production and Kaizen, commonly applied at modern companies.

A method for increasing the cutting tool utilization during turning and milling have been introduced and proven as plausible as part the research presented in this dissertation. However, much research still remains to be done on investigating the validity of the proposed method and especially its limitations. Thus, a significant amount of experimental research remains on how different process parameters, e.g. tool material and geometry, workpiece material and cutting data, influences the viability of the proposed method. Also, experiments should be performed where the proposed method is implemented in industry in order to validate its potentials during conventional production both from an economic as well as sustainable perspective.

References

[1] M. Andersson, J.-E. Ståhl, Polar Machinability Diagram - A Model to Predict the Machinability of a Work Material, *Proceedings of the Swedish Production Symposium*, Gothenburg, Sweden, 2007.

[2] G.E. Dieter, *Mechanical Metallurgy - SI Metric Edition*, McGraw-Hill, London, UK, 1988.

[3] J. Jablonowski, N. Eigel-Miller, *2013 World Machine-Tool Output and Consumption Survey*, Gardner Business Media Inc., Cincinnati, OH, USA, 2013.

[4] S. Kline, *2013 Tooling Equipment Report*, Gardner Business Media Inc., Cincinnati, OH, USA, 2012.

[5] J.-E. Ståhl, *Metal Cutting - Theories and models*, Division of Production and Materials Engineering, Lund University in cooperation with Seco Tools AB, Lund/Fagersta, Sweden, 2012.

[6] J. Olsson, M. Snis, Duplex - A new generation of stainless steels for desalination plants, *Desalination*, 205 (2007) 104-113.

[7] I. Weibull, Duplex stainless steels and their application, particularly in centrifugal separators. Part A History & Development, *Materials & Design*, 8 (1987) 35-40.

[8] J.-E. Ståhl, *Development of Manufacturing Systems - The link between technology and economics*, Division of Production and Materials Engineering, Lund University, Lund, Sweden, 2013.

[9] J.-E. Ståhl, The development of NEXT STEP beyond Lean Production - The link between technology and economics with focus on sustainable developments, *Proceedings of the International Conference on Applied Mechanics, Materials and Manufacturing*, Shenzhen, China, 2011.

[10] F.W. Taylor, *On the Art of Cutting Metals*, 3rd ed., The American Society of Mechanical Engineers, New York, USA, 1906.

[11] E. Befring, *Forskningsmetodik och statistik*, Studentlitteratur, Lund, Sweden, 1994.

[12] K. Williams, *Research methods for students, academics and professionals*, 2nd ed., Centre for Information Studies, Charles Stuart University, Wagga Wagga, Austrailia, 2002.

[13] J. Bell, *Introduktion till forskningsmetodik*, 4th ed., Studentlitteratur, Lund, Sweden, 2010.

[14] J.E.M. Sale, L.H. Lohfeld, K. Brazil, Revisiting the quantitative-qualitative debate: Implications for mixed-methods research, *Quality & Quantity*, 36 (2002) 43-53.

[15] M. Kolodnitsky, *Fundamentals of the theory of mathematical modeling of various systems*, ZSTU, Zhytomyr, Ukraine, 2001.

[16] D.C. Montgomery, *Design and Analysis of Experiments*, 8th ed., John Wiley & Sons, Singapore, 2012.

[17] W.L. Oberkampf, T.G. Trucano, C. Hirsch, Verification, validation, and predictive capability in computational engineering and physics, *Applied Mechanics Reviews*, 57 (2004) 345-384.

[18] R.K. Yin, *Fallstudier: design och genomförande*, Liber, Malmö, Sweden, 2007.

[19] H. Hallendorf, *Slagsten och Automat - Bilder från verktygsmaskinens utveckling*, Maskinaktiebolaget Karlebo, Stockholm, Sweden, 1967.

[20] E.O. Ezugwu, Key improvements in the machining of difficult-to-cut aerospace superalloys, *International Journal of Machine Tools & Manufacture*, 45 (2005) 1353-1367.

[21] G. Vieregge, *Zerspanung der Eisenwerkstoffe*, Verlag Stahleisen M.B.H., Düsseldorf, Germany, 1959.

[22] E.M. Trent, P.K. Wright, *Metal Cutting*, 4th ed., Butterworth-Heinemann, Stoneham, MA, USA, 2000.

[23] M.C. Shaw, *Metal cutting principles*, Clarendon Press, Oxford, UK, 1997.

[24] S. Kalpakjian, S.R. Schmid, *Manufacturing Engineering and Technology - Sixth Edition in SI Units*, Prentice Hall, Singapore, 2010.

[25] I.S. Jawahir, The Chip Control Factor in Machinability Assessments - Recent Trends, *Journal of Mechanical Working Technology*, 17 (1988) 213-224.

[26] Sandvik, *Modern skärande bearbetning*, Sandvik Coromant, Sandviken, Sweden, 1994.

[27] W.A. Knight, Application of the universal machinability chart to the prediction of machine tool stability, *International Journal of Machine Tool Design and Research*, 8 (1968) 1-14.

[28] R. Venkata Rao, O.P. Gandhi, Digraph and matrix methods for the machinability evaluation of work materials, *International Journal of Machine Tools and Manufacture*, 42 (2002) 321-330.

[29] J.P. Davim, F. Mata, A new machinability index in turning fiber reinforced plastics, *Journal of Materials Processing Technology*, 170 (2005) 436-440.

[30] E.W. Thiele, K.J.A. Kundig, D.W. Murphy, G. Saloway, B. Duffin, *Comparative machinability of brasses, steels and aluminum alloys: CDA's universal machinability index*, SAE Technical Paper 900365, (1990).

[31] N. Boubekri, J. Rodriguez, S. Asfour, Development of an aggregate indicator to assess the machinability of steels, *Journal of Materials Processing Technology*, 134 (2003) 159-165.

[32] W.T. Chien, C.Y. Chou, The predictive model for machinability of 304 stainless steel, *Journal of Materials Processing Technology*, 118 (2001) 442-447.

[33] A. Stoić, J. Kopač, G. Cukor, Testing of machinability of mould steel 40CrMnMo7 using genetic algorithm, *Journal of Materials Processing Technology*, 164-165 (2005) 1624-1630.

[34] R. Venkata Rao, Machinability evaluation of work materials using a combined multiple attribute decision-making method, *International Journal of Advanced Manufacturing Technology*, 28 (2006) 221-227.

[35] S.V. Wong, A.M.S. Hamouda, A fuzzy logic based expert system for machinability data-on-demand on the Internet, *Journal of Materials Processing Technology*, 124 (2002) 57-66.

[36] J.Y. Tan, S. Wong, A.M.S. Hamouda, N. Ismail, Strategy for generalizing the development of alloy steel fuzzy model for machinability data selection, *Journal of Materials Processing Technology*, 155-156 (2004) 2080-2086.

[37] S.H. Yeo, M. Rahman, V.C. Venkatesh, Development of an Expert System for Machinability Data Selection, *Journal of Mechanical Working Technology*, 17 (1988) 51-60.

[38] S.H. Yeo, M. Rahman, Y.S. Wong, Towards Enhancement of Machinability Data by Multiple-Regression, *Journal of Mechanical Working Technology*, 19 (1989) 85-99.

[39] S. Rawat, H. Attia, Characterization of the dry high speed drilling process of woven composites using Machinability Maps approach, *CIRP Annals - Manufacturing Technology*, 58 (2009) 105-108.

[40] J.P. Davim, L. Figueira, Machinability evaluation in hard turning of cold work tool steel (D2) with ceramic tools using statistical techniques, *Materials & Design*, 28 (2007) 1186-1191.

[41] A. Medvedeva, J. Bergstrom, S. Gunnarsson, P. Krakhmalev, L.G. Nordh, Influence of nickel content on machinability of a hot-work tool steel in prehardened condition, *Materials & Design*, 32 (2011) 706-715.

[42] D. Ulutan, T. Ozel, Machining induced surface integrity in titanium and nickel alloys: A review, *International Journal of Machine Tools & Manufacture*, 51 (2011) 250-280.

[43] I.S. Jawahir, E. Brinksmeier, R. M'Saoubi, D.K. Aspinwall, J.C. Outeiro, D. Meyer, D. Umbrello, A.D. Jayal, Surface integrity in material removal processes: Recent advances, *CIRP Annals - Manufacturing Technology*, 60 (2011) 603-626.

[44] P.G. Benardos, G.C. Vosniakos, Predicting surface roughness in machining: a review, *International Journal of Machine Tools & Manufacture*, 43 (2003) 833-844.

[45] C. Spaans, *The Fundamentals of Three-Dimensional Chip Curl, Chip Breaking and Chip Control*, Afdeling der werktuigbouwkunde, Laboratorium voor werkplaatstechniek, Delft University of Technology, Delft, The Netherlands, 1971.

[46] W. Kluft, W. Konig, C. Van Luttervelt, K. Nakayama, A. Pekelharing, Present knowledge of chip control, *Annals of the CIRP*, 28 (1979) 441-455.

[47] I.S. Jawahir, C.A. van Luttervelt, Recent Developments in Chip Control Research and Applications, *CIRP Annals - Manufacturing Technology*, 42 (1993) 659-693.

[48] R. Kiessling, G. Sandén, *Skärteknik*, Sveriges Mekanförbund, Stockholm, Sweden, 1980.

[49] ISO, ISO 3685:1993, *Tool-life testing with single point turning tools*, International Organization for Standardization, Geneva, Switzerland, 1993.

[50] M. Kronenberg, Replacing the Taylor formula by a new tool life equation, *International Journal of Machine Tool Design and Research*, 10 (1970) 193-202.

[51] B.N. Colding, A Tool-Temperature/Tool-Life Relationship Covering a Wide Range of Cutting Data, *CIRP Annals - Manufacturing Technology*, 40 (1991) 35-40.

[52] B.N. Colding, The Machining Productivity Mountain and its Wall of Optimum Productivity, *Proceedings of the 9th NAMRAC*, (1981) 37-42.

[53] G.H. Brundtland, *Our Common Future*, World Commision on Environment and Development, Oxford University Press, Oxford, UK, 1987.

[54] UNCED, *Agenda 21: Programme of Action for Sustainable Development*, United Nations, New York, USA, 1992.

[55] F. Jovane, H. Yoshikawa, L. Alting, C.R. Boer, E. Westkamper, D. Williams, M. Tseng, G. Seliger, A.M. Paci, The incoming global technological and industrial revolution towards competitive sustainable manufacturing, *CIRP Annals - Manufacturing Technology*, 57 (2008) 641-659.

[56] F. Schultheiss, J.-E. Ståhl, Machinability of duplex stainless steels - A study with focus on the tool wear behaviour, *Proceedings of the 4th International Swedish Production Symposium*, Lund, Sweden, 2011, pp. 271-277.

[57] G. Berglund, P. Wilhelmsson, Fabrication and practical experience of duplex stainless steels, *Materials & Design*, 10 (1989) 23-28.

[58] I. Weibull, Duplex stainless steels and their application, particularly in centrifugal separators: Part B Corrosion resistance, *Materials & Design*, 8 (1987) 82-88.

[59] J. Paro, H. Hanninen, V. Kauppinen, Tool wear and machinability of HIPed P/M and conventional cast duplex stainless steels, *Wear*, 249 (2001) 279-284.

[60] B. Larsson, B. Lundqvist, Fabrication of ferritic-austenitic stainless steels - Part A, *Materials & Design*, 7 (1986) 33-37.

[61] M. Vosough, *Effect of high-pressure cooling on the residual stress in Ti-alloys during machining*, Department of Applied Physics and Mechanical Engineering, Luleå University of Technology, Luleå, Sweden, 2005.

[62] E.O. Ezugwu, J. Bonney, Y. Yamane, An overview of the machinability of aeroengine alloys, *Journal of Materials Processing Technology*, 134 (2003) 233-253.

[63] P.J. Arrazola, A. Garay, L.M. Iriarte, M. Armendia, S. Marya, F. Le Maitre, Machinability of titanium alloys (Ti6Al4V and Ti555.3), *Journal of Materials Processing Technology*, 209 (2009) 2223-2230.

[64] Sandvik, *Sandvik Bioline Ti6Al4V ELI (Bar)*, Sandvik Materials Technology, www.smt.sandvik.com, 2013-06-10.

[65] E.O. Ezugwu, Z.M. Wang, Titanium alloys and their machinability - a review, *Journal of Materials Processing Technology*, 68 (1997) 262-274.

[66] E.A. Loria, The Status and Prospects of Alloy 718, *Journal of Metals*, 40 (1988) 36-41.

[67] H.J. Wagner, A.M. Hall, *Physical metallurgy of alloy 718*, DMIC Report No. 218, Battelle Memorial Institute, Columbus, OH, USA, 1965.

[68] P. Avdovic, *Machinability variations in Alloy 718*, Division of Production and Materials Engineering, Lund University, Lund, Sweden, 2011.

[69] S. Olovsjö, *Influence of microstructure in machining of nickel and nickel-iron based alloys*, Department of Materials and Manufacturing Technology, Chalmers University of Technology, Gothenburg, Sweden, 2011.

[70] D. Dudzinski, A. Devillez, A. Moufki, D. Larrouquere, V. Zerrouki, J. Vigneau, A review of developments towards dry and high speed machining of Inconel 718 alloy, *International Journal of Machine Tools & Manufacture*, 44 (2004) 439-456.

[71] P. Avdovic, L. Xu, M. Andersson, J.-E. Ståhl, Evaluating the Machinability of Inconel 718 Using Polar Diagrams, *Journal of Engineering for Gas Turbines and Power*, 133 (2011).

[72] S. Olovsjö, P. Hammersberg, P. Avdovic, J.-E. Ståhl, L. Nyborg, Methodology for evaluating effects of material characteristics on machinability - theory and statistics-based modelling applied on Alloy 718, *International Journal of Advanced Manufacturing Technology*, 59 (2012) 55-66.

[73] S. Olovsjö, P. Hammersberg, L. Nyborg, A method for evaluation of potential machinability correlated with material properties between different batches of material, *Proceedings of the 4th International Swedish Production Symposium*, Lund, Sweden, 2011, pp. 250-256.

[74] L.H. Xu, Z.F. Jiang, J.-E. Ståhl, Machinability Prediction of Workpiece Material with a Diagraph Method, *Advanced Materials Research*, 97-101 (2010) 2072-2075.

[75] X.J. Ren, R.D. James, E.J. Brookes, L. Wang, Machining of high chromium hardfacing materials, *Journal of Materials Processing Technology*, 115 (2001) 423-429.

[76] L. Xu, F. Schultheiss, M. Andersson, J.-E. Ståhl, General conception of polar diagrams for the evaluation of the potential machinability of workpiece materials, *International Journal of Machining and Machinability of Materials*, 14 (2013) 24-44.

[77] H. Chandrasekaran, J.O. Johansson, Chip Flow and Notch Wear Mechanisms during the Machining of High Austenitic Stainless Steels, *CIRP Annals - Manufacturing Technology*, 43 (1994) 101-105.

[78] BE Group, *42CrMoS4 (SS 2244)*, BE Group Sverige AB, 2013, www.begroup.com, 2013-10-26.

[79] O. Kienzle, Die Bestimmung von Kräften und Leistungen an spanenden Werkzeugen und Werkzeugmaschinen, *VDI-Z*, 94 (1952) 299-305.

[80] W.F. Hastings, P. Mathew, P.L.B. Oxley, A Machining Theory for Predicting Chip Geometry, Cutting Forces etc. From Work Material Properties and Cutting Conditions, *Proceedings of the Royal Society of London. A. Mathematical and Physical Sciences*, 371 (1980) 569-587.

[81] P.G. Katsev, *Statistical methods in cutting tool analysis*, 2nd ed., Mashinostroenie, Moscow, Russia, 1974.

[82] W. König, K. Essel, L. Witte, *Specific Cutting Force Data for Metal-Cutting*, Verein Deutscher Eisenhüttenleute, Verlag Stahleisen m.b.H., Düsseldorf, Germany, 1982.

[83] ISO, ISO 513:2004, *Classification and application of hard cutting materials for metal removal with defined cutting edges - Designation of the main groups and groups of application*, International Organization for Standardization, Geneva, Switzerland, 2004.

[84] ISO, ISO 4287:1997, *Geometrical Product Specifications (GPS) - Surface texture: Profile method - Terms, definitions and surface texture parameters*, International Organization for Standardization, Geneva, Switzerland, 1997.

[85] C.X. Feng, X. Wang, Development of empirical models for surface roughness prediction in finish turning, *International Journal of Advanced Manufacturing Technology*, 20 (2002) 348-356.

[86] Y. Sahin, A.R. Motorcu, Surface roughness model in machining hardened steel with cubic boron nitride cutting tool, *International Journal of Refractory Metals and Hard Materials*, 26 (2008) 84-90.

[87] X.D. Fang, H. Safi-Jahanshahi, A new algorithm for developing a reference-based model for predicting surface roughness in finish machining of steels, *International Journal of Production Research*, 35 (1997) 179-199.

[88] Y. Sahin, A.R. Motorcu, Surface roughness prediction model in machining of carbon steel by PVD coated cutting tools, *American Journal of Applied Sciences*, 1 (2004) 12-17.

[89] I.A. Choudhury, M.A. ElBaradie, Surface roughness prediction in the turning of high-strength steel by factorial design of experiments, *Journal of Materials Processing Technology*, 67 (1997) 55-61.

[90] D.J. Whitehouse, *Handbook of surface metrology*, Institute of Physics Publishing, Bristol, UK, 1994.

[91] V. Puhasmägi, *Finsvarvning med hårdmetall*, Department of Mechanical Enginnering, Lund University, Lund, Sweden, 1973.

[92] C. Bus, N.A.L. Touwen, P.C. Veenstra, A.C.H. Van Der Wolf, On the Significance of Equivalent Chip Thickness, *CIRP Annals - Manufacturing Technology*, 19 (1971) 121-124.

[93] A.I. Isaev, *Microgeometry of a surface generated in turning*, Academy of Science USSR, Moscow, 1950.

[94] J.-E. Ståhl, F. Schultheiss, S. Hägglund, Analytical and Experimental Determination of the Ra Surface Roughness during Turning, *Procedia Engineering*, 19 (2011) 349-356.

[95] W.B. Palmer, R.C.K. Yeo, Metal flow near the tool point during orthogonal cutting with a blunt tool, *Advances in Machine Tool Design and Research - Proceedings of the Fourth International MTDR Conference, Manchester*, UK, 1963, pp. 61-71.

[96] R.V. Kazban, J.J. Mason, Fluid Mechanics Approach to Machining at High Speeds: Part II: A Potential Flow Model, *Machining Science and Technology*, 11 (2007) 491-514.

[97] F. Schultheiss, *Duplexa rostfria ståls skärbarhet - En studie med inriktning mot skärverktygens nedbrytningsbeteende*, Department of Production and Materials Engineering, Lund University, Lund, Sweden, 2009.

[98] F. Schultheiss, M. Agmell, B. Högrelius, V. Bushlya, J.-E. Ståhl, Experimental Study of the Minimum Chip Thickness during the Machining of Duplex Stainless Steel, *Proceedings of AMST'11 - Advanced Manufacturing Systems and Technology*, Rijeka, Croatia, 2011, pp. 175-189.

[99] Z.J. Yuan, M. Zhou, S. Dong, Effect of diamond tool sharpness on minimum cutting thickness and cutting surface integrity in ultraprecision machining, *Journal of Materials Processing Technology*, 62 (1996) 327-330.

[100] M.E.A. Moneim, The Tribology of Orthogonal Finish Machining - a Review, *Wear*, 63 (1980) 303-318.

[101] Y.-C. Yen, A. Jain, T. Altan, A finite element analysis of orthogonal machining using different tool edge geometries, *Journal of Materials Processing Technology*, 146 (2004) 72-81.

[102] S.M. Son, H.S. Lim, J.H. Ahn, Effects of the friction coefficient on the minimum cutting thickness in micro cutting, *International Journal of Machine Tools and Manufacture*, 45 (2005) 529-535.

[103] M. Agmell, A. Ahadi, J.E. Ståhl, A fully coupled thermomechanical two-dimensional simulation model for orthogonal cutting: formulation and simulation, *Proceedings of the Institution of Mechanical Engineers, Part B: Journal of Engineering Manufacture*, 225 (2011) 1735-1745.

[104] G.R. Johnson, W.H. Cook, Fracture characteristics of three metals subjected to various strains, strain rates, temperatures and pressures, *Engineering Fracture Mechanics*, 21 (1985) 31-48.

[105] Z. Xu, Y. Li, Dynamic behaviors of 0Cr18Ni10Ti stainless steel welded joints at elevated temperatures and high strain rates, *Mechanics of Materials*, 41 (2009) 121-130.

[106] K. Liu, S.N. Melkote, Effect of plastic side flow on surface roughness in micro-turning process, *International Journal of Machine Tools & Manufacture*, 46 (2006) 1778-1785.

[107] P.-H. Brammertz, *Ursachen für Form und Massfehler an feinbearbeiten Werkstüchken*, RWTH Aachen, Aachen, Germany, 1960.

[108] W. Grzesik, A revised model for predicting surface roughness in turning, *Wear*, 194 (1996) 143-148.

[109] M.M.W. Knüfermann, *Machining surfaces of optical quality by hard turning*, School of Industrial and Manufacturing Science, Cranfield University, Cranfield, UK, 2003.

[110] W. Grzesik, K. Zak, Surface integrity generated by oblique machining of steel and iron parts, *Journal of Materials Processing Technology*, 212 (2012) 2586-2596.

[111] P.G. Petropoulos, Statistical basis for surface roughness assessment in oblique finish turning of steel components, *International Journal of Production Research*, 12 (1974) 345-360.

[112] T.H.C. Childs, Friction modelling in metal cutting, *Wear*, 260 (2006) 310-318.

[113] W. Grzesik, The influence of thin hard coatings on frictional behaviour in the orthogonal cutting process, *Tribology International*, 33 (2000) 131-140.

[114] N.A. Shevchenko, E.I. Kruglov, *Influence of tool surface microtopography on tool wear*, in: G.L. Haet (Ed.) Reliability of cutting tools, Donetsk, USSR, 1975, pp. 177-182.

[115] E.M. Trent, Metal cutting and the tribology of seizure: I seizure in metal cutting, *Wear*, 128 (1988) 29-45.

[116] E.M. Trent, Metal cutting and the tribology of seizure: II movement of work material over the tool in metal cutting, *Wear*, 128 (1988) 47-64.

[117] R. M'Saoubi, S. Ruppi, Wear and thermal behaviour of CVD α-Al2O3 and MTCVD Ti(C,N) coatings during machining, *CIRP Annals - Manufacturing Technology*, 58 (2009) 57-60.

[118] U. Höglund, *Skäreggens förslitningsprocess i mikroskala, fysikaliska villkor - förslitningsmekanismer*, Chalmers University of Technology, Gothenburg, Sweden, 1976.

[119] N.N. Zorev, Interrelationship between shear processes occurring along tool face and shear plane in metal cutting, *International Research in Production Engineering*, 49 (1963) 42-49.

[120] E. Usui, H. Takeyama, A Photoelastic Analysis of Machining Stresses, *Journal of Engineering for Industry*, 82 (1960) 303-307.

[121] M.E. Merchant, Mechanics of the Metal Cutting Process. II. Plasticity Conditions in Orthogonal Cutting, *Journal of Applied Physics*, 16 (1945) 318-324.

[122] P.L.B. Oxley, *The mechanics of machining: an analytical approach to assessing machinability*, Ellis Horwood Ltd., Chichester, UK, 1989.

[123] N.N. Zorev, *Metal cutting mechanics*, Pergamon Press, Oxford, UK, 1966.

[124] H.O. Gekonde, S.V. Subramanian, Tribology of tool–chip interface and tool wear mechanisms, *Surface and Coatings Technology*, 149 (2002) 151-160.

[125] T. Özel, T. Altan, Determination of workpiece flow stress and friction at the chip–tool contact for high-speed cutting, *International Journal of Machine Tools and Manufacture*, 40 (2000) 133-152.

[126] M. Fallqvist, F. Schultheiss, R. M'Saoubi, M. Olsson, J.E. Ståhl, Influence of the tool surface micro topography on the tribological characteristics in metal cutting: Part I experimental observations of contact conditions, *Wear*, 298-299 (2013) 87-98.

[127] W.C. Oliver, G.M. Pharr, An Improved Technique for Determining Hardness and Elastic-Modulus Using Load and Displacement Sensing Indentation Experiments, *Journal of Materials Research*, 7 (1992) 1564-1583.

[128] O. Bayard, *Investigation of Forces and Contact Area for Modelling Turning Processes*, Department of Production Engineering, Royal Institute of Technology, Stockholm, Sweden, 2003.

[129] H. Ernst, M.E. Merchant, Chip Formation, Friction and High Quality Machined Surfaces, *Surface Treatment of Metals, American Society for Metals*, Cleveland, Ohio, USA, 1941, pp. 299-328.

[130] F. Schultheiss, M. Fallqvist, R. M'Saoubi, M. Olsson, J.E. Ståhl, Influence of the tool surface micro topography on the tribological characteristics in metal cutting - Part II Theoretical calculations of contact conditions, *Wear*, 298-299 (2013) 23-31.

[131] R. Woxén, *Theory and an equation for the life of lathe tools*, Ingenjörsvetenskapsakademins Handlingar Nr. 119, Stockholm, Sweden, (1932).

[132] T. Hodgson, P.H.H. Trendler, G.F. Micheletti, Turning Hardened Tool Steels with Cubic Boron Nitride Inserts, *CIRP Annals - Manufacturing Technology*, 30 (1981) 63-66.

[133] T. Carlsson, T. Stjernstoft, B. Lindström, A model for calculation of the geometrical shape of the cutting tool - work piece interface, *CIRP Annals - Manufacturing Technology*, 50 (2001) 41-44.

[134] S. Hägglund, *Methods and Models for Cutting Data Optimization*, Department of Materials and Manufacturing Technology, Chalmers University of Technology, Gothenburg, Sweden, 2013.

[135] H.J.J. Kals, J.A.W. Hijink, A.C.H. Van Der Wolf, A Computer Aid in the Optimization of Turning Conditions in Multi-Cut Operations, *CIRP Annals - Manufacturing Technology*, 27 (1978) 465-469.

[136] J.P. Choi, S.J. Lee, Efficient chip breaker design by predicting the chip breaking performance, *International Journal of Advanced Manufacturing Technology*, 17 (2001) 489-497.

[137] J.-E. Ståhl, F. Schultheiss, Analytical Calculation of the True Equivalent Chip Thickness for Cutting Tools and its Influence on the Calculated Tool Life, *Advanced Materials Research*, 576 (2012) 80-86.

[138] V.P. Astakhov, The assessment of cutting tool wear, *International Journal of Machine Tools and Manufacture*, 44 (2004) 637-647.

[139] E. Kuljanic, Macro Plastic Deformation of Cutting Edge - A Method for Maximum Utilization of Cutting Tool, *CIRP Annals - Manufacturing Technology*, 41 (1992) 151-154.

[140] E.O. Ezugwu, R.B. Da Silva, J. Bonney, Á.R. Machado, Evaluation of the performance of CBN tools when turning Ti–6Al–4V alloy with high pressure coolant supplies, *International Journal of Machine Tools and Manufacture*, 45 (2005) 1009-1014.

[141] R. Komanduri, B.F. Von Turkovich, New Observations on the Mechanism of Chip Formation When Machining Titanium-Alloys, *Wear*, 69 (1981) 179-188.

[142] A.R. Machado, J. Wallbank, Machining of titanium and its alloys - a review, *Proceedings of the Institution of Mechanical Engineers, Part B: Journal of Engineering Manufacture*, 204 (1990) 53-60.

[143] A.K. Nandy, M.C. Gowrishankar, S. Paul, Some studies on high-pressure cooling in turning of Ti–6Al–4V, *International Journal of Machine Tools and Manufacture*, 49 (2009) 182-198.

[144] S.Y. Hong, Y.C. Ding, Cooling approaches and cutting temperatures in cryogenic machining of Ti-6Al-4V, *International Journal of Machine Tools & Manufacture*, 41 (2001) 1417-1437.

[145] A. Jawaid, S. Sharif, S. Koksal, Evaluation of wear mechanisms of coated carbide tools when face milling titanium alloy, *Journal of Materials Processing Technology*, 99 (2000) 266-274.

[146] Q. Meng, J.A. Arsecularatne, P. Mathew, Prediction of the cutting conditions giving plastic deformation of the tool in oblique machining, *International Journal of Machine Tools & Manufacture*, 38 (1998) 1165-1182.

[147] J.-E. Ståhl, *Skäreggars spontanhaverier*, Division of Production and Materials Engineering, Lund University, Lund, Sweden, 1986.

[148] M. Vosough, F. Schultheiss, M. Agmell, J.-E. Ståhl, A method for identification of geometrical tool changes during machining of titanium alloy Ti6Al4V, *International Journal of Advanced Manufacturing Technology*, 67 (2013) 339-348.

[149] J.P. Womack, D.T. Jones, D. Roos, *The machine that changed the world, Rawson Associates*, New York, USA, 1990.

[150] C. Voss, D. Clutterbuck, *Just-in-time: A Global status report*, IFS Publications Ltd, Bedford, England, 1989.

[151] E.J. Hay, *The just-in-time breakthrough: implementing the new manufacturing basics*, John Wiley & Sons Inc., New York, USA, 1988.

[152] Y. Monden, *Toyota production system: an integrated approach to just-in-time*, 2nd ed., Chapman & Hall, London, UK, 1989.

[153] J.-E. Ståhl, C. Andersson, M. Jönsson, A basic economic model for judging production development, *Proceedings of the Swedish Production Symposium*, Göteborg, Sweden, 2007.

[154] M. Jönsson, C. Andersson, J.-E. Ståhl, A general economic model for manufacturing cost simulation, *Proceedings of the 41st CIRP Conference on Manufacturing Systems*, Tokyo, Japan, 2008, pp. 33-38.

[155] F. Schultheiss, B. Lundqvist, J.-E. Ståhl, Cost Based Process Optimization by Incrementally Changing the Cutting Data during Sustainable Machining, *Advanced Materials Research*, 576 (2012) 742-746.

[156] L. Smith, P. Ball, Steps towards sustainable manufacturing through modelling material, energy and waste flows, *International Journal of Production Economics*, 140 (2012) 227-238.

[157] J.R. Duflou, J.W. Sutherland, D. Dornfeld, C. Herrmann, J. Jeswiet, S. Kara, M. Hauschild, K. Kellens, Towards energy and resource efficient manufacturing: A processes and systems approach, *CIRP Annals - Manufacturing Technology*, 61 (2012) 587-609.

[158] M. Garetti, M. Taisch, Sustainable manufacturing: Trends and research challenges, Production Planning & Control, 23 (2012) 83-104.

[159] M. Despeisse, M.R. Oates, P.D. Ball, Sustainable manufacturing tactics and cross-functional factory modelling, *Journal of Cleaner Production*, 42 (2013) 31-41.

[160] A.D. Jayal, F. Badurdeen, O.W. Dillon, I.S. Jawahir, Sustainable manufacturing: Modeling and optimization challenges at the product, process and system levels, *CIRP Journal of Manufacturing Science and Technology*, 2 (2010) 144-152.

[161] F. Pusavec, P. Krajnik, J. Kopac, Transitioning to sustainable production – Part I: application on machining technologies, *Journal of Cleaner Production*, 18 (2010) 174-184.

[162] E. Kuram, B. Ozcelik, M. Bayramoglu, E. Demirbas, B.T. Simsek, Optimization of cutting fluids and cutting parameters during end milling by using D-optimal design of experiments, *Journal of Cleaner Production*, 42 (2013) 159-166.

[163] F. Schultheiss, J. Zhou, E. Gröntoft, J.-E. Ståhl, Sustainable machining through increasing the cutting tool utilization, *Journal of Cleaner Production*, 59 (2013) 298-307.

[164] S. Hägglund, *Global optimization of cutting processes*, Department of Product and Production Development, Chalmers University of Technology, Gothenburg, Sweden, 2002.

[165] R. Woxén, *Tool-life and balance of heat in lathe work*, Ingenjörsvetenskapsakademin, Handling 142, Stockholm, Sweden, 142 (1937).

[166] V.A. Balogun, P.T. Mativenga, Modelling of direct energy requirements in mechanical machining processes, *Journal of Cleaner Production*, 41 (2013) 179-186.

[167] T. Behrendt, A. Zein, S. Min, Development of an energy consumption monitoring procedure for machine tools, *CIRP Annals - Manufacturing Technology*, 61 (2012) 43-46.

[168] L. Li, J. Yan, Z. Xing, Energy requirements evaluation of milling machines based on thermal equilibrium and empirical modelling, *Journal of Cleaner Production*, 52 (2013) 113-121.